IFM-GEOMAR REPORT

IFM-GEOMAR

Leibniz-Institut für Meereswissenschaften
an der Universität Kiel

FS POSEIDON
Fahrtbericht / Cruise Report
P399 - 2&3

P399-2
31.05.2010 – 17.06.2010
Las Palmas - Las Palmas (Canary Islands)

P399-3
18. – 24.06.2010
Las Palmas (Canary Islands), Vigo (Spain)

IBM (Hamburg), IUP (Heidelberg), IFM-GEOMAR (Kiel): Diurnal and Regional Variability of halogen Emissions

DRIVE

S PRAN

Poseidon Cruise P399
Legs 2 and 3
Eastern Tropical North Atlantic
31 May – 24 June 2010

Berichte aus dem Leibniz-Institut
für Meereswissenschaften an der
Christian-Albrechts-Universität zu Kiel

Nr. 48

August 2011

IFM-GEOMAR
Leibniz-Institut für Meereswissenschaften
an der Universität Kiel

FS Poseidon
Fahrtbericht / Cruise Report
P399 - 2&3

P399-2
31.05.2010 – 17.06.2010
Las Palmas - Las Palmas (Canary Islands)

P399-3
18. – 24.06.2010
Las Palmas (Canary Islands), Vigo (Spain)

Berichte aus dem Leibniz-Institut
für Meereswissenschaften an der
Christian-Albrechts-Universität zu Kiel

Nr. 48
August 2011

ISSN Nr.: 1614-6298

IFM-GEOMAR
Leibniz-Institut für Meereswissenschaften
an der Universität Kiel

Das Leibniz-Institut für Meereswissenschaften ist ein Institut der Wissenschaftsgemeinschaft Gottfried Wilhelm Leibniz (WGL)

The Leibniz-Institute of Marine Sciences is a member of the Leibniz Association (Wissenschaftsgemeinschaft Gottfried Wilhelm Leibniz).

Herausgeber / Editor:
H. Bange

IFM-GEOMAR Report
ISSN Nr.: 1614-6298

Leibniz-Institut für Meereswissenschaften / Leibniz Institute of Marine Sciences
IFM-GEOMAR
Dienstgebäude Westufer / West Shore Building
Düsternbrooker Weg 20
D-24105 Kiel
Germany

Leibniz-Institut für Meereswissenschaften / Leibniz Institute of Marine Sciences
IFM-GEOMAR
Dienstgebäude Ostufer / East Shore Building
Wischhofstr. 1-3
D-24148 Kiel
Germany

Tel.: ++49 431 600-0
Fax: ++49 431 600-2805
www.ifm-geomar.de

IFM-GEOMAR,
Leibniz-Institut für
Meereswissenschaften
an der Universität Kiel

15 August 2011

Cruise Report

Compiled by: PD Dr Hermann W. Bange, IFM-GEOMAR, Kiel, Germany

R/V Poseidon Cruise No.: 399 leg 2 (P399/2) and 399 leg 3 (P399/3)

Dates of Cruise: P399/2: 31 May 2010 – 17 June 2010; P399/3: 18 – 24 June 2010

Research Topics: Mar. Biogeochem., Phys. Oceanogr., Atmos. Chem.

Oceanic Region: P399/2 – Eastern Tropical North Atlantic Ocean and coastal upwelling off Mauritania; P399/3 – subtropical North Atlantic Ocean

Port Calls: P399/2 – Las Palmas (Canary Islands), Mindelo (Cape Verde Islands), Las Palmas (Canary Islands); P399/3 – Las Palmas (Canary Islands), Vigo (Spain)

Institute: IFM-GEOMAR, Kiel, Germany

Chief Scientist: PD Dr Hermann W. Bange, IFM-GEOMAR, Kiel, Germany

Number of Participants: 10 scientists

Project: SOPRAN (Surface Ocean PRocesses in the ANthropocene): DRIVE (Diurnal and RegIonal Variability of halogen Emissions)

This cruise report consists of 74 pages including cover page:

The SOPRAN II / DRIVE campaign – Poseidon cruise 399 legs 2 and 3 to the eastern tropical North Atlantic/upwelling off Mauritania and eastern subtropical North Atlantic

H.W. Bange[1], E. Atlas[2], E. Bahlmann[3], A. Baker[4], A. Bracher[5], A. Cianca[6], M. Dengler[1], S Fuhlbrügge[1], K. Großmann[7], H. Hepach[1], J. Lavrič[8], C. Löscher[9], K. Krüger[1], A. Orlikowska[10], I. Peeken[11], B. Quack[1], J. Schafstall[1], T. Steinhoff[1], J. Williams[12], and F. Wittke[1]

[1] IFM-GEOMAR, Kiel
[2] Rosenstiel School Marine Atmospheric Science (RSMAS), Miami, Fl, USA
[3] IfBM, Universität Hamburg
[4] School Environ. Sci., Univ. East Anglia, Norwich, UK
[5] AWI, Bremerhaven
[6] Instituto Canario de Sciencias Marinas (ICCM), Telde, Gran Canaria, Spain
[7] IUP, Universität Heidelberg
[8] MPI für Biogeochemie, Jena
[9] Institut für Allgem. Mikrobiol., Universität Kiel
[10] IOW, Warnemünde
[11] AWI/MARUM, Bremerhaven/Bremen
[12] MPI für Chemie, Mainz

Summary

The DRIVE (Diurnal and RegIonal Variability of Halogen Emissions) campaign to the eastern tropical North Atlantic Ocean and the upwelling off Mauritania (NW Africa) was funded by the BMBF as part of the German SOLAS project SOPRAN II (Surface Ocean Processes in the Anthropocene; www.sopran.pangaea.de): The second leg of the 399th cruise of R/V Poseidon (P399/2) took place from 31 May to 17 June 2010 (Las Palmas-Mindelo (Cape Verde Islands) – Mauritanian upwelling – Las Palmas). It was followed by the transit leg 3 (P399/3) which took place from 18 June to 24 June 2010 (Las Palmas – Vigo (Spain)) with only one stop at ESTOC. Ten scientists from IFM-GEOMAR (Kiel), IfAM (U Kiel), IfBM (U Hamburg) and IUP (U Heidelberg) representing various SOPRAN II subprojects took part in the cruise which was the sixth of a series of German SOLAS cruises to the tropical North Atlantic Ocean. The major objective of P399/2 was to investigate the regional and diurnal atmospheric and oceanic variations of halogenated compounds in the eastern tropical North Atlantic Ocean with a special focus on the Mauritanian upwelling. The main working packages of P399/2 and P399/3 included measurements of

- Atmospheric BrO and IO
- Atmospheric halocarbons
- Other atmospheric trace gases such as ozone, methane etc.
- Aerosol composition
- Vertical structure of the atmosphere
- Dissolved halocarbons, nitrous oxide and carbon dioxide
- CTD, dissolved nutrients, O_2, and chlorophyll
- Microstructure of the upper water column

Besides an extensive underway measurement program of dissolved (halocarbons, N_2O, CO_2) and atmospheric (BrO, halocarbons, other trace gases, aerosol) compounds, six 24h stations were performed and 23 regular CTD stations with depth profiles covering the entire water column were occupied.

1. Scientific team

1.1 List of participants

31 May – 5 June 2010 (Las Palmas – Mindelo)			
01 Hermann W. Bange	*Chief Scientist*	IFM-GEOMAR	hbange@ifm-geomar.de
02 Enno Bahlmann	Scientist	Univ. Hamburg	enno.bahlmann@zmaw.de
03 Mirja Dunker	Student	IFM-GEOMAR	mdunker@ifm-geomar.de
04 Katja Großmann	Student	Univ. Heidelberg	katja.grossmann@iup.uni-heidelberg.de
05 Helmke Hepach	Student	IFM-GEOMAR	hhepach@ifm-geomar.de
06 Uwe Koy	Technician	IFM-GEOMAR	ukoy@ifm-geomar.de
07 Carolin Löscher	Student	Univ. Kiel	cloescher@ifam.uni-kiel.de
08 Gert Petrick	Technician	IFM-GEOMAR	gpetrick@ifm-geomar.de
09 Jens Schafstall	Scientist	IFM-GEOMAR	jschafstall@ifm-geomar.de
10 Franziska Wittke	Student	IFM-GEOMAR	fwittke@ifm-geomar.de

5 June – 17 June 2010 (Mindelo – Las Palmas)			
01 Hermann W. Bange	*Chief Scientist*	IFM-GEOMAR	
02 Ralf Lendt	Scientist	Univ. Hamburg	ralf.lendt@zmaw.de
03 Mirja Dunker	Student	IFM-GEOMAR	
04 Katja Großmann	Student	Univ. Heidelberg	
05 Helmke Hepach	Student	IFM-GEOMAR	
06 Uwe Koy	Technician	IFM-GEOMAR	
07 Carolin Löscher	Student	Univ. Kiel	
08 Karen Stange	Technician	IFM-GEOMAR	kstange@ifm-geomar.de
09 Jens Schafstall	Scientist	IFM-GEOMAR	
10 Franziska Wittke	Student	IFM-GEOMAR	

18 June – 24 June 2010 (Las Palmas – Vigo)			
01 Hermann W. Bange	*Chief Scientist*	IFM-GEOMAR	
02 Ralf Lendt	Scientist	Univ. Hamburg	
03 Mirja Dunker	Student	IFM-GEOMAR	
04 Katja Großmann	Student	Univ. Heidelberg	
05 Helmke Hepach	Student	IFM-GEOMAR	
06 Carolin Löscher	Student	Univ. Kiel	
07 Karen Stange	Technician	IFM-GEOMAR	
08 Franziska Wittke	Student	IFM-GEOMAR	
09 Andres Cianca	Scientist	ICCM*	andres@iccm.rcanaria.es
10 Ahmed Makaoui	Observer	INRH**	makaouireda@yahoo.fr

* Instituto Canario de Sciencias Marinas, Telde, Gran Canaria, Spain; www.iccm.rcanaria.es/ .
** Institut National de Recherche Halieutique, Casablanca, Morocco; www.inrh.org.ma/ .

Chief Scientist

PD Dr Hermann W. Bange

Marine Biogeochemistry Research Division
IFM-GEOMAR
Düsternbrooker Weg 20
24105 Kiel, Germany.

e-mail: hbange@ifm-geomar.de
ph.: +49-431 600 4204
fax: +49-431 600 4202

1.2 National and international collaborators

- Elliot Atlas, RSMAS, Miami, Florida: Atm. compounds; flask sampling
- Alex Baker, University of East Anglia, Norwich, UK: Aerosols
- Astrid Bracher, AWI, Bremerhaven: Remote sensing of phytoplankton
- Marcus Dengler, IFM-GEOMAR: Microstructure
- Gernot Friedrichs, Univ. Kiel: Atmospheric $^{13}CO_2$
- Martin Heimann & Jost Lavric, MPI für Biogeochemie, Jena: Flask sampling; atmos. CH_4, CO_2
- Kirstin Krüger, IFM-GEOMAR: Meteorology
- Anna Orlikowska, IOW, Warnemünde: Isotope signature of diss. VOC
- Ilka Peeken, AWI/MARUM, Bremerhaven: Phytoplankton distribution
- Ulrich Platt, Univ. Heidelberg: Atmospheric halogen compounds
- Ruth Schmitz-Streit, Univ. Kiel: Molecular biology
- Tobias Steinhoff, IFM-GEOMAR: pCO_2
- Jonathan Williams, MPI für Chemie, Mainz: Atmospheric ozone

For the list of e-mail addresses of the collaborators see Appendix.

2. Research programme

The major objective of cruise P399 leg 2 (P399/2) was to investigate the the regional and diurnal atmospheric and oceanic variability of halogenated compounds in the eastern tropical North Atlantic Ocean with special focus on the Mauritanian upwelling.

The target areas of P399/2 were

(i) the eastern tropical North Atlantic (West-to-East transect along 18°N) and
(ii) the coastal upwelling region off Mauritania.

Leg 3 of P399 (P399/3) was a transit leg from Las Palmas to Vigo with only one stop at ESTOC (European Station for Time Series in the Ocean).

The main working packages of P399/2 and P399/3 included measurements of

- Atmospheric BrO and IO
- Atmospheric halocarbons (in cooperation with E. Atlas, RSMAS, Miami)
- Isotope signature of atmospheric halocarbons
- Other atmospheric trace gases such as ozone, methane etc. (in cooperation with M. Heimann, MPI Biogeochemie, Jena; J. Williams, MPI Chemie, Mainz; G. Friedrichs, U Kiel)
- Aerosol composition (in cooperation with A. Baker; UEA, Norwich)
- Vertical structure of the atmosphere
- Dissolved halocarbons, nitrous oxide and carbon dioxide
- CTD, dissolved nutrients, O_2, and chlorophyll
- Microstructure of the upper water column

3. Narrative of cruise

R/V Poseidon left Las Palmas on 31 May 2010 heading SW. A successful CTD test station was performed on 2 June at 22°N 21°W. The CVOO (Cape Verde Ocean Observatory, formerly called TENATSO) station was reached on 3 June and the first 24h station was performed. After a short stopover at the port of Mindelo (Cape Verde) for the exchange of two members of the scientific crew, the cruise was continued with a short transect from Mindelo to the northern tip of the island of Sal. Then Poseidon steamed east along 18°N transect toward the Mauritanian coast which was reached on 10 June. Then Poseidon headed north following a cruise track parallel to the Mauritanian coast. The last 24h station was performed on 13/14 June at 20°N 17.25°W. P399/2 was finished on 17 June in Las Palmas.

The transit from Las Palmas to Vigo (P399/3) took place from 18 June to 24 June 2010 with only one stop at ESTOC on 19 June.

For further details see the weekly cruise reports (in German, see appendix).

4. Technical report

4.1 Cruise track

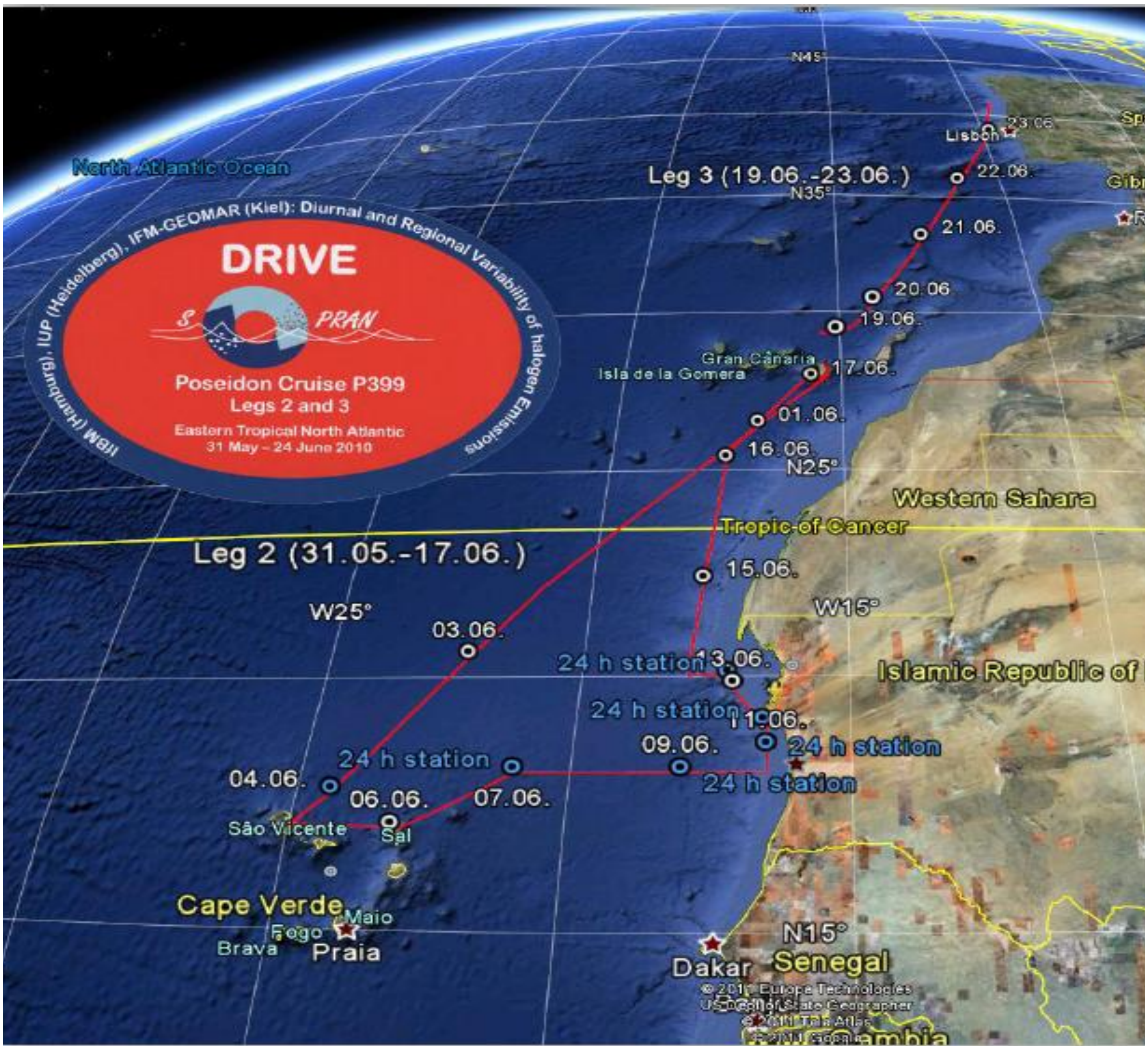

(map by S. Fuhlbrügge, IFM-GEOMAR, Kiel)

4.2 List of stations

(24h stations are marked in grey)

Station #	CTD #	Date Start UTC	Time UTC	Lat. (start)		Long. (start)		Water depth	Max. pressure[a]
305*	1	02.06.2010	11:26	22° N	0.0'	21° W	0.0'	4328	507
307**	2	03.06.2010	21:56	17° N	36.0'	24 °W	18.0'	3598	509
307**	3	04.06.2010	10:06	17 °N	36.0'	24 °W	18.0'	3598	3642
307**	4	04.06.2010	12:48	17 °N	36.0'	24 °W	18.0'	3598	401
308	5	06.06.2010	17:06	18 °N	0.0'	21 °W	0.0'	3068	236
308	6	07.06.2010	06:43	18 °N	0.0'	21 °W	0.0'	3068	3094
308	7	07.06.2010	09:00	18 °N	0.0'	21 °W	0.0'	3156	303
309	8	08.06.2010	01:37	18 °N	0.0'	20 °W	0.0'	3192	503
310	9	08.06.2010	10:01	18 °N	0.0'	19 °W	0.0'	3150	504
311	10	08.06.2010	17:38	18 °N	0.0'	18 °W	0.0'	2810	505
311	11	09.06.2010	07:00	18 °N	0.0'	18 °W	0.0'	2801	2819
311	12	09.06.2010	09:56	18 °N	0.0'	18 °W	0.0'	2803	466
312	13	09.06.2010	20:38	18 °N	0.0'	17 °W	30.0'	2514	505
313	14	10.06.2010	01:26	18 °N	0.0'	17 °W	0.0'	1716	507
314	15	10.06.2010	04:01	18 °N	0.0'	16 °W	45.0'	988	506
315	16	10.06.2010	06:24	18° N	00.0'	16° W	30.0'	190	186
316	17	10.06.2010	10:51	18 °N	30.0'	16 °W	30.0'	98	92
316	18	10.06.2010	23:02	18 °N	30.0'	16 °W	30.0'	94	95
317	19	11.06.2010	19:02	19 °N	0.0'	16 °W	34.1'	64	63
317	20	12.06.2010	07:02	19 °N	0.1'	16 °W	34.1'	64	63
318	21	12.06.2010	20:00	19 °N	30.0'	17° W	0.0'	105	103
319	22	13.06.2010	07:04	20° N	0.0‘	17° W	15.0	24.5	23
319	23	13.06.2010	17:11	20 °N	0.0'	17 °W	15.0'	25	23
320***	24	19.06.2010	04:40	29 °N	10.0‘	15 °W	30.0‘	3608	600
320***	25	19.06.2010	06:15	29° N	10.0‘	15° W	30.0‘	3608	3500

* Test station; ** CVOO; *** ESTOC.
[a] max. depth of CTD cast.

4.3 Water column measurements/sampling:

- CTD (incl. O_2 and fluorescence sensors)
- Microstucture
- Nutrients (NO_3^-, NO_2^-, PO_4^{3-}, SiO_2)
- O_2
- N_2O
- Halocarbons
- Stable carbon isotope ratio of volatile halogenated organic compounds (VHOCs)
- Chl. a and other pigments
- DNA/RNA
- Flow Cytometry

4.4 Underway water measurements/sampling:

- ADCP
- Thermosaliograph (available only for P399/2)
- O_2
- Total gas tension
- N_2O
- CO_2
- Halocarbons
- Chl. a and other pigments

4.5. Atmospheric measurements/sampling:

- Standard meteorological data
- Radio sondes
- Aerosol composition
- BrO, IO
- O_3 (continuous)
- Hg (continuous)
- CH_4 and CO_2 (continuous)
- $^{13}CO_2$ (continuous)
- Flask samples (Miami): halocarbons, hydrocarbons, CFCs, DMS, COS, alkyl nitrates
- Flask samples (Jena): SF_6, O_2/N_2, Ar/N_2, $^{13}C^{18}O_2$, N_2O, CO, CH_4, H_2
- Discrete samples (Hamburg): stable carbon isotope ratio of halocarbons

4.6 Deployments:

none

4.7 Remarks

Please note that the originally proposed quasi-Lagrangian experiment which also included a concurrent land sampling campaign at the Mauritanian coast (Banc d'Arguin) could not take place because of the unforeseen shift of the allocated ship time from Sept/Oct 2010 to May/Jun 2010.

- All sampling devices and instruments worked well.
- Unfortunately, thermosalinograph data have not been recorded during P399/3 because of a handling error.
- Some filter samples for Chl a and marker pigments were lost on Charles de Gaulle Airport (Paris) while changing flights (obviously the box with the frozen filter samples was opened by personnel of the airport; the box arrived in Kiel one day later in a bad condition).
- The submersible seawater pump in the moon pool used on the transect from Las Palmas to Mindelo did not work properly replaced during the stopover in Mindelo.
- The originally proposed underway measurements of dissolved CH_4 in the surface layer were not performed because of the unavailability of the instrument (as a result of the unforeseen shift of the allocated ship time, see above).

4.8 Data management

The data from P399/2 and P399/3 will be made available by July 2011. Data requests should be submitted to Hermann Bange and/or to the PI of the individual working packages, see section 7.

All data will be archived at the PANGAEA database: www.pangaea.de .

5. Scientific equipment

The major scientific equipment on board consisted of:
– 12x 10L water sampler rosette with CTD
– Free-falling microstructure probe
– ADCP
– Thermosalinograph
– Submersible water pump
– Equilibrator/Gas chromatograph with ECD
– Equilibrator/IR CO_2 gas analyzer
– O_2 optode
– Gas tension device
– GC/MS
– Autoanalyzer
– O_2 titration device
– Seawater filtration racks
– Aerosol collector
– Air pump
– O_3 analyzer
– Hg analyzer

– CH_4 analyzer (Picarro)
– $^{13}CO_2$ analyzer (Picarro)
– MAX-DOAS
– Radio sondes

6. Acknowledgements

I am indebted to all participants of P399 and the many other colleagues for their excellent collaboration without P399 would not have been successful. Moreover, I especially acknowledge the excellent support by the officers and crew of R/V Poseidon. I thank the authorities of Mauritania, Cape Verde Islands and Morocco for the permissions to work in their territorial waters. The cruise P399 was funded by the BMBF joint project SOPRAN II with grant no. 03F0611A.

7. First results

7.1 Hydrographic setting during P399/2

Marcus Dengler, Jens Schafstall, Uwe Koy, IFM-GEOMAR, Kiel;
mdengler@ifm-geomar.de

7.1.1 Hydrographic measurements

Altogether, 23 conductivity-temperature-depth/oxygen (CTD/O_2) profiles were sampled at 14 stations (Tab. A1). The CTD/O_2 system was attached to a rosette holding 12 Niskin bottles for water sampling. During the cruise, a hydrographic section from 21°W to the Mauritanian coast along 18°N was completed and several profiles were collected on a northward transect along the Mauritanian continental slope and shelf (Fig. 1).

7.1.1.1 Technical aspects and performance of the CTD/O_2 system

The instrument in use was a SBE 911 plus CTD-system manufactured by Seabird Electronics Inc. of Bellevue, Washington, USA, referred to as "IFM-GEOMAR SBE1" (Seabird s/n 0618). It was equipped with a pressure sensor (s/n 75760) and two independent sets of temperature (s/n 4875 and 4823), conductivity (s/n 2443 and 3374) and oxygen sensors (s/n 1739 and 1718). In addition, a fluorescence (Dr. Haardt Chlorophyll a) sensor and an altimeter (s/n 41839) were attached to the CTD/O_2 frame. Different methodologies were used for the calibration of the CTD sensors. While the temperature and pressure sensors were calibrated in the laboratory of IFM-GEOMAR prior to the cruise, the conductivity and oxygen sensors were calibrated against data obtained from water samples collected during the cruise. In total, 234 oxygen samples were analyzed for oxygen content during the cruise and subsequently used for calibration of the oxygen sensor. For conductivity sensor calibration, 92 water samples were collected during the cruise. The samples were analyzed upon return from the cruise by Guideline laboratory salinometers at IFM-GEOMAR.

Conductivity sensor calibration was performed using a multi-linear fit of temperature, conductivity and pressure minimizing the least square difference to the salinity data from the water samples. Tests using quadratic fits in some or all of the dependencies did not improve the overall quality of the calibration. After applying the corrections to the conductivity sensor, a root mean square (rms) difference of $5x10^{-4}$ S/m was obtained from the water sample conductivities. This corresponds to a rms salinity of about 0.005 that can be taken as the uncertainty of the salinity values. For oxygen, a multi-linear fit of pressure, temperature and oxygen let to a rms difference of 3 µmol/kg that again can be taken as the uncertainty of the sensor data. Only three deep CTD/O_2 casts were collected during the cruise, leading to larger uncertainties of the data below 500 m as only few calibration data were available for this part of the water column. The data from the primary sensors were used to create the final 1-dbar averaged CTD/O_2 profiles. Chlorophyll data from the fluorescence were not calibrated. The raw data, however, was included in the final data files.

CTD/O_2 casts collected in water depths shallower than 500 m along the continental slope and the shelf regions were made from surface to bottom (Fig. 1). In deeper waters (>500m) top to bottom CTD data was only collected at the CVOO time series station (17°36'N, 24°18'W) and along the 18°N section at 21°W and 18°W. All other CTD/O_2 casts were terminated at 500 m. On some stations, a repeat cast was necessary to fulfill the demand of water for biogeochemical sampling. The extra casts typically extended from the surface to about 250 m depth.

The CTD/O_2 system performed well throughout the cruise. During two deep cast (>2000 m) data transmitted by the primary sensors showed some occasional spikes which disappeared at shallower depth. These spikes were removed during post-processing. The Seabird bottle release unit attached to the rosette also worked well throughout the cruise. The CTD data were recorded using Seabird Seasave V7.12 software.

7.1.1.2 Preliminary results

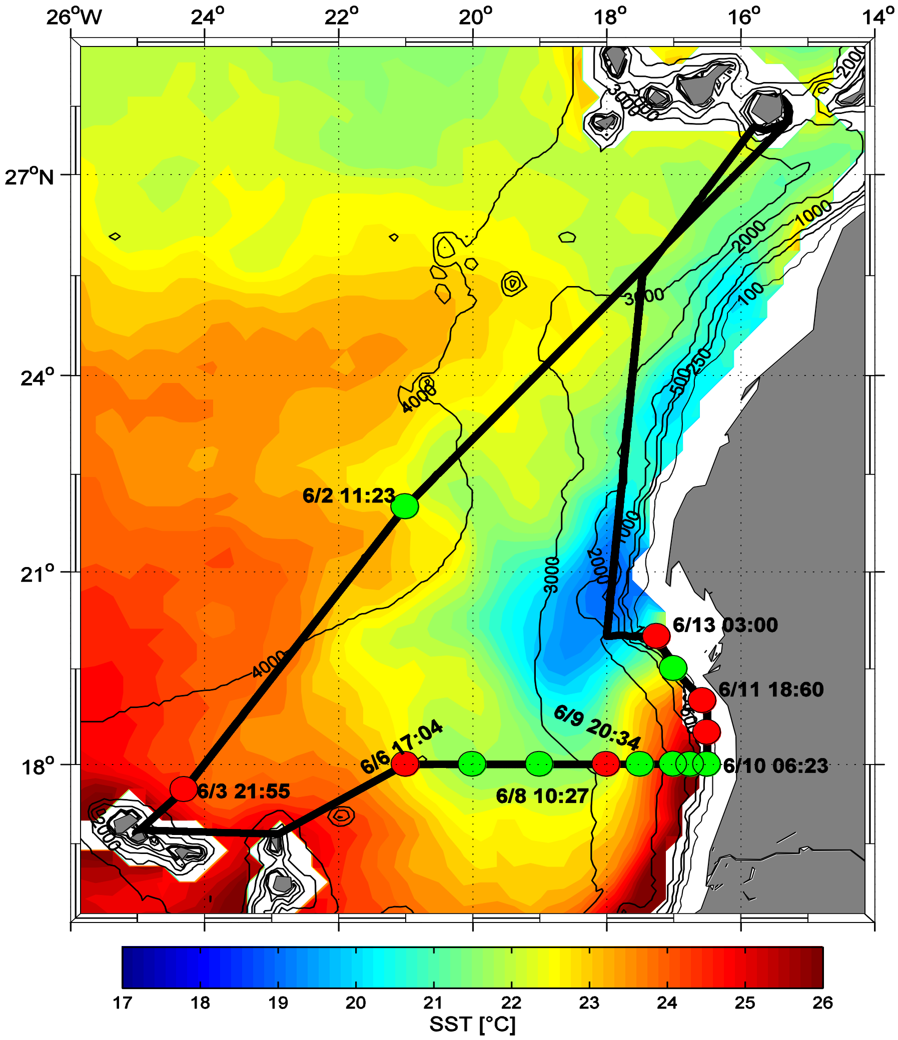

Fig. 1: Cruise track and station overview. Colored dots mark station positions (red dots indicate 24-h stations). Sea surface temperature is shown as a three day average (June 8th-10th) observed by TRMM satellite.

The surface waters in the region off Mauritania south of 20°N exhibited temperatures of up to 26°C (Fig. 1) indicating that upwelling was suppressed. During late winter and early spring when upwelling peaks, sea surface temperatures (SST) as low as 17°C have been observed in this region. However, north of 20°N off Cape Blanc (21°N), cold SSTs were still observed suggesting active upwelling conditions.

In general, the deeper ocean between the Cape Verde Islands and Africa is occupied by two central water masses, the North Atlantic Central Water (NACW) and South Atlantic Central Water (SACW). While the NACW is more saline and oxygen rich, the SACW is characterized by higher nutrient concentrations. The hydrographic section along 18°N (Fig. 2) reveals the presence of low salinity and low oxygen waters close to the continental slope off Mauritania east of 18.5°W, while west of this longitude salinities and oxygen increases. The regions close to the continental slope is thus occupied by the oxygen-poor SACW. The oxygen minimum was found between 300 and 500 m depth well inside the central water layer which is bounded by the isopycnals 25.8 kg m^{-3} and 27.1 kg m^{-3} (Fig. 2). Lowest oxygen values found in this layer were 42 □mol kg^{-1}. It should be noted that there is a second oxygen minimum in the upper water column between 50 m and 100 m close to the continental slope. Here, oxygen values below 60 □mol kg^{-1} are commonly found.

It should be noted that the upper isopycnals strongly slope downward towards the east in the proximity of the continental slope. This downward slope is less evident for the deeper isopycnals indicating a strong baroclinic geostrophic current flowing northward in this region. The circulation at 18°N is further discussed in section 7.2.3.

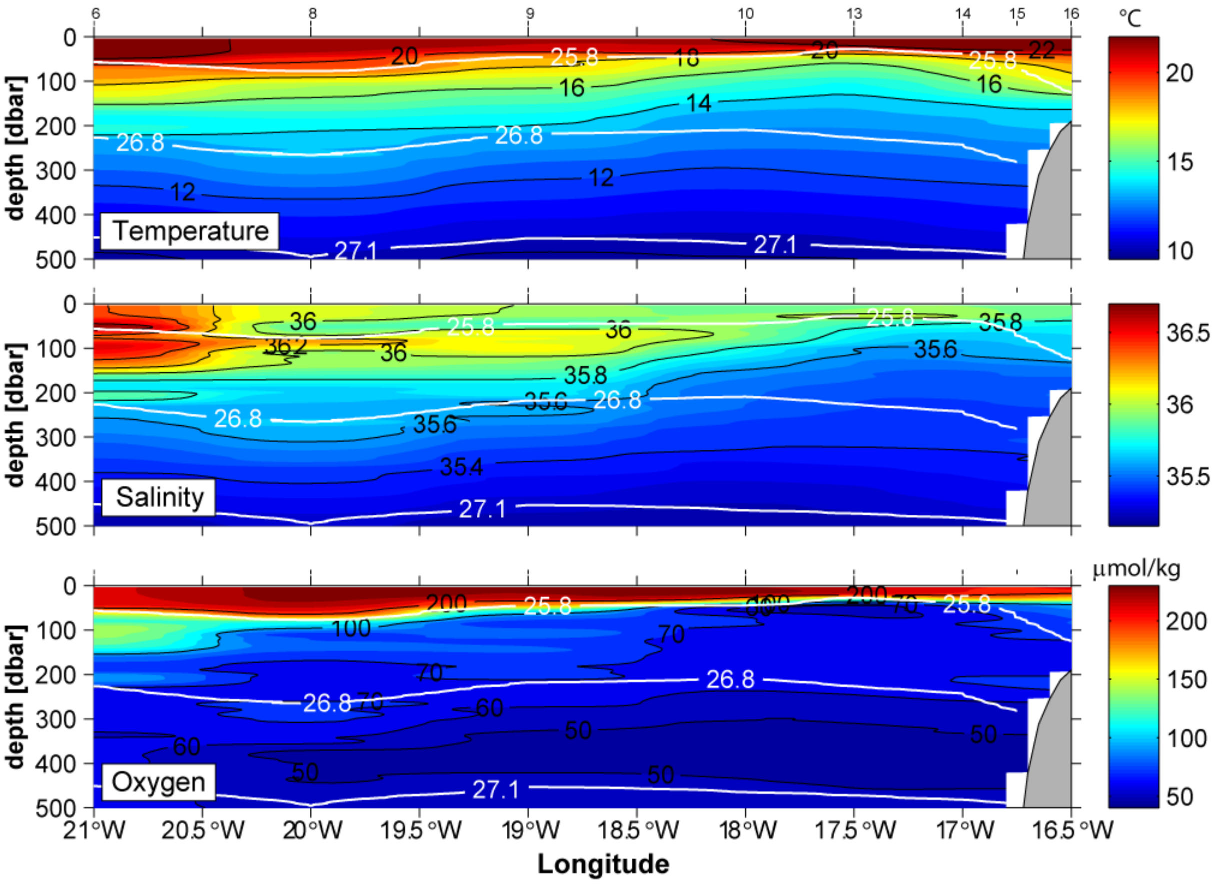

Fig. 2: Temperature (in °C, ITS-90) salinity (PSS-78) and oxygen (in □mol/kg) distribution along 18°N. Isopycnals (white lines) are superimposed on the distributions. The central waters are found between isopycnals 25.8 and 27.1. CTD/O2 profile positions and station numbers are indicated above the top panel.

7.1.2 Microstructure sampling

In total 123 profiles of microstructure shear and temperature were sampled with a loosely-tethered microstructure profiler (MSS) at 20 stations during the cruise (Tab. A1 and Fig. 1). The microstructure profiling system used was manufactured by ISW-Messtechnik in collaboration with Sea and Sun Technology (Trappenkamp, Germany) and consisted of a profiler (s/n 32), a winch and a data interface. The profiler can operate 16 channels in a high data transmission mode (1024 Hz) that is sufficient to resolve the small vertical scales of turbulent fluctuations in the ocean.

7.1.2.1 Technical aspects

The MSS 32 profiler was equipped with four shear probes (airfoil, 4 ms response time), a fast-responding temperature sensor (microthermistor FP07, 12 ms response time), an acceleration sensor and conductivity, temperature, depth sensors that sample at a lower frequency (24 Hz). Additionally, the profiler is equipped with two tilt sensors (for details see Tab. 1). The profiler was optimized to sink at a rate of about 0.6 m/s and is designed to measure up to a depth of 2000 m. During the cruise, microstructure data was collected from the surface to about 200-250 m depth or to a few meters above the bottom in shallower waters. During each CTD/O_2 station, 3-5 microstructure profiles were routinely collected. In addition, continuously MSS profiling along several transects near the continental shelf (consisting of 10-20 profiles) were collected during the 24-hour CTD/O_2 stations. Profiles were sampled from the stern (port side) of the vessel while steaming at about 0.5 kn.

In general, the instrument performed well during the cruise. During a few profiles we had trouble with the data transmission (especially during the up-cast) due to water leaking into cable tethering the profiler. After removing about 15 m of the cable, this problem was resolved. Post-processing of the data is currently underway.

Tab. 1: Sensors used with the microstructure profiler (MSS 32) during the cruise.

Sensor	Type	Response time	Serial No.
Temperature	PT100	160 ms	
Conductivity	ADM	100 ms	
Pressure	Keller PA7-200	40 ms	
Acceleration	ACC	4 ms	
Tilt X	ADXL 203	~100ms	
Tilt Y	ADXL 203	~100ms	
Shear 1	Airfoil	4 ms	003
Shear 2	Airfoil	4 ms	029
Shear 3	Airfoil	4 ms	6052 / 044
Shear 4	Airfoil	4 ms	6058 / 045
Temperature	NTC; FP07	12 ms	40

7.1.3 ADCP measurements

During P399, continuous upper ocean velocity data were recorded by a vessel-mounted Ocean Surveyor that was installed in R/V Poseidon's moon pool. The Ocean Surveyor (OS) uses a phased array transducer consisting of 36 by 36 individual ceramic elements. In contrast to the older narrow band four transducer VMADCP, the OS produces sound pulses at all four beams during the same time and can be operated in either broadband or narrowband mode. R/V Poseidon is equipped with a 75kHz OS that allows to survey velocity in the upper 600 m of the water column.

7.1.3.1 Technical aspects

The systems configuration used during the cruise was different to the standard configuration usually used on R/V Poseidon, in particular due to a malfunctioning of the Ashtech ADU2 system. The OS was controlled by RDI's vessel-mounted data acquisition system (VMDAS). Heading information from the ships gyro compass was directly supplied to the electronic chassis via a synchro interface to convert the measured velocities from beam to earth coordinates, which were then recorded by the VMDAS as single ping data. In addition to the velocities, the VMDAS was supplied directly with heading information from the gyro compass ($GPHDT NMEA string) and with GPS position via two serial interfaces. Due to malfunctioning of the Ashtech receiver, no NMEA GGA position string was available. Instead, a RMC (recommended minimum data for GPS) string was used which, however, could not be interpreted by the VMDAS software. Thus, no positions were stored in the binary data files and the NMEA data were recorded in separate files ending on N2R. The velocity and position data sets were merged during post-processing.

The OS was set-up to record 100 bins at a sampling rate of about 1.6s having a bin length of 8m, a pulse length of 8m and a blanking interval of 4m. Considering that the OS is mounted to the moon pool at 5m water depth, the uppermost bin is located in a water depth of 17m. For pinging, a narrow band mode was chosen. Data was recorded from June 1, 08:10 UTC to June 17, 07:50 UTC. The OS worked well throughout the cruise and a near-continuous upper ocean velocity data set was obtained. However, data inferences were obvious during periods of intense use of R/V Poseidon's bow thrusters which degraded data quality, particularly on station.

During post-processing, the misalignment angle between the axis of the ADCP and the axis of the ship's gyro compass was determined. A water track calibration, where changes of measured velocities during acceleration periods of the vessel are compared the compass changes, resulted in a misalignment angle of -0.8045° with a standard deviation $\sigma = 0.92°$ (Fig. 3). No significant amplitude calibration factor was determined and it was thus set to 1. Similarly, a temporal dependency of the misalignment angle was not significant. The standard deviation of the misalignment angle which reflects data accuracy while underway is about twice as high as during previous cruises where heading information from the Ashtech ADU2 receiver was available. The increase in uncertainty stems from several errors of the gyro compass. The most severe errors are caused by Schuler oscillations of the gyro compass that have a period of about 84 minutes which cannot be removed during post-processing. Additional errors inherent to the gyro compass are due to approximations of the compensations for latitudinal positions and speed of the vessel influencing the heading data. Apart from the known errors of the gyro compass, the gyro heading data showed several jumps of about 10° occurring within a few seconds for periods of 10-20 minutes. The reason for this error could not be determined, but they were clearly distinguishable from the heading changes by the vessel as they occurred much faster than the vessel can turn. As the gyro heading was unreliable during these periods and no other heading source was available, the data were removed. Finally, only 134 values for misalignment angle and amplitude calibration were available. Usually, 500 to 1000 values are available from a single cruise.

The small number of calibration values is due to few stations performed during the cruise and due to the fact that during the 24 hour stations the vessels speed was much reduced.

Due to the errors inherent to the gyro heading and the uncertainties in the calibration of the misalignment angle, the velocity data obtained during P399 are of lower quality compared to previous cruises. The error of hourly averages of velocity is estimated to be above 5 cm s^{-1} during periods when the vessel is underway with 8.5 knots. However, on station or while the ship is steaming slowly, the error of hourly-averaged velocity is between 1 and 2 cm s^{-1}

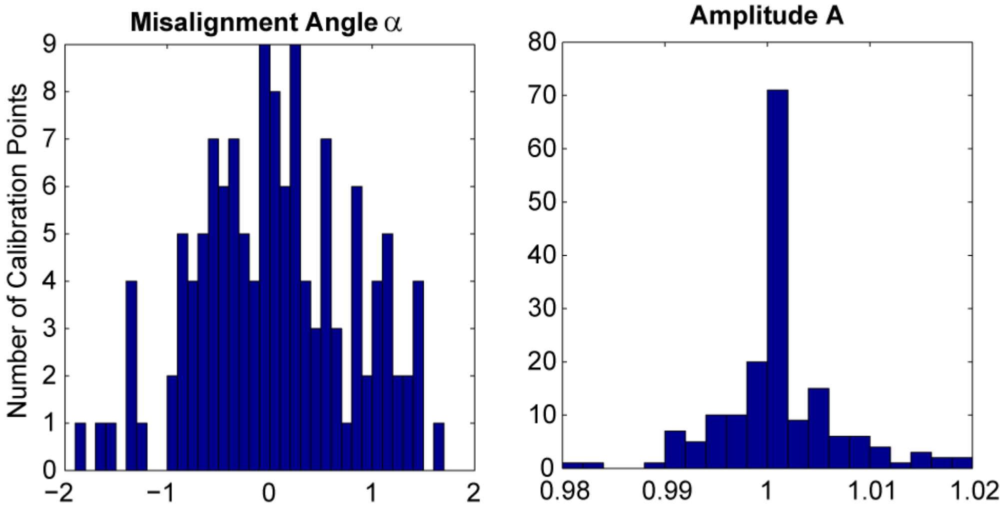

Fig. 3: *Frequency distribution of calibration points for misalignment angle (left) and amplitude (right) determined from 134 values available from the cruise. The average misalignment angle of -0.8045° is subtracted from each value.*

7.1.3.2 Preliminary results

Previous measurement programs have suggested that the large scale circulation in the region between the Cape Verde Islands and Mauritania presents a cyclonic gyre which intensifies during summer (e.g. Mittelsteadt, 1983). During this season, a strengthened eastern boundary current is flowing northward along the continental slope, while a weaker northward flow along the continental slope and an equatorward current on the shelf is present during winter. During previous measurement programs carried out with R/V Poseidon during winter in 2005 and 2007 (P320, P347/P348) an equatorward flow on the continental slope was not evident and instead a broad northward flow was found along the continental slope and on the shelf region having maximum velocities of about 20 cm s^{-1} (Schafstall et al., 2010).

As already indicated by the sloping isopycnals at the continental slope (section 7.2.1), meridional velocity during P399 along 18°N shows a strong northward flow along the continental slope with maximum velocities of above 50 cm s^{-1} (Fig. 4). This current extends from the surface to about 150m depth and has a width of about 50 km. It is not surface intensified by exhibits maximum velocities at a depth of about 60m depth. This northward flow is also pronounced in the ocean surveyor data from 20°N to 20.5°N suggesting that the northward current is pronounced at least up to Cape Blanc.

Along 18°N, northward velocity is not only limited to the eastern boundary regime. Instead, a broad band of northward flow was evident during the cruise extending from the continental slope to about 19.5°W (Fig. 4). It is hypothesized that this northward flow represents the eastern flank of the cyclonic gyre between Cape Verde Islands and Mauritania, which is presumably forced by elevated cyclonic wind stress curl in this region. Several previous investigations (e.g. Mittelsteadt, 1983; Stramma et.al., 2008; Schafstall, 2010) have suggested the presence of the cyclonic gyre which, however, is usually observed to be weak.

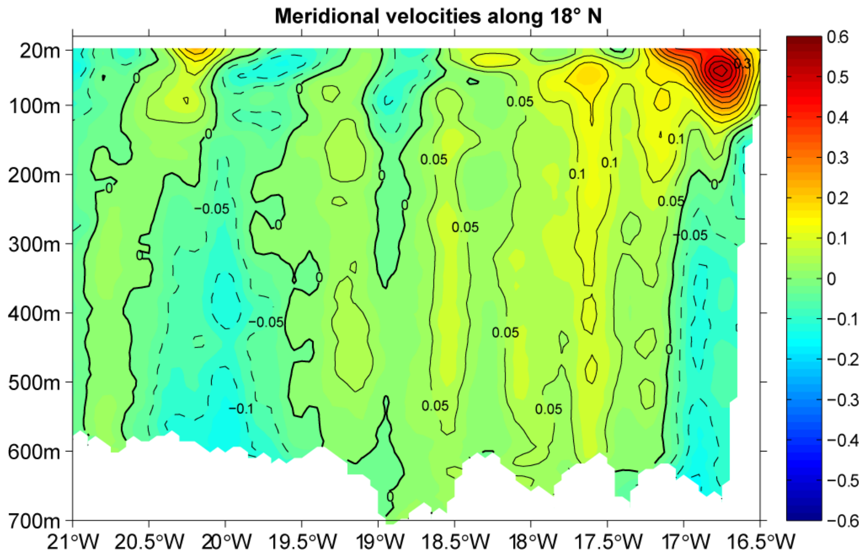

Fig. 4: Meridional velocity along the 18°N section as measured by the R/V Poseidon's Ocean Surveyor.

References:

Mittelsteadt, E. (1983) The upwelling Area off northwest Africa - a description of phenomena related to coastal upwelling. *Prog. Oceanogr.*, 12, 307–331.

Schafstall, J. (2010), Turbulente Vermischungsprozesse und Zirkulation im Auftriebsgebiet vor Nordwestafrika, *PhD Thesis thesis*, IFM-GEOMAR, Leibniz Institute for Marine Sciences, Kiel, 219 pp.

Schafstall, J., M. Dengler, P. Brandt, and H. Bange (2010), Tidal-induced mixing and diapycnal nutrient fluxes in the Mauritanian upwelling region, *J. Geophys. Res.*, 115, C10014, doi:10.1029/2009JC005940.

Stramma, L., P. Brandt, J. Schafstall, F. Schott, J. Fischer und A. Körtzinger (2008), Oxygen minimum zone in the North Atlantic south and east of the Cape Verde Islands. *J. Geophys. Res.*, 113. C04014, doi:10.1029/2007JC004369.

Tab. A1: Schedule and positions and of CTD /O_2 and MSS profiles collected during P399

Station No.	*Gear*	CTD/O_2 No.	Date Start UTC	Time UTC	Latitude Start		Longitude Start		Water depth	Max. pressure
305	CTD	1	02.06.2010	11:26	22° N	0.0'	21° W	0.0'	4328	507
305	MSS	1	02.06.2010	11:59	22° N	0.0'	21 °W	0.0'	4328	280
307	CTD	2	03.06.2010	21:56	17° N	36.0'	24 °W	18.0'	3598	509
307	MSS	2	03.06.2010	22:33	17 °N	36.0'	24 °W	18.0'	3598	254
307	MSS	3	04.06.2010	09:15	17 °N	36.0'	24 °W	18.1'	3598	270
307	CTD	3	04.06.2010	10:06	17 °N	36.0'	24 °W	18.0'	3598	3642
307	CTD	4	04.06.2010	12:48	17 °N	36.0'	24 °W	18.0'	3598	401
307	MSS	4	04.06.2010	13:16	17 °N	36.0'	24 °W	18.0'	3598	254
307	MSS	5	04.06.2010	16:54	17 °N	36.0'	24 °W	18.0'	3598	240
307	MSS	6	04.06.2010	21:10	17 °N	36.0'	24 °W	18.1'	3068	502
308	CTD	5	06.06.2010	17:06	18 °N	0.0'	21 °W	0.0'	3068	236

308	MSS	7	06.06.2010	18:07	18 °N	0.0'	21 °W	0.0'	3068	235
308	CTD	6	07.06.2010	06:43	18 °N	0.0'	21 °W	0.0'	3068	3094
308	CTD	7	07.06.2010	09:00	18 °N	0.0'	21 °W	0.0'	3156	303
308	MSS	8	07.06.2010	05:13	18 °N	0.0'	21 °W	0.1'	3068	212
308	MSS	9	07.06.2010	15:00	18 °N	0.0'	21 °W	0.0'	3068	212
309	CTD	8	08.06.2010	01:37	18 °N	0.0'	20 °W	0.0'	3192	503
310	CTD	9	08.06.2010	10:01	18 °N	0.0'	19 °W	0.0'	3150	504
311	CTD	10	08.06.2010	17:38	18 °N	0.0'	18 °W	0.0'	2810	505
311	MSS	10	08.06.2010	18:25	18 °N	0.0'	18 °W	0.0'	2810	275
311	CTD	11	09.06.2010	07:00	18 °N	0.0'	18 °W	0.0'	2801	2819
311	MSS	11	09.06.2010	08:50	18 °N	0.1'	18 °W	0.0'	2801	251
311	CTD	12	09.06.2010	09:56	18 °N	0.0'	18 °W	0.0'	2803	466
311	MSS	12	09.06.2010	15:25	18 °N	0.1'	18 °W	0.0'	2810	241
312	CTD	13	09.06.2010	20:38	18 °N	0.0'	17 °W	30.0'	2514	505
312	MSS	13	09.06.2010	21:10	18 °N	0.0'	17 °W	30.0'	2514	266
313	CTD	14	10.06.2010	01:26	18 °N	0.0'	17 °W	0.0'	1716	507
314	CTD	15	10.06.2010	04:01	18 °N	0.0'	16 °W	45.0'	988	506
315	CTD	16	10.06.2010	06:24	18° N	00.0'	16° W	30.0'	190	186
316	CTD	17	10.06.2010	10:51	18 °N	30.0'	16 °W	30.0'	98	92
316	MSS	15	10.06.2010	12:07	18 °N	29.9'	16 °W	30.1'	98	137
316	MSS	16	10.06.2010	18:07	18 °N	30.1'	16 °W	30.0'	92	117
316	CTD	18	10.06.2010	23:02	18 °N	30.0'	16 °W	30.0'	94	95
316	MSS	17	11.06.2010	09:34	18 °N	30.0'	16 °W	30.1'	95	102
317	CTD	19	11.06.2010	19:02	19 °N	0.0'	16 °W	34.1'	64	63
317	MSS	18	11.06.2010	19:20	19 °N	0.0'	16 °W	34.1'	64	67
317	CTD	20	12.06.2010	07:02	19 °N	0.1'	16 °W	34.1'	64	63
317	MSS	19	12.06.2010	08:36	19 °N	0.3'	16 °W	34.2'	64	68
317	MSS	20	12.06.2010	14:18	19 °N	0.1'	16 °W	34.2'	64	68
318	CTD	21	12.06.2010	20:00	19 °N	30.0'	17° W	0.0'	105	103
318	MSS	21	12.06.2010	20:28	19 °N	30.0'	16 °W	60.0'	105	108
319	CTD	22	13.06.2010	07:04	20 °N	0.0'	17 °W	15.0'	25	23
319	CTD	23	13.06.2010	17:11	20 °N	0.0'	17 °W	15.0'	25	23

7.2 P399/3: ESTOC water column sampling

Andres Cianca, Instituto Canario de Ciencias Marinas (ICCM), Telde, Gran Canaria, Spain; andres@iccm.rcanaria.es

ICCM was invited to participate in the Poseidon 399 leg 3 cruise with the aim to carry out the seasonal ESTOC sampling. ESTOC (European Station for Time-Series in the Ocean Canary Islands) was initialized as a cooperative project established by four research institutions: Institut für Meereskunde, Kiel (IFMK) and the Fachbereich Geowissenschaften der Universität Bremen (UBG) in Germany, and in Spain the Instituto Español de Oceanografía (IEO) and the Instituto Canario de Ciencias Marinas (ICCM). Observations started in 1994 (Llinás et al., 1994) and the objectives are maintained until nowadays. Many cruises have taken place to the north and east of the Canary Islands; among them it is worth mentioning those made within the European project CANIGO, ANIMATE and MERSEA. ESTOC is currently a Spanish open ocean observatory and internationally is belonging to the current European network “EuroSITES”.

7.2.1 Narrative of the ESTOC sampling with technical details

ESTOC sampling started on June 19th 2010 at 04:40 in the morning. The sampling was run in two profiles (shallow and deep). The equipment was a Seabird 911 plus CTD and a 12 bottles water sampler. The shallow and deep profiles ran along the depth ranges from surface to 600 m and from 600 to bottom, respectively. Temperature, conductivity, dissolved oxygen and chlorophyll were measured by the CTD, whereas samples of dissolved oxygen, nutrients (nitrate, phosphate and silicate), and pigments were taken to analyze on board (O_2, DINN, DIP, DISi) and ashore (DINN, DIP, DISi and pigments). Samples were collected immediately after the bottles were on board from each depth.

The sampling sequence was as follows: Oxygen: was taken in glass bottles of about 125 ml of volume which were previously cleaned and washed with HCl acid and was fixed at once; then it was kept for at least six hours according to WOCE regulations and finally it was analysed at the laboratory on board the ship by the tritation method described in the WOCE Operations Manual, WHP Office Report No. 68/91. The nutrients were taken in polypropylene bottles which were previously cleaned and washed with HCl acid and were completely dry. Samples were duplicated, the first ones were measured on board and the other were immediately frozen at -20°C, to analyze them as soon as possible ashore. The nutrient determination ashore was performed with a segmented continuous-flow autoanalyser, a Skalar® San Plus System in the ICCM laboratory. Freezing the samples is a common practice; it does not or only in a non-significant way affect the nitrate+nitrite and the phosphate values (by a slight decrease) and is not noticeable in the silicate values (Kremling and Wenck,1986; McDonald and McLunghlin, 1982).

Nitrate+Nitrite: The automated procedure for the determination of nitrate and nitrite is based on the cadmium reduction method; the sample is passed through a column containing granulated copper-cadmium to reduce the nitrate to nitrite (Wood et al.,1967), using ammonium chloride as pH controller and complexer of the cadmium cations formed (Strickland and Parsons, 1972). The optimal column preparation conditions are described by several authors (Nydahl, 1976; Garside, 1993).

Phosphate: Orthophosphate concentration is understood as the concentration of reactive phosphate (Riley and Skirpow,1975) and according to Koroleff (1983a) is a synonym of “dissolved inorganic phosphate”. The automated procedure for the determination of phosphate is based on the following reaction: ammonium molybdate and potassium antimony tartrate react in an acidic medium with diluted solution of phosphate to form an antimony-phospho-molybdate complex. This complex is reduced to an intensely blue-coloured complex, ascorbic acid. The complex is measured at 880nm. The basic methodology for this anion determination is given by Murphy and Riley (1962); the used methodology is the one adapted by Strickland and Parsons (1972).

Silicate: The determination of the soluble silicon compounds in natural waters is based on the formation of the yellow coloured silicomolybdic acid; the sample is acidified and mixed with an ammonium molybdate solution forming molybdosilicic acid. This acid is reduced with ascorbic acid to a blue dye, which is measured at 810nm. Oxalic acid is added to avoid phosphate interference. The used method is described in Koroleff (1983b).

Pigment samples of one liter of water were taken and duplicated. The chlorophyll samples were filtered inmediatelly and the filters were measured in a Turner fluorometer 10-AU-000 whereas pigment samples were filtered and frozen at -60°C to analyze by HPLC method, both ashore. The HPLC method used is that described by Wright et al. (1991).

7.2.2 Results

The biochemical samples were analyzed ashore and the values included in the ESTOC time-series. Similarly, the CTD data were validated and included in the ESTOC ctd time-series. Dissolved oxygen and chlorophyll values from the CTD were calibrated by a regression with the samples measured by winkler method and chlorophyll using a fluorometer, respectively.
The figure 1 shows the TS diagram and highlighted using the color bar the dissolved oxygen from the oxygen sensor attached to the CTD. The TS profiles shows typical values for this season in the upper waters (around 21ºC and 36.8 psu).In addition, the profile do not show any special signal from MEDDY structures. The dissolved oxygen minimum is located in the temperature- salinity range from 8º to 10ºC potential temperature and near 35 psu as common.

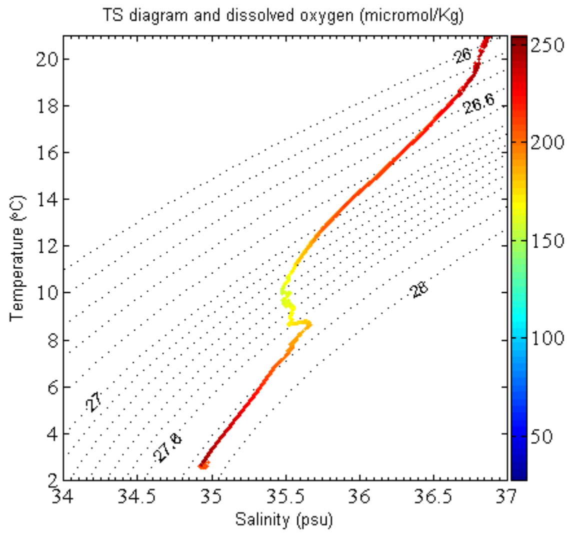

Figure 1. TS diagram from the CTD data. Dissolved oxygen is highlighted using the color bar.

A comparative experiment was carry out in order to compare nutrient measurements made in situ (analyzed by IFMK staff) and ashore (analyzed by ICC staff, conserved at -20ºC). The Figure 2 shows a good agreement between both data sets, with a very high root mean square values. Silicate samples appear to be a bit less stable in the coservation regarding the agreement between samples.

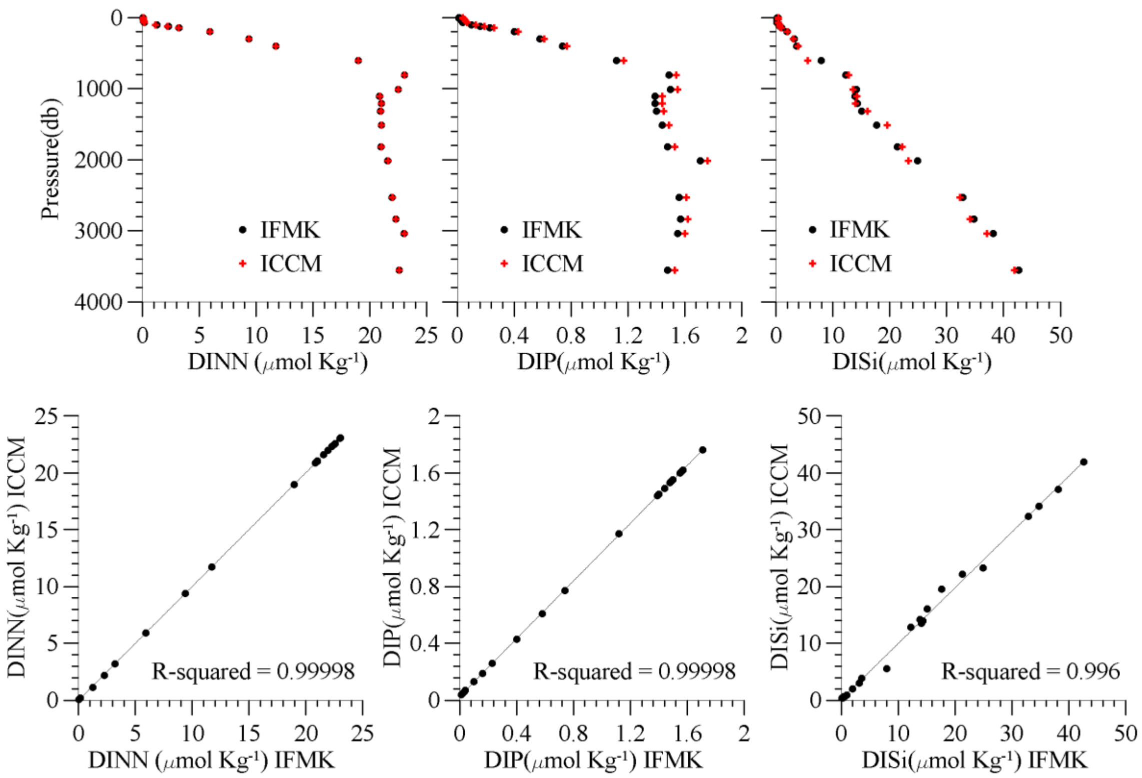

Figure 2. Upper plots from left to right show the DINN, DIP and DISi measured by IFMK and ICCM staff, respectively. Down plots show the regression between both analysis.

Finally, The Figure 3 A (see below) shows the comparative plots between dissolved oxygen values from the sensor attached to the CTD and those obtained by Winkler method from bottle samples. Previously, CTD was calibrated by a linear fit between both sample sets. We can observe electrical problems in the deep part of the profiles, likely motivated by a sensor malfunction due to the high pressure. Similarly for the chlorophyll results in the Figure 3 B (see below), the data from the sensor attached to the CTD was calibrated using the bottles samples measured with the fluorometer ashore.

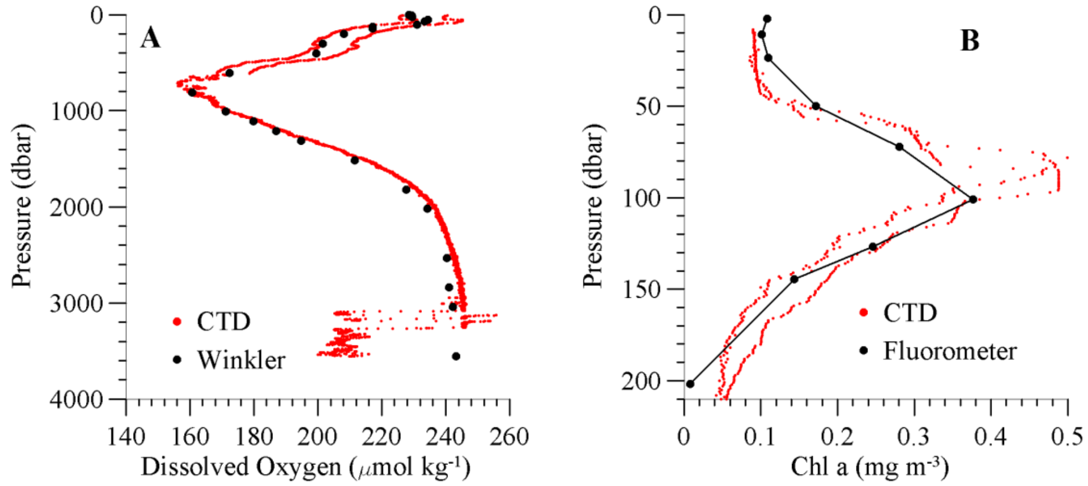

7.3 Dissolved nutrients and oxygen

Hermann W. Bange and Mirja Dunker, IFM-GEOMAR, Kiel; hbange@ifm-geomar.de

Dissolved nutrients (NO_3^-, NO_2^-, PO_4^{3-}, SiO_2) and oxygen (O_2) were measured according to the methods described in Grasshoff et al. (1999). The concentrations of dissolved nutrients and O_2 during P399/2 were in the same range as observed during previous SOPRAN/SOLAS cruises to the eastern tropical North Atlantic Ocean (ETNA): P320/1, M68/3, P348, and ATA03. The minimum O_2 concentration of 43.2 µmol L^{-1} was measured in the bottom layer (104 m) at CTD station # 21 on the shelf off Mauritania (19.5°N 17°W). O_2 profiles generally mirror the NO_3^- profiles (Figure 1: lower panel). At ESTOC nutrient concentrations in the in mid-water depths (i.e. thermocline – 2000m) were considerably lower compared to the nutrient concentrations measured in the ETNA (Figure 1). Accordingly O_2 concentrations in the mid-water depths at ESTOC were considerably higher compared to those found in the ETNA (Figure 1, lower panel). This is caused by the pronounced different hydrographic (see Figure 1: upper panel) and biogeochemical settings of ESTOC. The low nutrient concentrations observed at ESTOC indicate a pronounced oligotrophic status of the marine ecosystem.

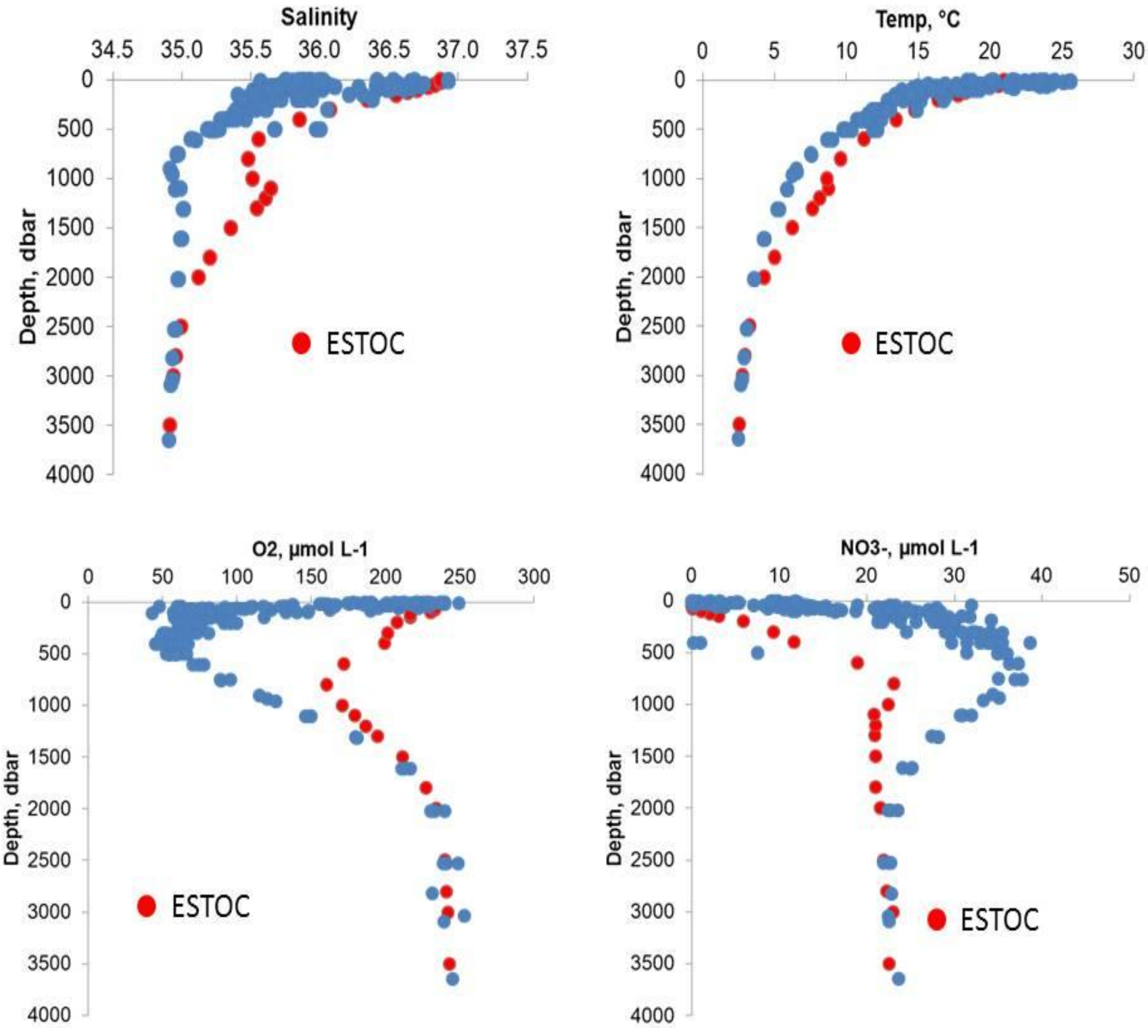

Figure 1: Depth profiles of salinity, temperature, O_2 and NO_3^- during P399/2 (blue dots) and P399/3 (ESTOC, red dots).

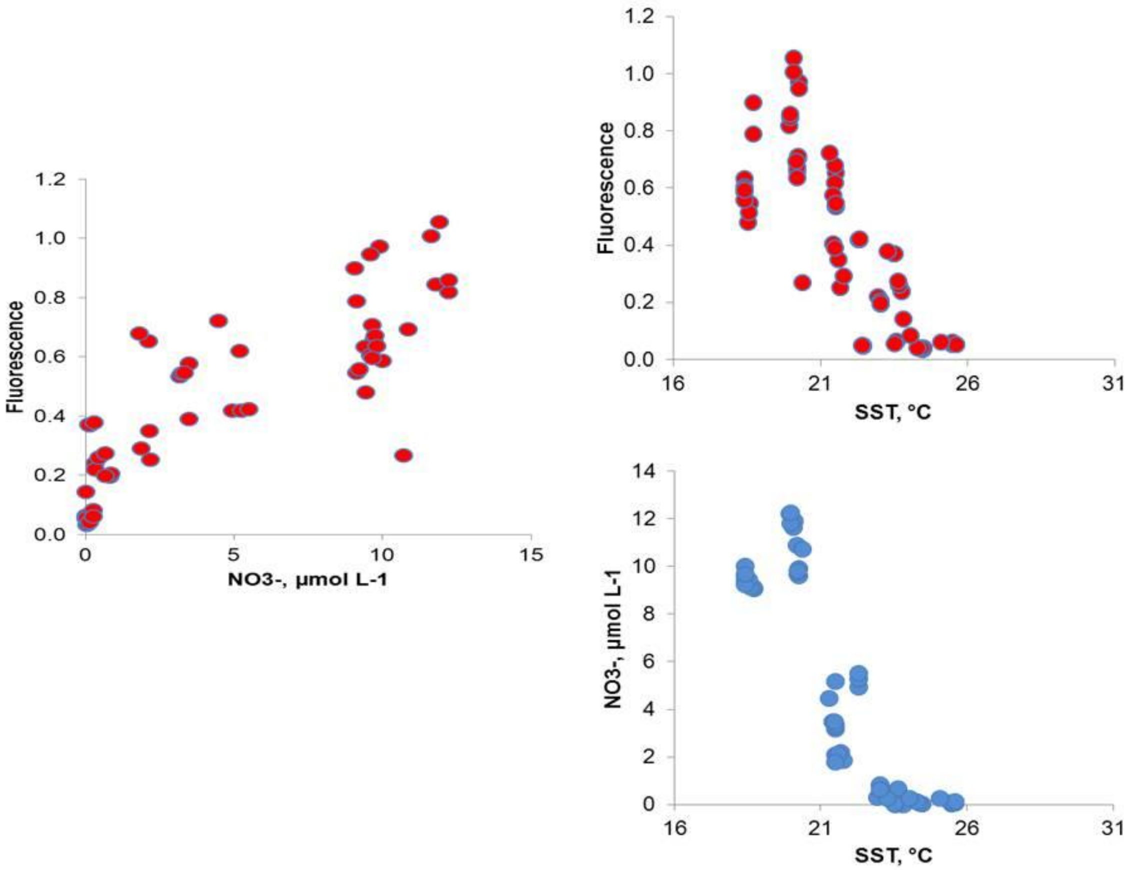

Figure 2: Dissolved NO_3^-, fluorescence (not calibrated, arbitrary units) and sea surface temperature (SST) in the surface layer (0-25m) in the ETNA/Mauritanian upwelling during P399/2.

The upwelling along the Mauritanian coast was clearly visible in the temperature nutrient and fluorescence data from the mixed layer (see Figure 2), here defined as 0–25m. In the open ocean of the ETNA surface temperatures were as high as 26°C. In the upwelling along the Mauritanian coast water temperatures dropped to 18.4°C. The decrease in the water temperature was associated with an increase in nutrients (NO_3^- and PO_4^{3-}) and fluorescence (which can be taken as a rough indicator for chlorophyll/productivity). It is worth to note that the max. values of NO_3^- and fluorescence are not associated with the min. water temperatures (Figure 2, right panel) despite the fact that fluorescence and NO_3^- were well correlated (Figure 2, left panel). This might indicate different source water masses which have been upwelled along the coast. The min. surface water temperatures of 18.4°C were measured at the most northern station (CTD station # 22) at 20°N 17.25°W.

Reference

Grasshoff, K., et al. (1999), *Methods of seawater analysis*, 3rd ed., 600 pp., Wiley-VCH, New York.

7.4 Phytoplankton biomass and group composition by marker pigments

Ilka Peeken, AWI/MARUM, Bremerhaven/Bremen, ilka.peeken@awi.de

7.4.1 Work during cruise

For the determination of pigments, 1 L of sea water was filtered onto 25 mm Whatman GF/F filters with a pressure of less than 120 mbar. After filtration, the filters were folded and stored in 2 ml micro centrifuge tubes (Eppendorf cups) at -80 °C until analysis. Samples were taken from the surface pump system (n = 103) and CTD casts. For the CTD casts the upper 150 m were sampled with usually 8 depths (n = 96). Only close to the coast the number of samples was reduced to minimum of four samples according to the shallow water depth.

7.4.2 Pigment measurements

Samples were measured using a Waters HPLC-system, equipped with an auto sampler (717 plus), pump (600), PDA (2996), a fluorescence detector (2475) and EMPOWER software. For analytical preparation, 50 µl internal standard (canthaxanthin) and 1.5 ml acetone were added to each filter sample and then homogenised for 20 seconds in a PRECELLYS cell homogenisatior. After centrifugation, the supernatant liquid was filtered through a 0.2µm PTFE filter (Rotilabo) and placed in Eppendorf cups and an aliquot (100 µl) were transferred in the auto sampler (4°C). Just prior to analysis the sample was premixed with 1 M ammonium acetate solution in the ratio 1:1 (v/v) in the auto sampler and injected onto the HPLC-system. The pigments were analysed by reverse-phase HPLC, using a VARIAN Microsorb-MV3 C8 column (4.6x100mm) and HPLC-grade solvents (Merck). For further details see Hoffmann et al (2006). For correction of experimental losses and volume changes, the concentrations of the pigments were normalised to the internal standard, canthaxanthin. This method separates chlorophyll a and divinyl chlorophyll a as well as lutein and zeaxanthin completely. Chlorophyll b and divinyl chlorophyll b are also distinguishable from each other, but they are not baseline separated. Chlorophyll a and divinyl chlorophyll a are combined to total chlorophyll a (TChl a) to obtain a measure for the total amount of phytoplankton biomass in the sample. The taxonomic structure of phytoplankton communities was derived from photosynthetic pigment ratios using the multiple regression approach by Uitz, et al. (2006). The phytoplankton group composition is expressed in chlorophyll a concentrations.

7.4.3 Preliminary results:

Surface phytoplankton biomass (here shown as total chlorophyll a (chla; the sum of divinyl chl a and chl a) only reaches values above 1 µg/L in the Mauritanian upwelling area where total chlorophyll a values with a maximum of 11 µg/L were observed (Fig. 1 left). This biomass maximum is mainly consisting of diatoms determined with marker pigments. Divinyl chlorophyll a, the unique marker of prochlorophytes (Goericke and Repeta 1992) reaches only concentrations below 0.2µg/L and is a typical inhabitant of the oligotrophic water masses during this cruise (Fig. 1 right).

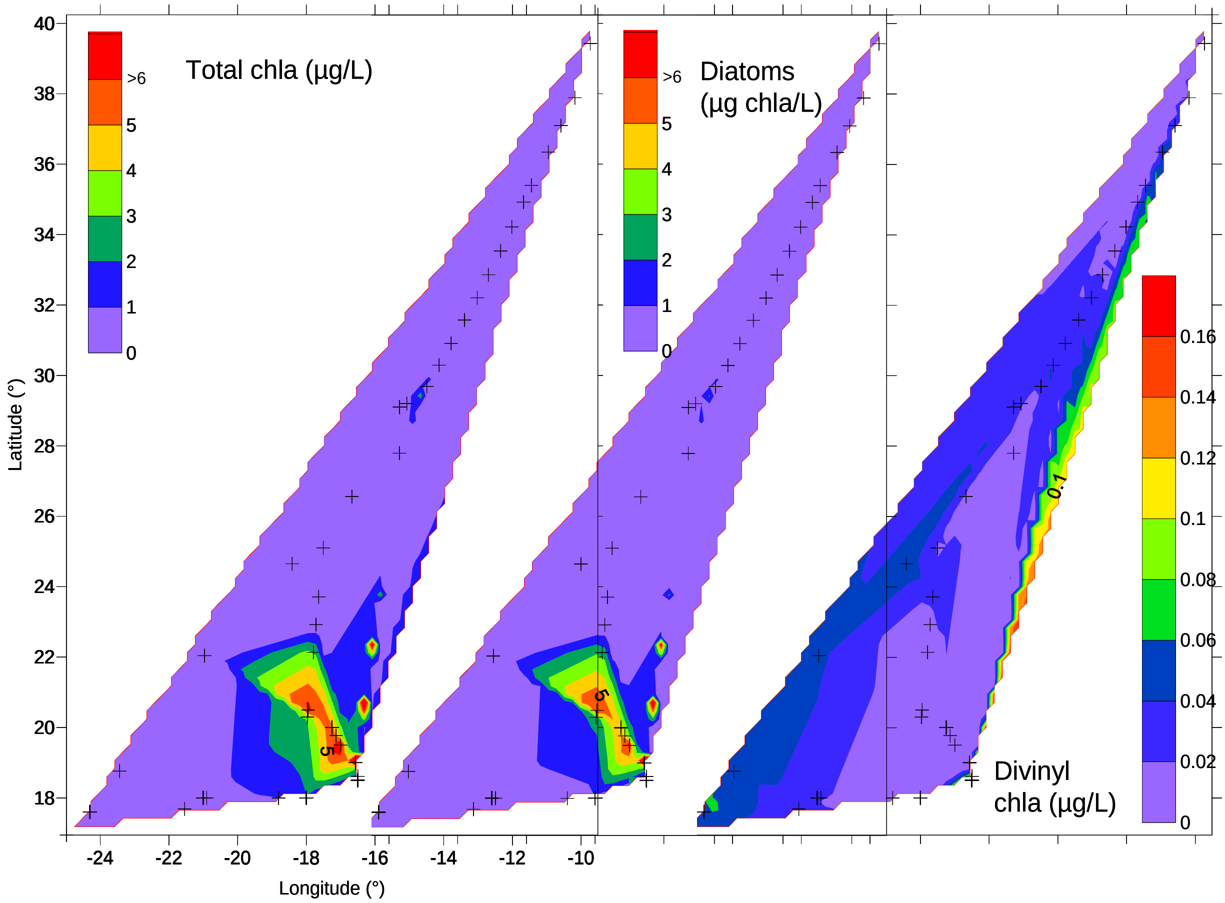

Figure 1: Surface contour maps of of all measured surface samples (5 and 6m) along the cruise track and on stations for total chlorophyll a (µg/L, left), diatoms (expressed in chla/L, middle) and divinyl chla (µg/L, right). The middle and right panel are inserted in the left figure and have the same x and y-axes. Crosses indicate sampling location.

A transect S-N station from the oligotrophic ocean into the upwelling region towards shallower water depth indicate the highest biomass closest to the coast with maximum concentrations > 6µg/L (Fig. 2). As already evident for the underway surface water samples, diatoms clearly dominate the high biomass at all depth horizons, reaching maximum concentrations of 5µg chla/L. In contrast, divinyl chla is mostly abundant in a subsurface maximum further south. Absolute biomass of all other phytoplankton is much lower (< 0.3 µg chla/L) but with different patterns e.g. for the three groups of autotroph dinoflagellates, haptophytes and Synecococcus-type cyanobacteria (Fig. 3). While dinoflagellates also inhabit the upwelling region, the haptophytes and Synecococcus are more abundant in the mixed water masses between the oligotrophic and upwelling regions in the middle of the S-N transect. While Synecococcus mainly exist in the surface ocean, haptophytes also show a deep maximum in 80 m in the oligotrophic deep chlorophyll maximum, which is also inhabited by prochlochlorophytes as is evident from slightly higher divinyl chla concentrations in this regions.

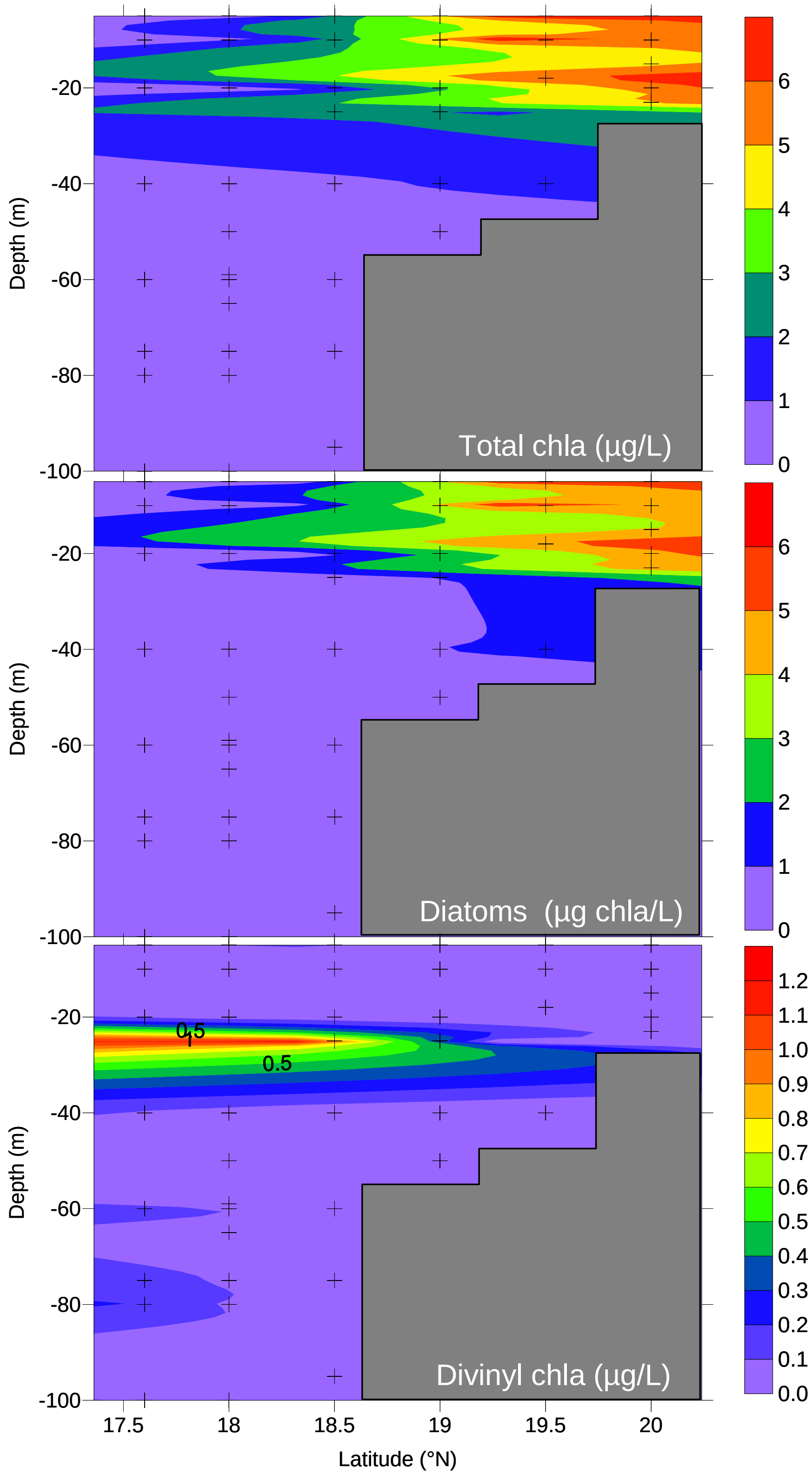

Figure 2: South-North transect ending on the shallow shelf for total chlorophyll a (µg/L, top), diatoms (expressed in chla/L, centre) and divinyl chla (µg/L, bottom). Crosses indicate sampling.

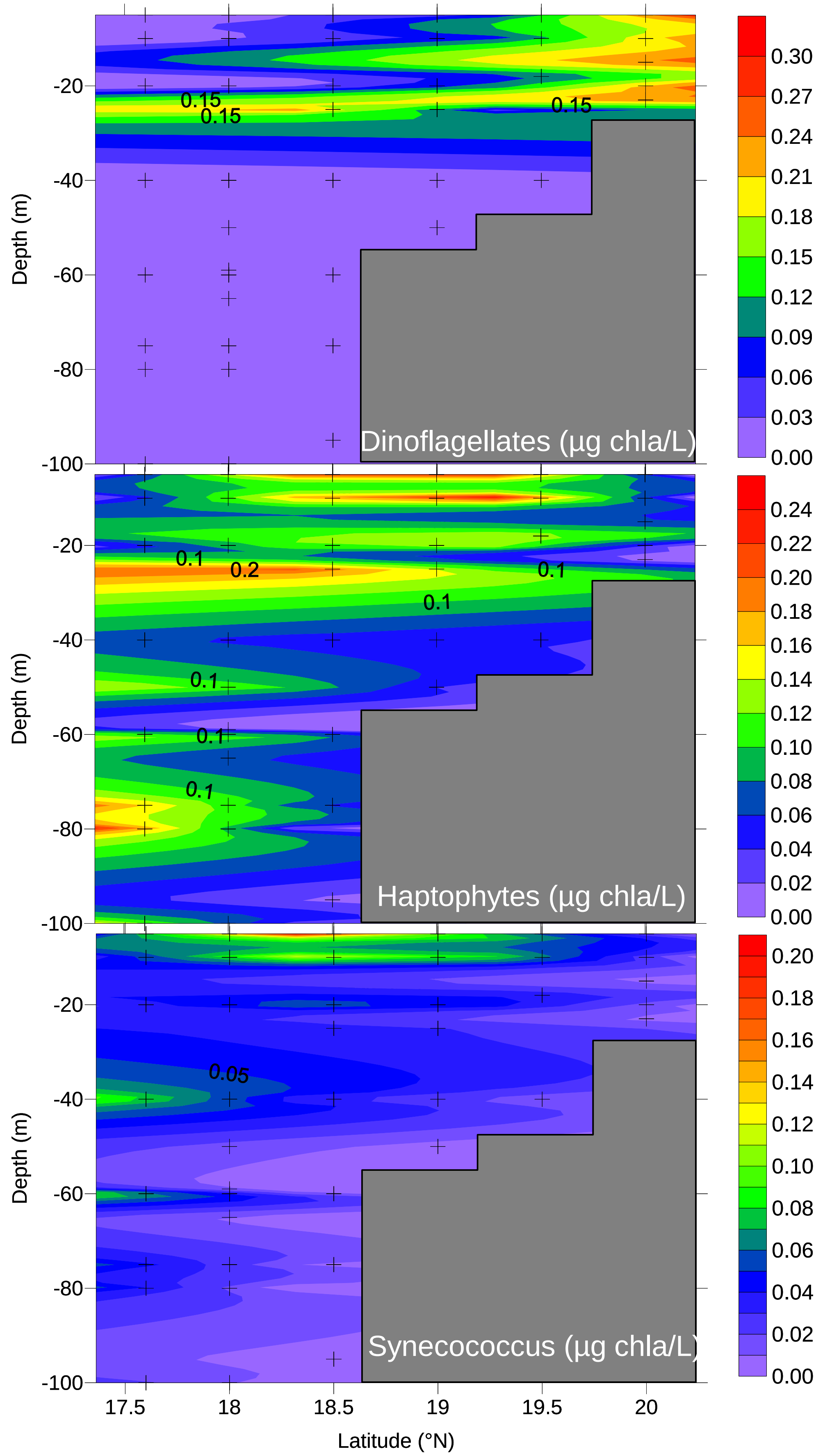

Figure 3: South-North transect ending on the shallow shelf for dinoflagellates (expressed in chla/L, top), haptophytes (expressed in chla/L, centre) and Syneccoccus (expressed in chla/L, bottom). Crosses indicate sampling.

In summary during this cruise diatoms mainly benefit from the upwelling of the coast of Mauretania as has already been observed during other seasons (Franklin et al. 2009; Quack et al. 2007). The occurrences of cyanobacteria including prochlorphytes are typical for the oligotrophic tropical Atlantic. Within the mixed water masses, a succession towards haptophytes is evident as has previously been reported by Barlow et al. (1993) and might have major implications for the DMS cycling (Franklin et al. 2009). Also the concentrations of autotroph dinoflagellates are low, they might also contribute significantly to the DMS production as has been previously reported for the Mauritanian upwelling (Zindler et al. 2011).

References

Barlow, R. G., R. F. C. Mantoura, M. A. Gough, and T. W. Fileman. 1993. Pigment signatures of the phytoplankton composition in the northeastern Atlantic during the 1990 spring bloom. Deep-Sea Research II **40:** 459-477.

Franklin, D., J. A. Poulton, M. Steinke, J. Young, I. Peeken, and G. Malin. 2009. Dimethylsulphide, DMSP-lyase activity and microplankton community structure inside and outside of the Mauritanian upwelling. Prog Oceanogr **83:** 134–142.

Goericke, R., and D. J. Repeta. 1992. The pigments of *Prochlorococcus marinus*: The presence of divinyl chlorophyll *a* and *b* in a marine procaryote. Limnol Oceanogr **37:** 425-433.

Hoffmann, L., I. Peeken, K. Lochte, P. Assmy, and M. Veldhuis. 2006. Different reactions of Southern Ocean phytoplankton size classes to iron fertilization. Limnol Oceanogr **51:** 1217-1229.

Quack, B., G. Petrick, I. Peeken, and K. Nachtigall. 2007. Oceanic distribution and sources of bromoform and dibromomethane in the Mauritanian upwelling. J Geophys Res-Oceans **112:** doi:10.1029/2006JC003803.

Uitz, J., H. Claustre, A. Morel, and S. B. Hooker. 2006. Vertical distribution of phytoplankton communities in open ocean: An assessment based on surface chlorophyll. J Geophys Res-Oceans **111:** -.

Zindler, C., I. Peeken, C. A. Marandino, and H. W. Bange. 2011. Environmental control on the variability of DMS and DMSP in the Mauritanian upwelling region. Biogeosciences Discussion, in preparation.

7.5 Phytoplankton charcterization via flow cytometry – comparisons to phytoplankton satellite data

Astrid Bracher, Bettina Taylor, Tilman Dinter, AWI, Bremerhaven;
astrid.bracher@awi.de

7.5.1 Description of the performed measurements

To assess the phytoplankton group composition at the waters studied during P399, measurements on water samples were performed. While Ilka Peeken (AWI) measured the pigment composition of all phytoplankton via HPLC technique (see section 7.4), our group measured with flow cytometry the composition of the pico- and nanoplankton and also took samples for microscopic analysis of the micro- and nanophytoplankton. Water samples were taken during the ship's steaming from the surface water only at 104 different stations and from the rosette water sampler at 8 profile-resolved CTD stations from 4 to 9 different depths. To expand these data sets spatially and temporarily, satellite measurements of phytoplankton composition and concentration are necessary which require verification by in-situ data, as the ones obtained during this cruise.

7.5.2 Flow cytometry

Samples for flow cytometry were preserved with 0.1% glutaraldehyde (final concentration), shock-frozen in liquid nitrogen and stored at -80°C. Back in the lab at AWI, phytoplankton cells were enumerated from preserved and frozen, unstained samples by using their specific chl *a* and phycoerythrin autofluorescence according to Marie et al. (2005). Both chl *a* and phycoerythrin are excited with the common 488-nm excitation line and fluoresce at 690nm (red) and 570nm (orange), respectively. Flow cytometry was performed on a FACScalibur with an excitation beam of 488 nm, two light scatter detectors at 180° (forward scatter) and at 90° (side scatter) and several photomultipliers detecting at 530nm (beads), 585nm (orange fluorescence) and 670nm (red fluorescence). Phytoplankton groups were separated according to their red and orange fluorescence and scattering characteristics. Yellow-green Fluoresbrite® Microspheres with a diameter of 1µm (Polysciences) were used as an internal standard. The data were analysed with the instrument software “CellQuest”. Using the carbon content approximations for prokarotic and eukaroytic cells by Charpy and Blanchot (1998) and Verity (1992), respectively, the carbon conc. in each sample was determined for each group using the information of average cell size and number of cells of the specific groups. As specific groups, nano- and picoeukaryotic, Prochlorococcus- and phycoerythrin-containing prokaryotic phytoplankton were identified.

7.5.3 Microscopy

Samples were fixated with 2% buffered formaldehyde (end concentration) and stored in brown glass bottles in a dark, cool and dry place. These samples still have to be analyzed at our lab, we will follow this method for analysis: the samples are introduced into a settling chamber and the phytoplankton is allowed to settle for 48 h. Phytoplankton cells are then identified and counted by the Utermöhl method (Utermöhl, 1958, Edler, 1979) using a Zeiss IM35 inverted microscope equipped with phase contrast and 400x magnification.

7.5.4 Phytoplankton satellite data

Biomass distributions of different dominant PFTs (Phytoplankton Functional Types; with 30 km by 60 km spatial resolution) were derived from measurements of the satellite sensor SCIAMACHY on ENVISAT analyzed with PhytoDOAS, a method of Differential Optical Absorption Spectroscopy (DOAS) specialized for diatoms and cyanobacteria (Bracher et al. 2009). This method has been improved for detecting four different types of PFTs by using simultaneous fitting of the differential specific absorption spectrum of each PFT to the satellite measurement (Sadeghi et al., revised). These PFTs are diatoms, cyanobacteria, dinoflagellates and coccolithophores. For the time period and region of the cruise, maps of the four phytoplankton groups using the PhytoDOAS method on SCIAMACHY data were produced as one month average. In addition, also the total phytoplankton concentration (i.e. total chl-a) was derived from the merged SeaWiFS-MODIS-MERIS total chl-a product GlobColour (http://hermes.acri.fr) for the same time period and region (see Fig. 1) which has a higher spatial resolution of 4.6 km by 4.6 km.

7.5.5 First results of phytoplankton groups and total biomass distributions during the cruise

Figures 1 and 2 show maps of the underlying monthly mean for June 2010 of total biomass from satellite data with the in-situ data on the surface carbon content from flowcytometry data measured at P399 stations for the various phytoplankton groups.

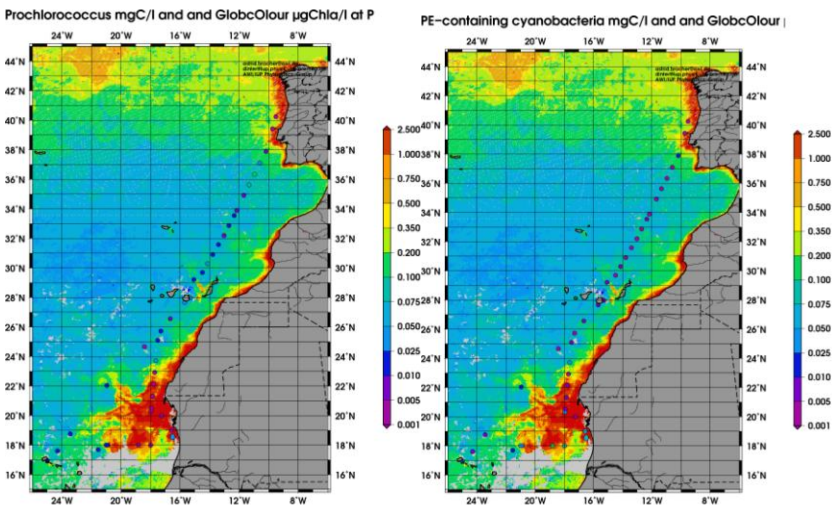

Figure 1: Color coded Chl-a concentration in [µg/l] as a monthly mean of June 2010 from GlobColour CHL1 product for the area around Poseidon P399 cruise with the carbon conc. in [mg/l] for Prochlorococcus (left) and phycoerythrin-containing cyanobacteria (right) measured at P399 surface water stations with flow cytometry.

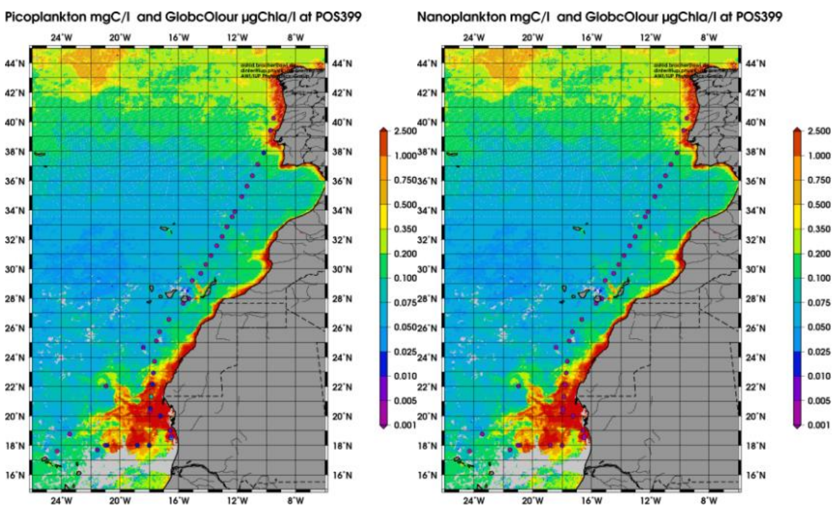

Figure 2: As Fig. 1 but for picoeukaroytic (left) and nanoeukaryotic phytoplankton (right).

The overall satellite chl-a map shows two blooms, one south at the African Coast which extends into the open ocean between 17°-23°N latitude, and one in the north, at the coast along Portugal. The flow cytometry data on carbon conc. show that the southern bloom does not consist of Prochlorococcus-type cyanobacteria and eukaryotic nanoplankton, but of picoeukaryotes and also at the south end of this bloom of elevated phycoerythrin containing cyanobacteria. All four groups have low carbon conc. in the northern bloom and in the low chl-a areas of the open ocean, except for Prochlorococcus. This group contributes as the highest to the carbon conc. in all oligotrophic open ocean waters south of 38°N. The PFT satellite data (Fig. 3) indicate that the blooms close to the coast are dominated by diatoms, which cannot be detected via flow cytometry because they belong to the microplankton, while off the coast in the bloom around 17°N-23°N coccolithophores are dominating. Satellite chl-a data of cyanobacteria (all prokaryotic phytoplankton) are low in the whole region (<0.025µg/l), while dinoflagellates chl-a provide a background conc. of 0.1 µg/l north of 17°N (results not shown). Coccolithophores can belong to the nano- (2-10µm) or the picoplankton (of about 1-2 µm) which conincides with the elevated picoeukarotic carbon content seen in the flowcytometric data from the offshore blooming areas. The satellite and flow cytometry results will be cross- checked with the microscopic and the pigment data, which give insight on the nano- and micro-phytoplankton composition and the overall distributions of phytoplankton groups regardless of their size composition, respectively.

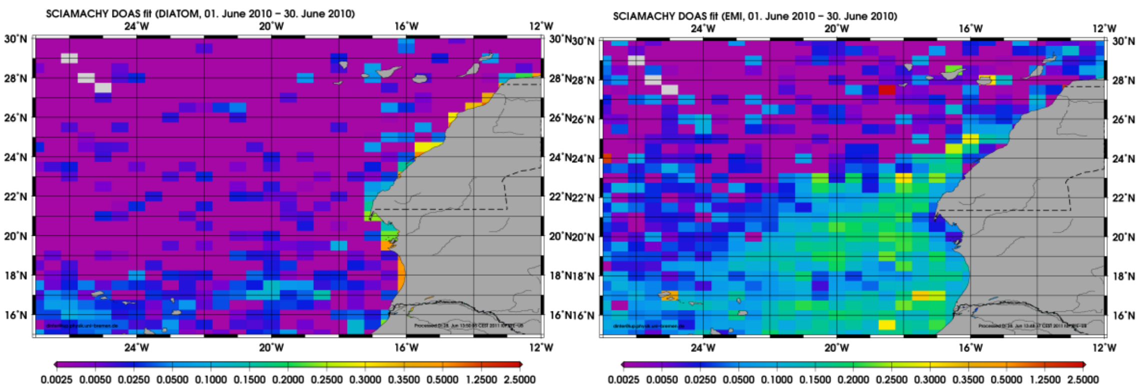

Figure 3: Chl-a concentration of coccolithophores (left) and diatoms (right) in [µg/l] as a monthly mean of June 2010 from PhytoDOAS retrieval using SCIAMACHY data in the area around P399.

References

Bracher A, Vountas M, Dinter T, Peeken I, Röttgers R, Burrows JP (2009) Quantitative observation of cyanobacteria and diatoms from space using PhytoDOAS on SCIAMACHY data. Biogeosciences 6: 751-764

Charpy L, Blanchot J (1998) Photosynthetic picoplankton in French Polynesian atoll lagoons: estimation of taxa contribution to biomass and production by flow cytometry. MEPS 162: 57-70

Sadeghi A, Dinter T, Vountas M, Taylor B, Peeken I, Bracher A (revision submitted 4 Juy 2011) Improvements to the PhytoDOAS method for the identification of major Phytoplankton groups using high spectrally resolved satellite data. Advances in Space Research

Verity PG, Robertson CY, Tronzo CR, Andrews MG, Nelson JR, Sieracki ME (1992) Relationship between cell volume and the carbon and nitrogen content of marine photosynthetic nanoplankton. Limno. Oceanogr. 37 (7): 1434-1446

7.6 Dissolved nitrous oxide (N_2O)

Hermann W. Bange, Carolin Löscher, Annette Kock, Marita Krumbholz, Maya Beyer; IFM-GEOMAR, Kiel; hbange@ifm-geomar.de

7.6.1 Depth profiles

N_2O depth profiles were measured according the method described in Walter et al. (2006): Triplicate water samples from each CTD depth were poisoned with $HgCl_2$ and then equilibrated at least 2h with a helium headspace. A 10 ml subsample from the headspace was used to flush a 2ml sampling loop. The injected gas samples were separated on packed column (5A molesieve) and N_2O was detected with an electron capture detector (ECD).

The N_2O depth profiles (Figure 1) showed maximum concentrations of up to 35 nmol L^{-1} in the oxygen minimum zone (OMZ) in water depths of about 400-500m.The N_2O profiles are mirrored by the O_2 profiles (Figure 1) nicely illustrating the well-known inverse relationships between O_2 and N_2O concentrations, on the one hand, and NO_3^- and N_2O, on the other hand (Figure 2). Since O_2 was far above the threshold for the onset of denitrification (5-20 µmol L–1), we conclude that N_2O in the ETNA is produced during nitrification (see also section 7.7: Biological sources of N_2O). The measurements during P399/2 are comparable to results from previous ship campaigns in the ETNA (M68/3, P348). O_2 concentrations in the OMZ at the ESTOC were considerably higher which is reflected by the lower N_2O concentrations measured at ESTOC (Figure 1), c.f. section 7.3: Dissolved nutrients and oxygen.

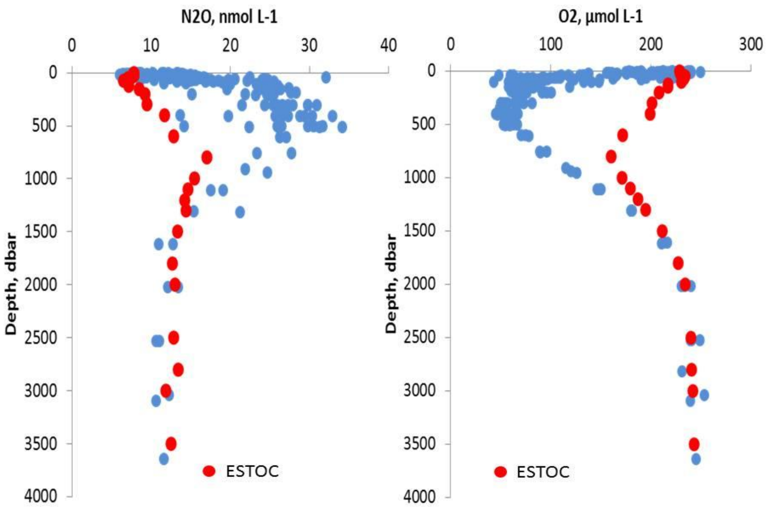

Figure 1: Depth profiles of N_2O and O_2 during P399/2 (ETNA, blue dots) and during P399/3 (ESTOC, red dots).

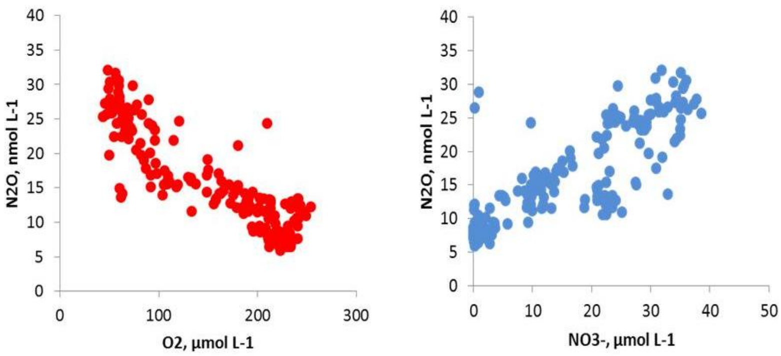

Figure 2: N_2O, O_2 and NO_3^- in the ETNA during P399/2 and at ESTOC during P399/3.

7.6.2 Underway surface measurements

The N_2O concentrations in the surface layer were determined with an underway GC/ECD-system which was connected to a Weiss-type shower head equilibrator (see Walter et al. (2004) and Bange et a. (1996)). The seawater was pumped by a submersible pump installed in the ship's moonpool. The water depth of the pumped water was about 3m. Please note that N_2O surface measurements were only performed during P399/2 (Las Palmas-Mindelo-Las Palmas) and not during P399/3 (Las Palmas-Vigo).

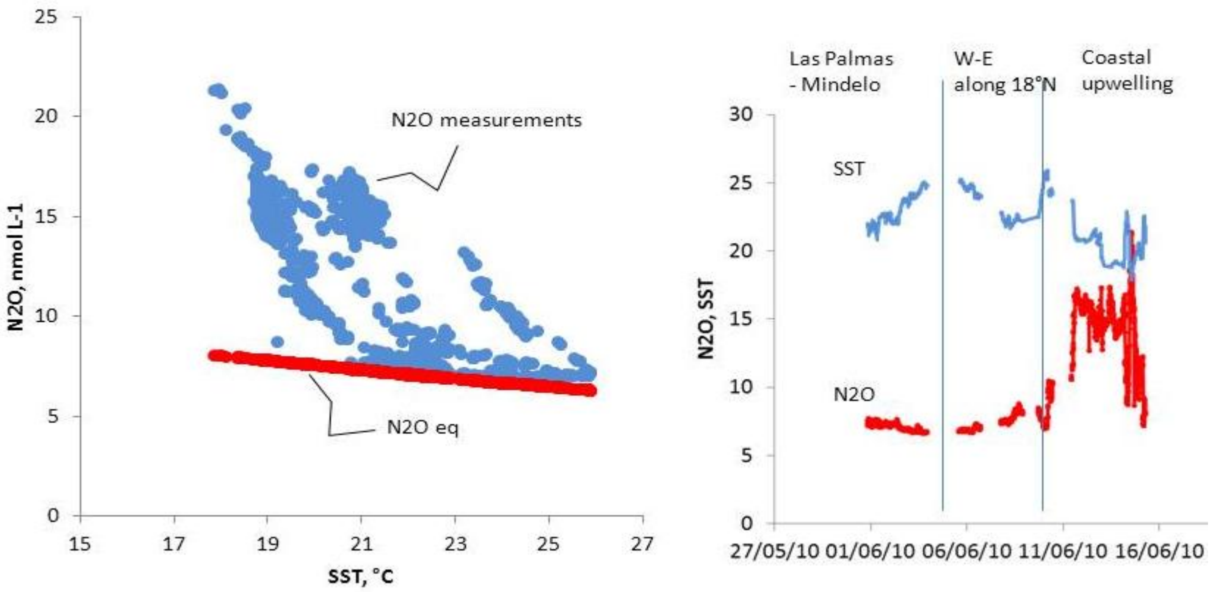

Figure 3: Surface N_2O and SST during P399/2: left figure shows both measured N_2O concentrations (blue dots) and calculated equilibrium concentrations (red dots; N_2O_{eq}). N2Oeq was calculated based on the atmospheric N_2O dry mole fraction (323-324 ppb) measured during P399/2.

N_2O was supersaturated during P399/2 indicating that the ETNA was a source of N_2O to the atmosphere during P399 (Figure 3, left). The max. N_2O concentration was 21.3 nmol L^{-1} (= 267% saturation) and was observed at 20.77°N 17.93°W in the coastal upwelling off Mauritania (SST = 17.9°C). Enhanced N_2O concentrations at the coast were associated with the decrease SST in the coastal upwelling off Mauritania (Figure 3, right). This is in agreement with previous findings (from P320/1 and P348) and underlines the fact that the coastal area off Mauritania is a significant source of atmospheric N_2O during the upwelling season.

References

Bange, H. W., et al. (1996), The Aegean Sea as a source of atmospheric nitrous oxide and methane, *Marine Chemistry*, *53*, 41-49.

Walter, S., et al. (2006), Nitrous oxide in the North Atlantic Ocean, *Biogeosciences*, *3*, 607-619.

Walter, S., et al. (2004), Nitrous oxide in the surface layer of the tropical North Atlantic Ocean along a west to east transect, *Geophysical Research Letters*, *31*, L23S07, doi:10.1029/2004GL019937.

7.7 Biological sources of dissolved nitrous oxide

Carolin Löscher, Institut für Allgemeine Mikrobiologie, Universität Kiel;
cloescher@ifam.uni-kiel.de

To study the biological source of nitrous oxide (N_2O) in the eastern tropical North Atlantic, a molecular genetic approach (PCR detection, qPCR, and sequencing) was combined with incubation experiments and high resolution measurements of N_2O (see also section 7.6.).

7.7.1 Performed measurements and sampling

7.7.1.1 Sampling

Samples for DNA/RNA extraction were taken at 10 stations by filtering a volume of about 1 L (exact volumes were recorded continuously) of seawater from 6-12 depths through 0.2 µm polyethersulfon membrane filters (Millipore, Billerica, MA, USA). The filters were immediately frozen and stored at -40°C. Specific RNA samples were treated with a RNA stabilizing agent before freezing.
DNA and RNA was extracted using the Qiagen DNA/RNA All prep Kit (Qiagen, Hilden, Germany) according to the manufacturers protocol.
As archaeal nitrifiers were hypothesized to be key producers of N_2O quantitative and phylogenetic screening studies concentrated on archaeal *amoA* as a functional marker. However, standard PCR screening was performed for bacterial *amoA* and the key gene of denitrification *nirS*. PCR and quantitative PCR conditions were chosen according to Löscher *et al.* (2011, submitted).

7.7.1.2 Seawater incubations

In order to quantify the N_2O production over time, seawater incubations were performed on board. 25mL serum bottles were filled with seawater from the OMZ (200- 250m) from the CTD, closed with an air-tight butyl rubber stopper and aluminium crimp-capped (comparable to N_2O samples). To identify the source of N_2O (bacterial archaeal nitrifiers), antibiotics to inhibit bacteria as well as the archaeal hypusination inhibitor *N*1-guanyl-1,7-diaminoheptane (GC_7) were used. Incubations were kept for the duration of the experiment (24h) in the dark at 8°C. The experiment was stopped by $HgCl_2$ addition, followed by the determination of the final N_2O concentrations.

7.7.2 Results

7.7.2.1 Molecular genetic studies

The archaeal *amoA* gene encoding for the alpha subunit of the ammonia monooxygenase was detected throughout the water column (Fig. 1) whereas copy numbers of bacterial *amoA* were negligible; maximum abundances were associated with low O_2 concentrations and high N_2O concentrations in samples from the upwelling system off Mauritania (Fig. 2). Contrastingly, samples from the ESTOC station showed high archaeal *amoA* abundances at comparably high O_2, while N_2O followed a similar trend as in the other samples. Phylogenetic analyses demonstrated that archaeal *amoA* sequences derived from ESTOC form a distinct cluster within cluster A of *Thaumarchaeota*. The genetic difference might result in a different behaviour for N_2O production.

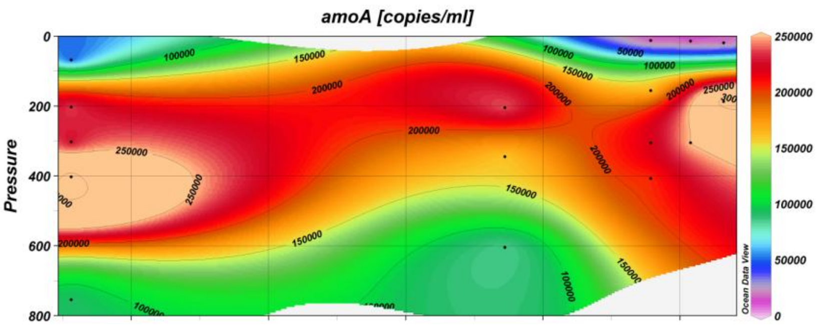

Fig. 1: Archaeal *amoA* along 18°N detected by qPCR, data points represent two technical replicates

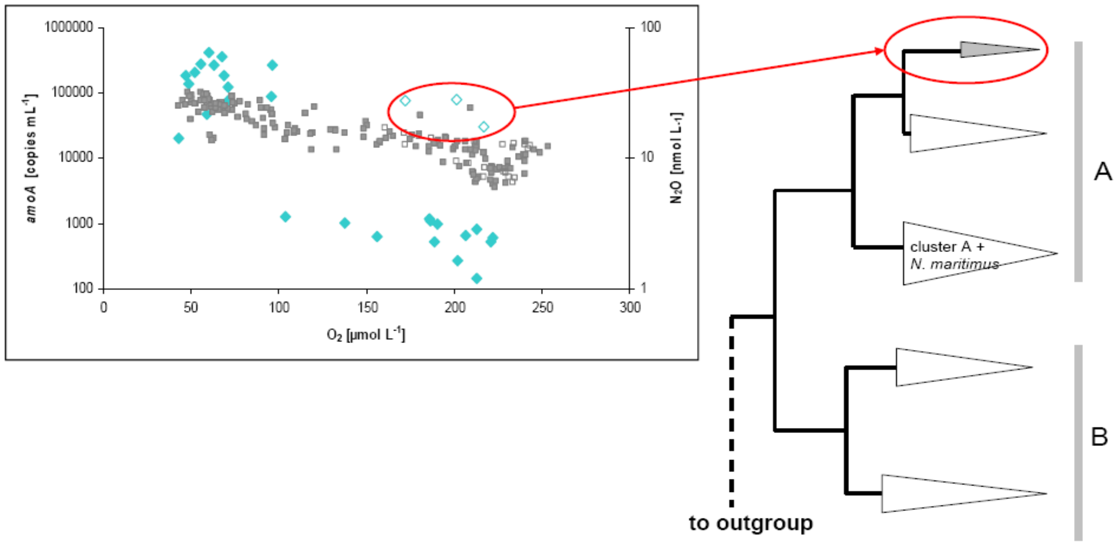

Fig. 2: Archaeal *amoA* and N_2O at present O_2 concentrations, open rectangles indicate samples from the ESTOC station, closed samples were derived from other stations. Distance-based neighbour-joining phylogenetic analysis of archaeal *amoA* sequences showed the typical clustering in clusters A and B, within cluster A sequences from ESTOC formed a distinct sub-cluster (grey triangle).

7.7.2.2 Seawater incubations

24h seawater incubations performed at three different stations in the ETNA showed significantly lower N_2O production in samples treated with N^1-guanyl-1,7-diaminoheptane (GC_7), a hypusination inhibitor shown to selectively inhibit the cell cycle of archaea (Fig. 3). In one experiment (18°N, 16.5°W) a similar trend was observed, however it was lacking a clear statistical significance. N_2O production seems therefore due to archaeal activity.

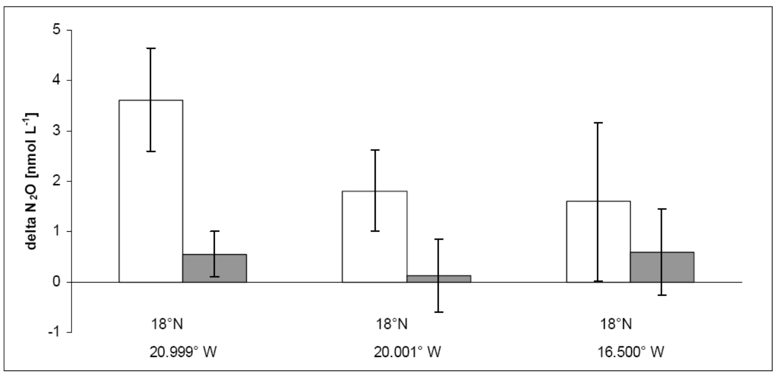

Fig. 3: N_2O production as delta N_2O determined from seawater incubations at three different stations. Delta N_2O was calculated as the difference of N_2O concentrations over the incubation time (24h). Open columns represent samples with no GC_7 inhibitor, filled columns represent samples with GC_7 inhibitor. Error bars indicate the standard deviation of three technical replicates

7.8 Underway measurements of dissolved CO_2, oxygen and total gas pressure

Tobias Steinhoff, IFM-GEOMAR, Kiel; tsteinhoff@ifm-geomar.de

On Poseidon cruise P399 legs 2 and 3 we ran several underway instruments to measure the following parameters: dissolved oxygen, total gas pressure of all dissolved gases and partial pressure of CO_2 (pCO_2). The instruments were fed with a seawater flow from a submersible pump that was installed in the ships moonpool (~ 3m depth). The pCO_2 system was directly connected to the water line while the other sensors were put in a bath (Coleman® cooling container) that was flushed with the seawater.

7.8.1 Underway measurements

7.8.1.1 pCO_2

The pCO_2 was measured with a GO pCO_2 instrument that is described in detail in Pierrot et al. (2009). The equilibrator contains a water spray head, and as the water flows through it the dissolved CO_2 equilibrates with the headspace. The headspace is dried and xCO_2 is determined by an infrared sensor (Licor, LI-7000). The pCO2 data were calibrated against standard gases. The accuracy of the pCO_2 data is estimated to be ±2µatm.

7.8.1.2 Oxygen

Dissolved Oxygen was determined via an optode (Aanderaa Instruments AS, Bergen, Norway). This technique is based on dynamic luminescence quenching. The raw data were corrected for salinity but not calibrated against discrete oxygen samples that were also taken during this cruise.

7.8.1.3 Gas Tension

The PSI-GTD-Pro (Pro-Oceanus Systems Inc., Halifax, Canada) measures the total dissolved gas pressure of all gases. A small sample volume of air is equilibrated to all dissolved gases in the water through a special membrane. The GTD was also installed in the water bath.

7.8.1.4 Sea surface temperature (SST) and salinity (SSS)

SST and SSS were measured by the ships thermosalinograph. Unfortunately no data were recorded during P399/3. A relationship between the temperature measurements in the equilibrator and SST during P399/2 will be used to correct data to SST during P399/3.

7.8.2 First results

Figure 1 shows underway data of P399/2. The upwelling along the northwest coast of Africa is indicated by the low sea surface temperature (SST) (<21°C) compared to temperatures around 24°C in the open ocean. In the upwelling region also the oxygen concentration is lowered and the pCO_2 values denote high supersaturation with respect to the atmosphere. In a small region north of 19°N low pCO_2 (~ 350 µatm) and high oxygen (~ 400 µmol L^{-1}) was measured. The pCO_2 measurements during P399/3 show values around saturation during most of the time. Only off the Iberian Peninsula undersaturation is observed. At the same time oxygen values are up to 400 µmol L^{-1}.

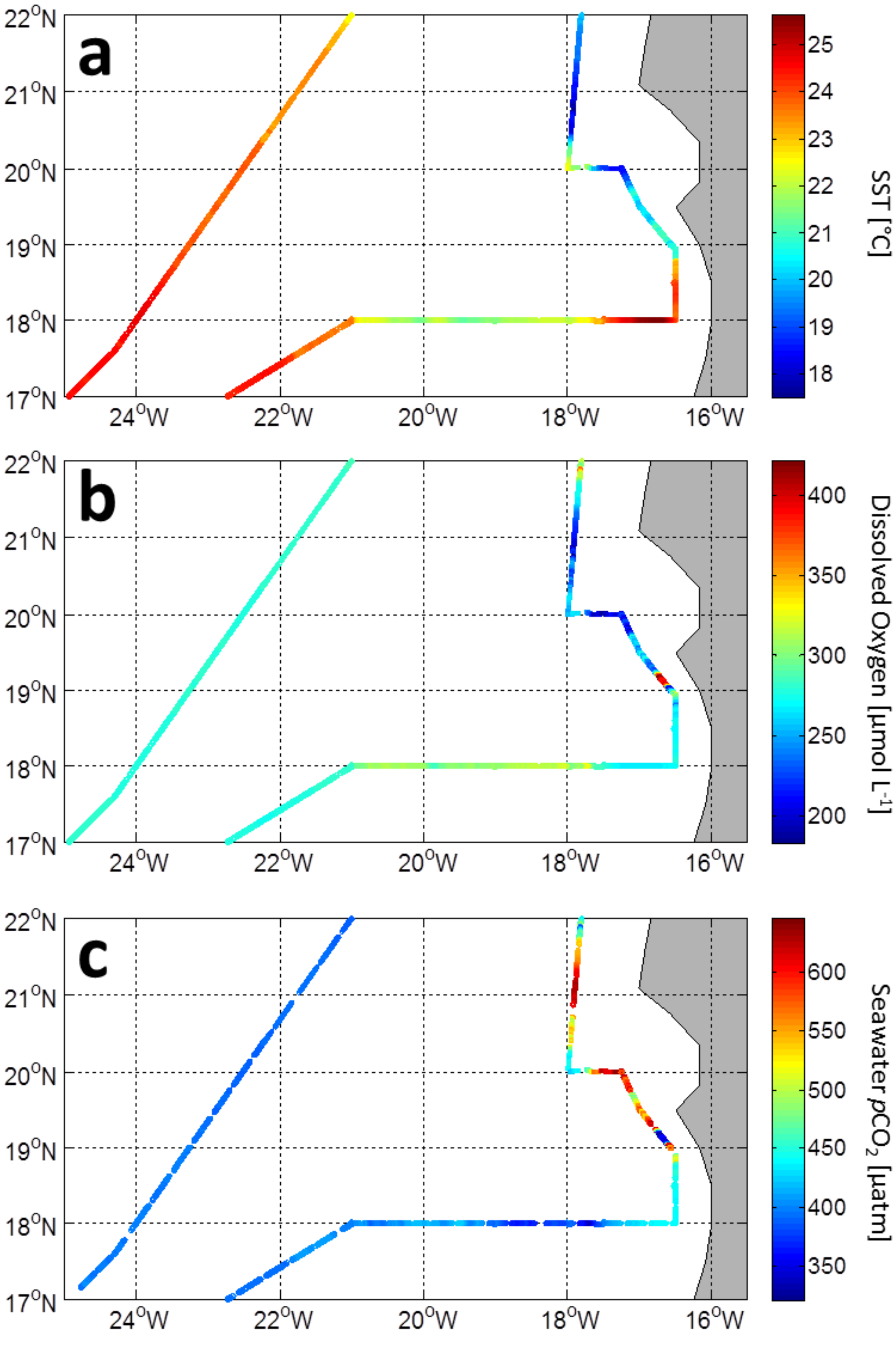

Figure 1: Underway data of Poseidon cruise P399/2. (a) Sea surface temperature (SST), (b) dissolved oxygen and (c) seawater pCO_2.

7.8 Atmospheric setting

Steffen Fuhlbrügge, Kirstin Krüger, Franziska Wittke, Helmke Hepach, Brigit Quack
IFM-GEOMAR, Kiel; sfuhlbruegge@ifm-geomar.de

7.8.1 Meteorology

With a velocity of 16.9 m/s the highest wind speed of the whole cruise was measured immediately after the start of P399/2 near Gran Canaria Island. This value lies by 9 m/s above the mean wind speed of 7.8 m/s (Leg 2: 7.38 m/s, Leg 3: 9.27 m/s) and forms together with stronger winds on June 14th the only velocities above 16 m/s. Contrary to the prior wind direction of the trade winds and westerlies, the mean measured absolute wind direction was 347° (Leg 2: 348°, Leg 3: 343°). A ten minute average of wind speed and direction is shown in Figure 1-2 for every six hours along the ship cruise. Most of the time maritime air masses influenced the ship measurement. Figure 1-3 shows a time series of the measured air and water temperature on the left and on the right the cruise track indicating the water temperature.

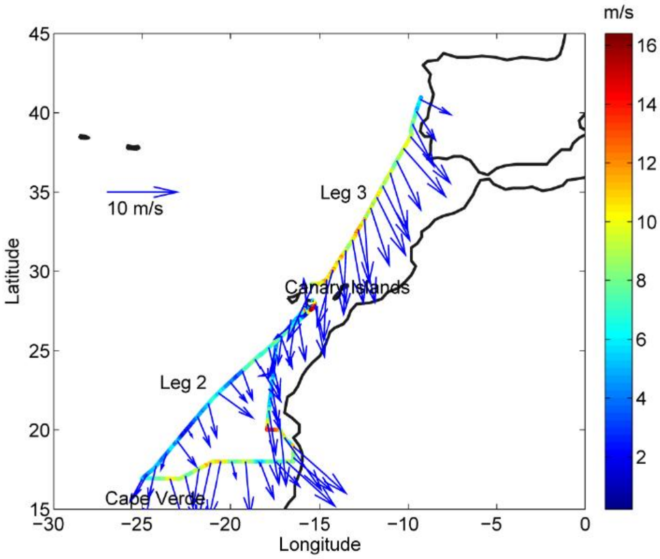

Figure 1-2: Ten minute average of wind speed and direction ship measurements for every six hours, except 24 h stations. The arrows indicate wind direction and speed. In addition the color of the cruise track indicates the wind speed as well

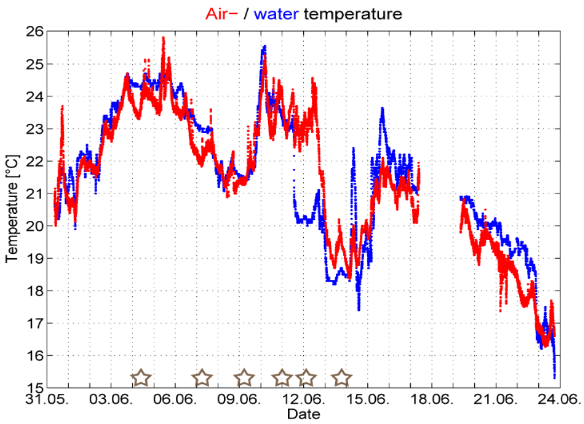

Figure 1-3: Left side: air-(red line) and water (blue line) temperature measured on POSEIDON during the DRIVE campaign from May 31th to June 24th 2010. The orange stars indicate the 24h stations.

A first intense increase of air temperature coincides with a collapse of the wind speed and a change of the wind direction to east on May 31th (see Figure 1-16 for wind speed and Figure 1-17 for wind direction). This wind speed collapse follows the maximum measured wind speed of the whole cruise just by about 4 hours. As the ship cruise started towards the equator, the air and water temperature increased until the maximum air temperature of 25.8 °C is recorded right after the stop at Mindelo. In the following both temperatures began to fall for the first time. This might be caused by southward winds, which transported cold water and air masses from the Mauritanian upwelling in the north towards the ships position. ERA-Interim surface winds confirm this assumption (see Figure 1-7). Right after the third 24 h station and close to the Mauritanian coast, air and water temperatures increased again. On June 11th the ship reached the Mauritanian upwelling at 18.75°N, 16.5°W. This is distinguishable from the abrupt decrease of the water temperature, followed by a drop of the air temperature with a time lag of about one day until both stabilize between 18° and 20° C. On June 14th 2010 a certain increase of the water temperature to about 23.5 °C is distinguishable from Figure 1-3. This increase coincides with the second wind speed maximum of about 16 m/s (Figure 1-16) from the north. Warmer water masses from outside the Mauritanian upwelling may be transported towards the ship at this time, or the ship actually left the upwelling region, until the water temperature dropped again to about 18 °C. On June 15th 2010 the ship left the area of upwelling water, due to increasing air and water temperature until both decreased again with increasing latitude. The total air pressure difference of 13.35 hPa shows, that the crew and the ship were exposed to relatively calm weather during the campaign (Figure 1-5 and Figure 1-6 respectively). The lowest value of 1007.6 hPa was reached near the Mauritanian coast on June 11th 2010 when the ship reached the edge of a low pressure system, originated on the African onshore at the boarder of Senegal and Mauritania (Figure 1-8). This was the only day dust from the Sahara was found in the air filter, as reported by the crew. The highest air pressure value of 1021 hPa was observed on June 19th during leg 3.

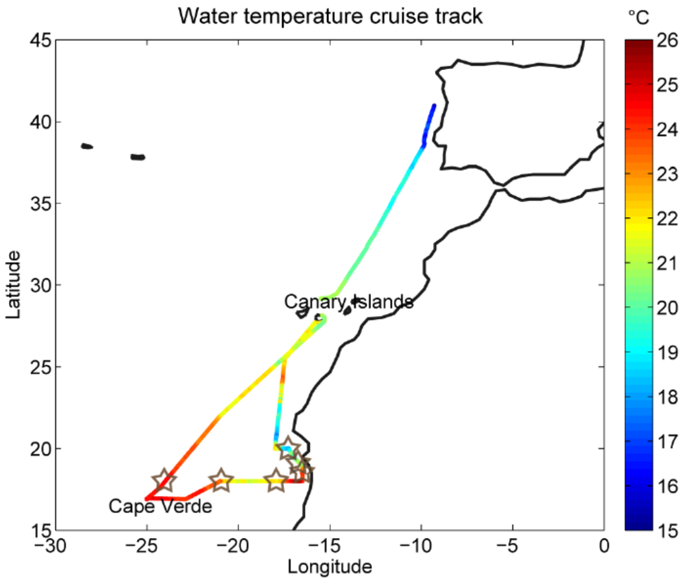

Figure 1-4: Water temperature cruise track measured on POSEIDON during the DRIVE campaign from May 31th to June 24th 2010. The orange stars indicate the 24h stations.

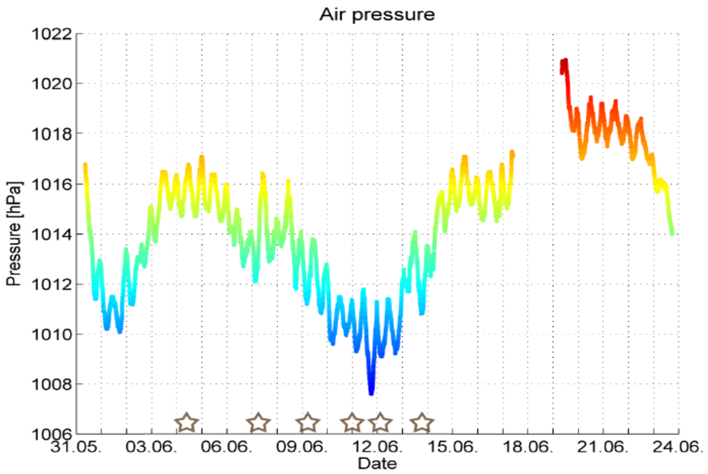

Figure 1-5: Time series of air pressure measured on POSEIDON during the DRIVE campaign from May 31th to June 24th 2010. Orange stars indicate the 24 h stations.
Figure 1-6: Cruise track of air pressure measured on POSEIDON during the DRIVE campaign from May 31th to June 24th 2010.

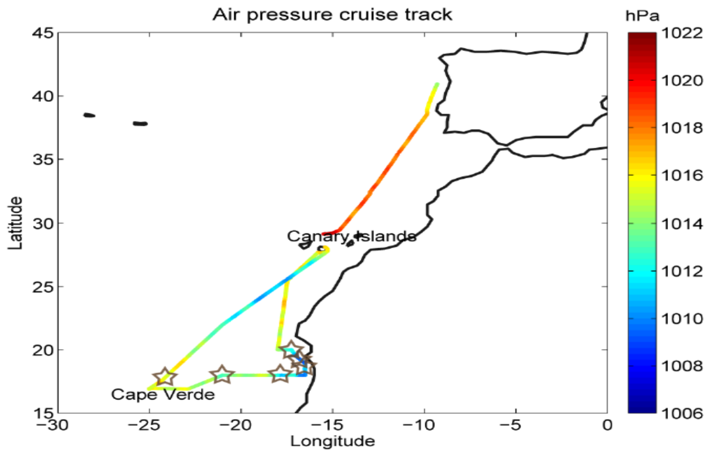

Figure1-6: Cruise track of air pressure measured on POSEIDON during the DRIVE campaign from May 31th to June 24th 2010.

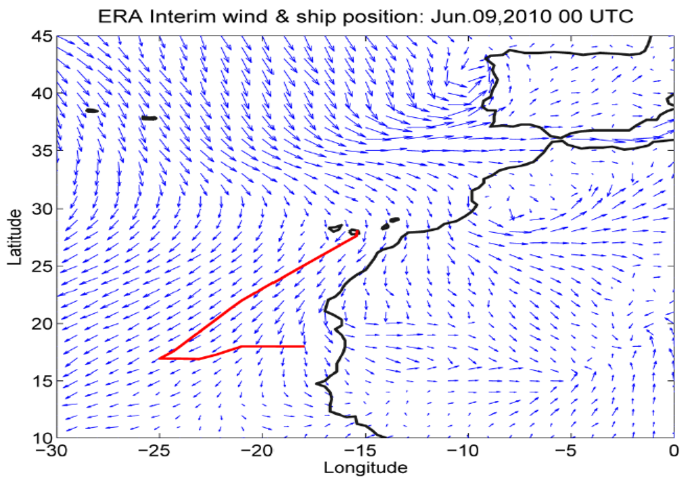

Figure 1-7: Surface winds of ERA Interim with covered ship track (red) of DRIVE campaign on June 9th 2010, 00 UTC.

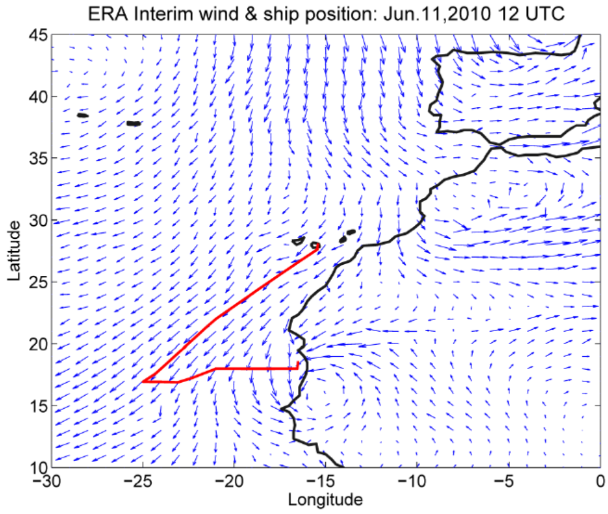

Figure 1-8: Surface winds of ERA Interim with covered ship track (red) of DRIVE campaign on June 11th 2010, 12 UTC.

7.8.2 Radiosoundings

During the DRIVE campaign 41 radiosondes have been launched to investigate the vertical structure of the troposphere and the mid stratosphere. The radiosondes were started every day at 12 UTC and at the 24 h stations at 00, 06, 12 and 18 UTC. The resulting profiles are shown in Figure 1-9 for temperature, Figure 1-10 for relative humidity, Figure 1-11for zonal wind and Figure1-12 for meridional wind respectively. The determined lapse rate (LRT) and cold point tropopause (CPT) is marked by the continuous and dash-dotted lines. Both tropopauses show short-timed variations in height. Except from 06.06.2010 to 09.06.2010 were the CPT is about 2 km higher than the LRT, both tropopauses show identic heights of 16 – 17 km from 03.06.2010 to 15.06.2010. After June 15th 2010 the height of the LRT in contrast to the CPT decreases to 15 km, while passing the Tropic of Cancer and entering the extratropics. Due to the less physical meaning of the CPT outside of the tropics this is an evidence for the changing climatic regime. This assumption is founded by the appearance of the subtropical jet (STJ) in the radiosondes measurements of the zonal wind. An abrupt increase of the wind speed with a maximum of 48 m/s between 10 and 15 km height is found on 16.06.2010 with a minor northern wind component (Figure 1-11 and Figure 1-12). The STJ is generally found at same altitudes and followed by a descent of the tropopause height towards increasing latitude. This descent is also shown by the LRT on 21.06.2010 immediately after the STJ weakens. Although it is not important for this diploma thesis it is worth mentioning, that above 20 km of altitude the stratospheric jet stream with easterly winds up to 35 m/s was determined by the radiosondes (Figure 1-11).
Taking a closer look to the lower temperature profile of Figure 1-9, several temperature inversions from the ground up to 2 km of height were detected by the radiosondes. Two examples are in addition given by Figure 1-14 and Figure 1-15. Due to their height and regional appearance the inversions are identified as trade inversions. These inversions suppress vertical motion of air and are reflected in the vertical relative humidity profile (Figure 1-10), the mixing layer height (1.1.2 Mixing Layer Height) and the backward calculated trajectories). The lower vertical profile of relative humidity already shows a rough trend of the mixing layer height, due to an intense decrease of relative humidity with height. From June 3rd to June 14th several clouds can be distinguished from the vertical relative humidity profile. These clouds were observed by the scientific crew on the ship as well and identified as a number of different cloud types like cirrostratus, altostratus, cirrocumulus, altocumulus et cetera.

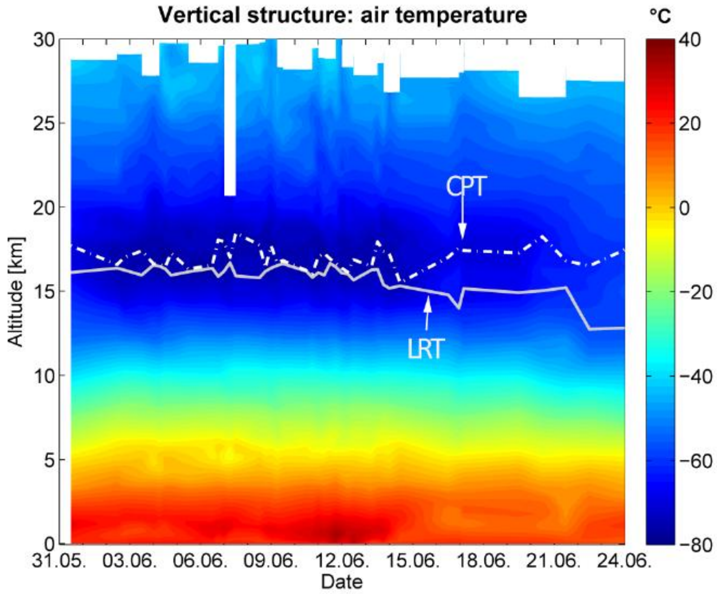

Figure 1-9: Vertical structure of air temperature measured by radiosondes with cold point tropopause (CPT) and lapse rate tropopause (LRT) during DRIVE campaign from May 31th to June 24th 2010.

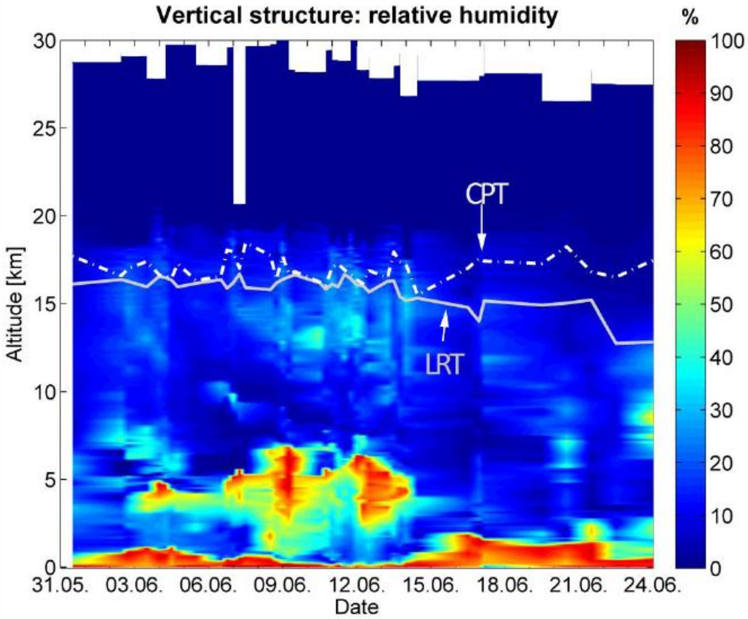

Figure 1-10: Vertical structure of relative humidity measured by radiosondes with cold point tropopause (CPT) and lapse rate tropopause (LRT) during DRIVE campaign from May 31th to June 24th 2010.

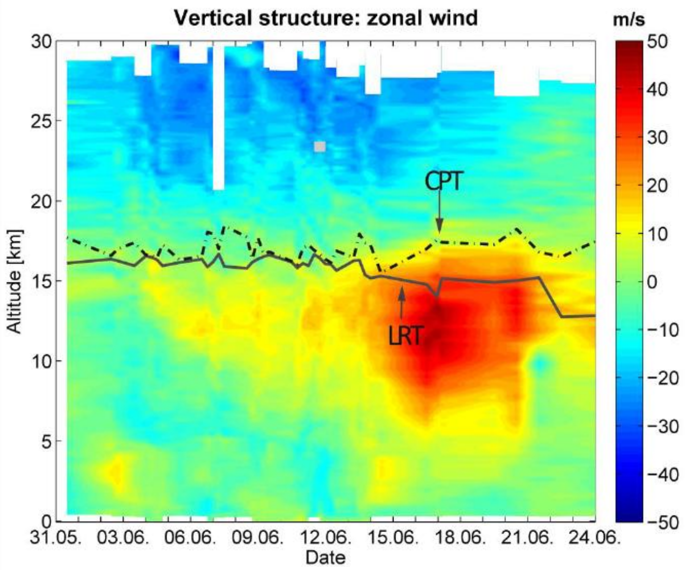

Figure 1-11: Vertical structure of zonal wind measured by radiosondes with cold point tropopause (CPT) and lapse rate tropopause (LRT) during DRIVE campaign from May 31th to June 24th 2010. Positive values indicate westerly winds.

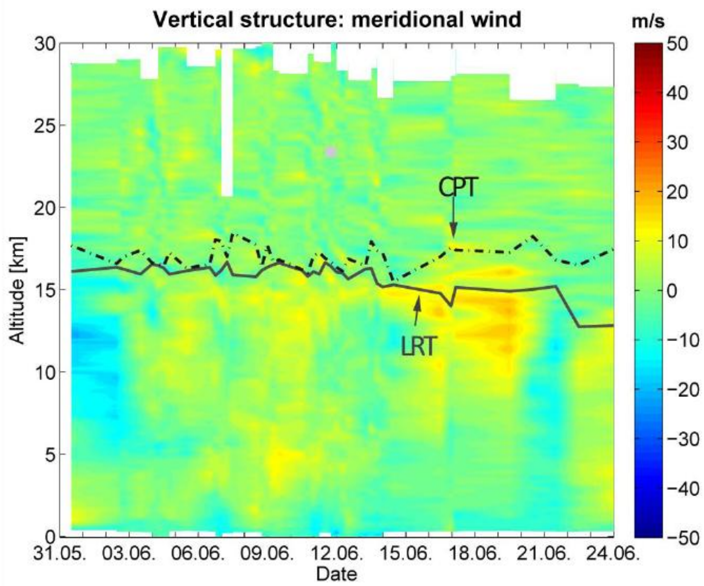

Figure 1-12: Vertical structure of meridional wind measured by radiosondes with cold point tropopause (CPT) and lapse rate tropopause (LRT) during DRIVE campaign from May 31th to June 24th 2010. Positive values indicate southern winds.

7.8.3 Mixing layer height

The mixing layer height for DRIVE is shown in Figure 1-13. It was determined for all 41 radiosoundings. A typical radiosounding for the case of a convective boundary layer at 21° W and 18° N on 06.06.2010 18 UTC is shown in Figure 1-14. The upper left plot shows the vertical profiles of air temperature T and virtual potential temperature Θv. The trade inversion, which limits the vertical extension of the mixing layer height, starts at h-= 400 m and ends at h+= 800 m altitude. A sharp bend in the virtual potential temperature profile is found at the same altitude of the trade inversions lower limit. This first evidence for the mixing layer identifies its height at about 500 m. The upper right plot of Figure 1-14 shows the water vapor mixing ratio in kg water per kg of dry air. As a conserved quantity it is essential for determining the mixing layer height and in contrast to the relative humidity,

which is measured by the radiosondes, not depending on the temperature. At 400 m of altitude the water vapor mixing ratio shows a sudden decrease from about 0.0125 kg water per kg dry air to about 0.0035 kg water per kg dry air at 600 m. The upper limit of the mixing layer is identified from this plot at about 500 m. A vertical wind shear in the lower left plot of Figure 1-14 is found between 300 m and 600 m, identifying the height of the mixing layer at 400 – 500 m. The lower right and last plot shows the Richardson number. Disregarding some outliers at about 250 m the Richardson number increases above 600 m of altitude due to the suppression of vertical motion. The definite height of the mixing layer for this radiosounding is finally stated at about 500 m altitude.
Another interesting radiosounding during DRIVE and especially during the time of several surface inversions from June 10th to June 13th is shown in Figure 1-15. This so-called stable boundary layer suppresses vertical motion of air from the ground to about 500 m of altitude. The mixing layer height for this case is zero meters. The earlier mentioned recorded air temperature oscillations are as well reflected in the lower profiles of air- and virtual potential temperature. However they do not influence the temperature pattern of the lowest 3 km due to the small amplitude at this level.

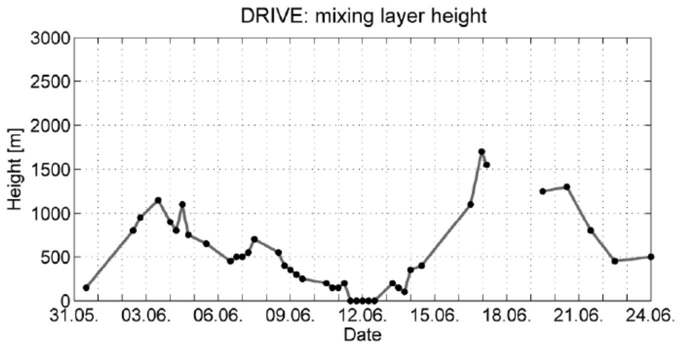

Figure1-13: Mixing layer height, determined from radiosoundings during DRIVE campaign from May 31th to June 24th 2010. The gap marks the break between leg 2 and leg 3.

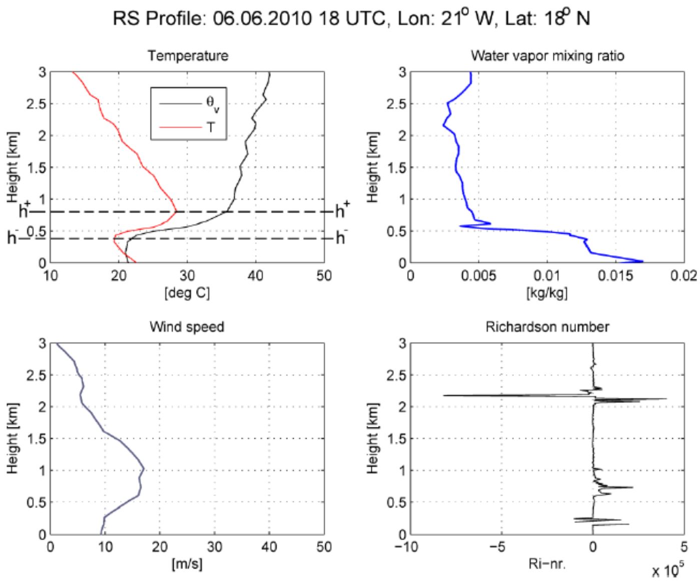

Figure 1-14: Radiosounding of the lowest 3 km of the atmosphere for the case of a convective boundary layer on June 6th 2010 18 UTC, 21° W and 18° N during DRIVE campaign from May 31th to June 24th 2010.

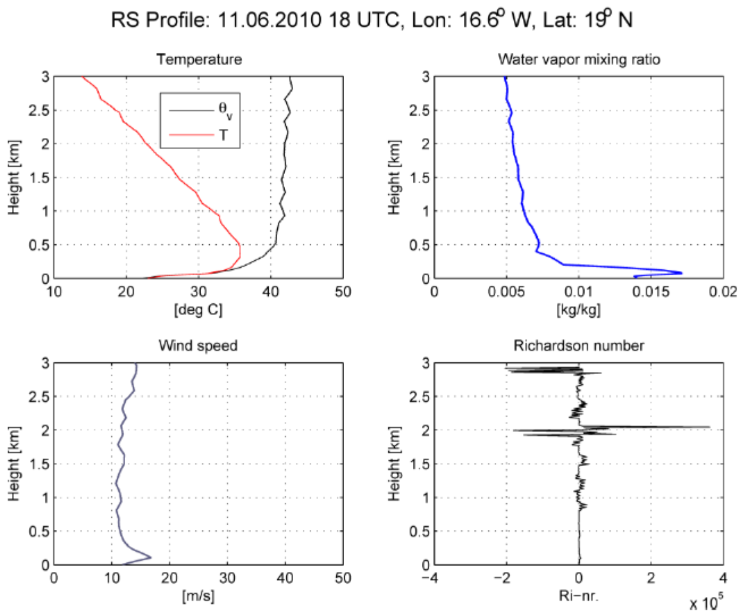

Figure 1-15: Radiosounding of the lowest 3 km of the atmosphere for the case of a stable boundary layer on June 6th 2010 18 UTC, 21° W and 18° N during DRIVE campaign from May 31th to June 24th 2010.

7.8.4 Data comparison

For the investigation of air masses and especially their origin it is important to distinguish the reliability of the meteorological data sets. For this reason the wind speed and direction measurements from the ship, averaged once per minute, and radiosondes are compared with a high-resolution ERA-Interim data set and NCEP/NCAR Reanalysis Project 1 (NNRP-1) model data due to its use for the trajectory calculation by HySplit. The results are shown in Figure 1-16 for wind speed and Figure 1-17 for wind direction. The blue curve indicates the ship measurements, the dark red curve the ERA-Interim model data and the light red curve NNRP-1 model data. The ship measurements were taken every second and are averaged for every minute. The original ERA-Interim grid of 0.25° x 0.25° and the NNRP-1 grid of 2.5° x 2.5° are interpolated to 0.125° x 0.125° horizontal grids. For the comparison the closest grid point to the ships position is determined and plotted. Depending on the latitude, the grid points have a distance of 10 – 14 km to each other. Consequently the maximum distance between a grid point and the ships position is always within a range of 7 km. The plots show a good agreement of both data sets with the ship measurements. For wind speed the correlation coefficient of the ship data and ERA-Interim is r = 0.91 and r = 0.79 for ship data and NNRP-1 respectively. Both assimilations seem to underestimate the wind speed extremes. Due to the higher horizontal resolution of the ERA-Interim data, the extremes may be better resolved than for NNRP-1. Nevertheless both data sets do have their problems with the wind speeds on May 31th, June 7th, June 14th and June 16th on leg 2 and underestimate these by 2 – 6 m/s. During leg 3 the wind speed is better resolved by NNRP-1. ERA-Interim seems to underestimate the mean velocity by about 2 – 4 m/s. Besides the horizontal resolution, the temporal resolution also plays an important role in the comparison of the data sets. Averaging the wind speed measured by the ship to 6 hours results in Figure 1-21 with correlation coefficients of r = 0.95 for ERA-Interim and r = 0.86 for NNRP-1. The wind direction comparison of the ship measurements and model data is shown in Figure 1-17 and for 6 hourly ship measurements in Figure 1-22. The y axis shows the direction from -180° to 180° (0° = northerly, -90°/90° = westerly/easterly, -180° and 180° = southerly winds). For the once per minute average of the ship measurements, the correlation coefficients are r = 0.69 (ERA-Interim) and r = 0.67 (NNRP-1) and for the 6 hourly averaged measurements r = 0.94 (ERA-Interim) and r = 0.88 (NNRP-1). Both assimilation data sets seem to simulate the surface winds quite well with regard to the temporal resolution. However they occasionally

overestimate the easterly winds by up to 20°. Despite the fact, that the original model data of ERA-Interim has a 10 times higher horizontal resolution than NNRP-1 the similar correlation coefficients for wind speed and direction are surprising. Unfortunately the accuracy of the measuring instruments of the ship is unknown.
For the investigation of the air mass origin within the boundary layer by trajectory calculations using NNRP-1 data sets, the wind measurements from radiosondes are compared with the 925 hPa (Figure 1-18) and 850 hPa pressure levels (Figure 1-19) from NNRP-1. Now the blue curve marks the observed wind from the radiosondes. To compare the NNRP-1 2.5° x 2.5° data with the radiosondes measurements, the data grid is interpolated to a 0.125° x 0.125° horizontal grid on each pressure level. The closest grid point to the current radiosondes positions of each pressure level is taken, resulting in a maximum distance of 7 km for grid point and radiosondes position. The correlation coefficients between radiosondes observations and NNRP-1 for the 925 hPa pressure level are r = 0.74 for wind speed and r = 0.66 for wind direction. For the 850 hPa pressure level the correlation results r = 0.67 (wind speed) and r = 0.82 (wind direction). In contrast to the surface measurements the model is not as accurate in determining the wind speed and direction in higher pressure levels. The higher correlation coefficient for wind direction at 850 hPa might be caused by distorted radiosondes measurements near the surface, due to an interpolation of the lowermost measurement values from the first measured value. This one is given by the ship and the following values are interpolated until measurements and interpolated values approximate. Nevertheless the curves roughly agree even though meteorological assimilation data over the open ocean are quite rare. As the DRIVE radiosondes measurements were not delivered to the WMO data net, they were not assimilated in global meteorological data sets.

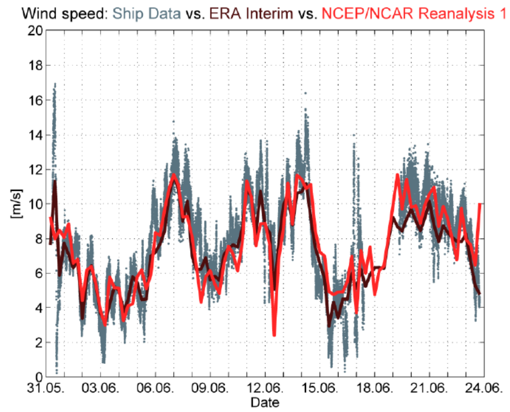

Figure 1-16: Wind speed comparison of ship measurement (blue) - ERA Interim (dark red) - NCEP/NCAR Reanalysis 1 (light red) during DRIVE campaign from May 31th to June 24th 2010.

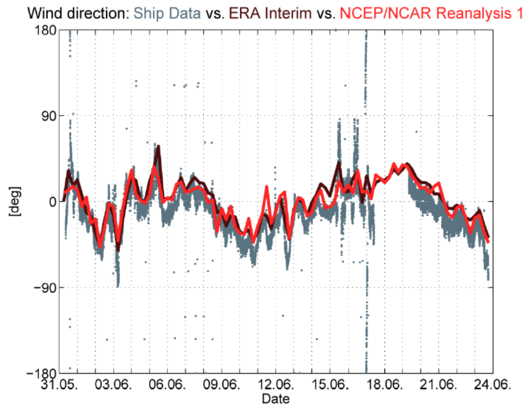

Figure 1-17: Wind direction comparison of ship measurement (blue) - ERA Interim (dark red) - NCEP/NCAR Reanalysis 1 (light red) during DRIVE campaign from May 31th to June 24th 2010. Most outliers have been filtered out from the ship data.

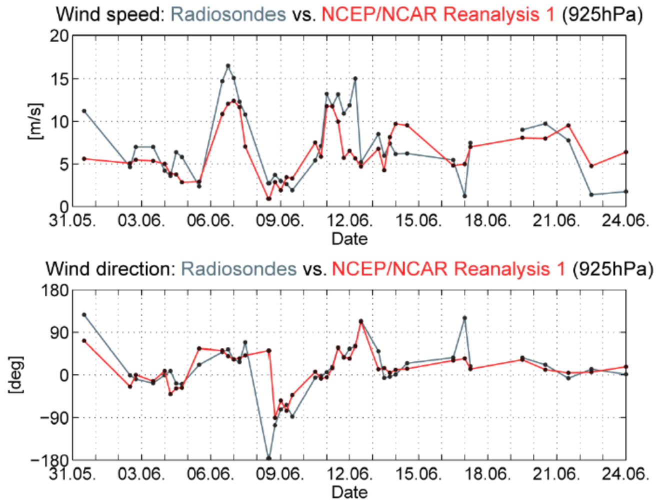

Figure 1-18: Comparison of wind speed and wind direction of radiosondes measurements and NCEP/NCAR Reanalysis Project 1 at 925 hPa during DRIVE campaign from May 31th to June 24th 2010.

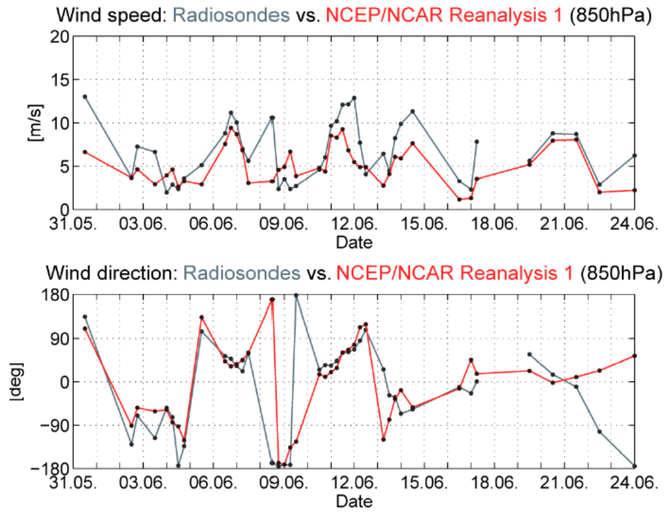

Figure 1-19: Comparison of wind speed and wind direction of radiosondes measurements and NCEP/NCAR Reanalysis Project 1 at 850 hPa during DRIVE campaign from May 31th to June 24th 2010.

7.9 Aerosols

Alex Baker, UEA, Norwich, Uk; alex.baker@uea.ac.uk

Sixteen daily aerosol samples were collected by Hermann Bange, IFM-GEOMAR between 5th and 23rd June 2010 aboard RV Poseidon during P399/2 and P399/3. Sample positions are summarised in Table 1. To date the samples have been analysed for their concentrations of soluble major cations (Na^+, Mg^{2+}, K^+, Ca^{2+}) (Figure 1). Analyses for aerosol trace metals (including Fe, Al, Mn, Ti and Zn), major anions (Cl^-, NO_3^-, SO_4^{2-}, Br^-, $C_2O_4^{2-}$), ammonium, total soluble nitrogen and soluble phosphate and silicate are yet to be completed.

Table 1 P399 aerosol sample start and end locations.

Sample	Start date	Start Position	End Date	End Position
TM01	05/06/2010	17.0N 24.9W	06/06/2010	17.7N 21.6W
TM02	06/06/2010	17.7N 21.6W	07/06/2010	18.0N 21.0W
TM03	07/06/2010	18.0N 21.0W	08/06/2010	18.0N 18.9W
TM04	08/06/2010	18.0N 18.9W	09/06/2010	18.0N 18.0W
TM05	09/06/2010	18.0N 18.0W	10/06/2010	18.5N 16.5W
TM06	10/06/2010	18.5N 16.5W	11/06/2010	18.6N 16.5W
TM07	11/06/2010	18.6N 16.5W	12/06/2010	19.0N 16.6W
TM08	12/06/2010	19.0N 16.6W	12/06/2010	20.0N 17.3W
TM09	13/06/2010	20.0N 17.3W	14/06/2010	20.4N 18.0W
TM10	14/06/2010	20.4N 18.0W	15/06/2010	23.6N 17.7W
TM11	15/06/2010	23.6N 17.7W	16/06/2010	26.5N 16.7W
TM12	16/06/2010	26.5N 16.7W	16/06/2010	27.7N 15.8W
TM13	19/06/2010	29.2N 15.5W	20/06/2010	31.1N 13.7W
TM14	20/06/2010	31.1N 13.7W	21/06/2010	33.7N 12.3W
TM15	21/06/2010	33.7N 12.3W	22/06/2010	36.5N 10.9W
TM16	22/06/2010	36.5N 10.9W	23/06/2010	39.5N 9.7W

7.9.1 Methods

All analytical methods employed are based on extraction of soluble aerosol components into aqueous solution, filtration and appropriate analysis. For major ions and total soluble nitrogen analysis the extraction solution is ultrapure water, while for the other species pH buffered solutions are employed (pH 4.7 for trace metals, pH 7 for phosphate and silicate). Analysis of extract solutions is by ion chromatography (major ions), high temperature catalytic oxidation (total soluble nitrogen), inductively coupled plasma – optical emission spectrometry (trace metals) or spectrophotometry (phosphate and silicate). Full details of analytical methods can be found in Baker et al., 2007.

7.9.2 Initial Results

Orange / brown Saharan dust was clearly visible on the aerosol filters for 3 samples collected during P399 (TM01, TM07, TM08). These samples contained the highest concentrations of non-seasalt calcium (nss Ca) observed during the cruise (Figure 1), which is consistent with the presence of $CaCO_3$ in the mineral dust. Sample TM09 also had a relatively high nssCa concentration (>20 nmol m^{-3}), but its colouration (grey) indicated that it also contained significant quantities of non-mineral aerosol. Figure 1 also shows concentrations of aerosol sodium (whose source is dominated by seaspray) and non-seasalt potassium (nss K), which is often an indicator of biomass burning products. Only one sample (TM08) showed significant quantities of nss K, but in this case mineral dust may be a more important source as P399 took place well outside the winter-time Sahel biomass burning season and the sample contained very high dust concentrations (nss Ca = 110 nmol m^{-3}).

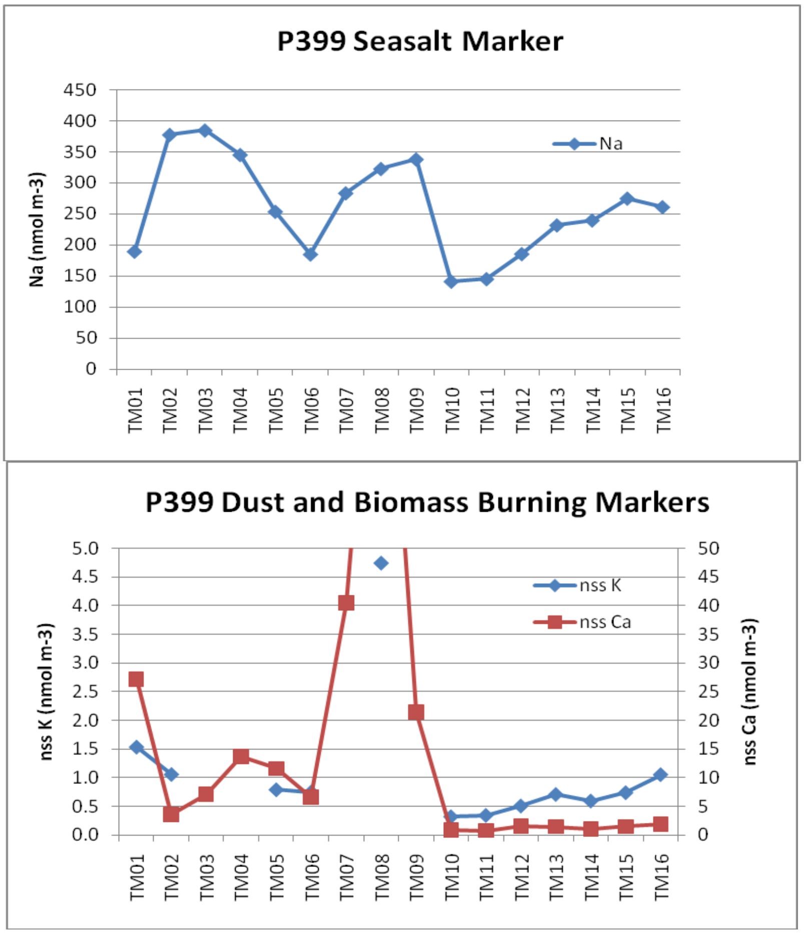

Figure 1: Concentrations of soluble sodium, non-seasalt calcium and non-seasalt potassium during cruise P399.

Reference

Baker, A. R., Weston, K., Kelly, S. D., Voss, M., Streu, P. and Cape, J. N., 2007. Dry and wet deposition of nutrients from the tropical Atlantic atmosphere: links to primary productivity and nitrogen fixation. *Deep-Sea Research Part I*, **54**, 1704-1720.

7.10 Atmospheric ozone (O_3) and mercury (Hg)

Enno Bahlmann, University Hamburg; enno.bahlmann@zmaw.de
Jonathan Williams, MPI für Chemie, Mainz

7.10 Preliminary Results

Ozone and mercury mixing ratios were continuously measured on board of R/V Poseidon during the cruise P399 leg 2 and 3 in order to assess changes of air masses and to examine whether intensive bromine chemistry in the marine boundary layer is accompanied with concurrent ozone and mercury depletions as previous reported for the high latitudes.. The preliminary results are presented in Figure 1 as 5 min averages. Between the 7th and 9th of June and between the 17th and 19th of June ozone data were not recorded and between the 3rd and 5th of June mercury data were not recorded due to a malfunction of the data logger. The peak in the ozone mixing ratio that occurred at the 20th of June is probably related to a plume of polluted air from the Portuguese Coast.On the 21.th of June a short mercury depletion event that did not coincide with decreasing ozone mixing ratios, was observed. At the beginning of the cruise between the first and 10th of June both compounds showed clear diurnal variations that are shown in Figure 2. In contrast to ozone that peaked in the morning and decreased over the day, Hg° showed a second peak in the afternoon. We suggest to examine the co-variations of ozone and mercury in more detail for periods of elevated BrO levels in the marine troposphere. A first comparison of the ozone data with the methane data presented by the MPI für Biogeochemie, Jena (see section 7.11) indicate similarities that should further be evaluated.

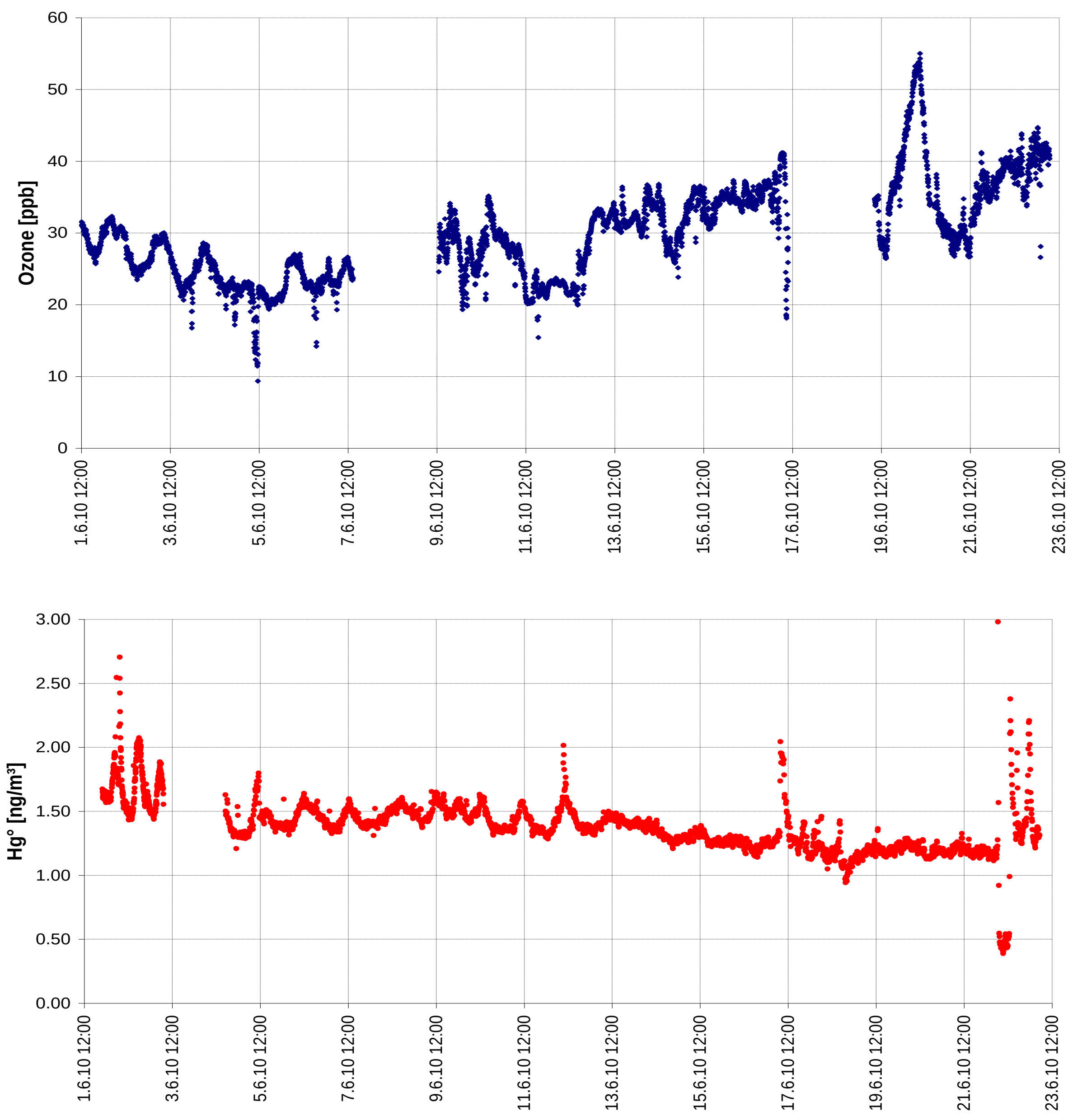

Fig. 1a and b Time series of atmospheric ozone (upper panel) and Hg° (lower panel) measured onboard of RV POSEIDON during cruise P399 leg 2 and 3. Data gaps result from a malfunction of the data logger.

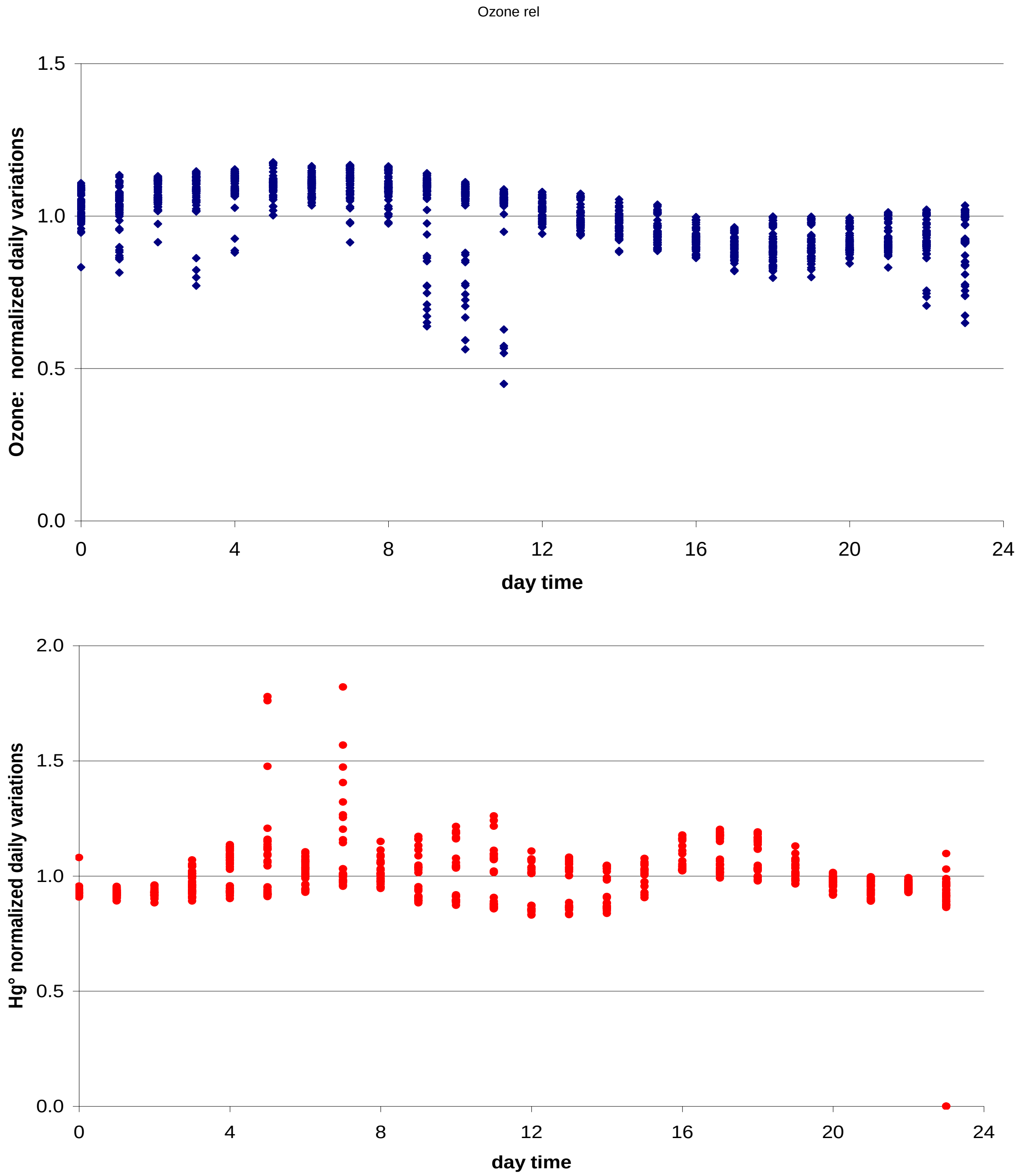

Fig. 2a and b: Normalized daily variations of ozone (upper panel) and mercury (lower panel) for the time period from June 1st to June 7th. Ozone mixing ratios typically peaked in the morning and decreased over the day.

7.11 Atmospheric CO_2, CH_4 and flask samples

Jošt Lavrič and Martin Heimann, MPI Biogeochemie, Jena; jlavric@bgc-jena.mpg.de

7.11.1 Introduction

The Max-Planck-Institute for Biogeochemistry (MPI-BGC) participated at the Poseidon cruise P399, legs 2 and 3 (31 May – 24 June 2010) with continuous measurement of the atmospheric mixing ratio of carbon dioxide (CO_2), methane (CH_4) and water vapour (H_2O). Additionally, 1 litre flask pair samples were taken daily.

7.11.2 Instrumental setup

The continuous measurement of the atmospheric mixing ratio of CO_2, CH_4 and H_2O was performed with a Picarro G1301 instrument attached to a PFA tube (OD = 1/4", length = 15 m) leading to the ship's upper deck. The tube was continuously flushed at ~ 3-4 litres/min. The instrument drifts less than 0.25 ppm and 3.2 ppb per year for CO_2 and CH_4, respectively. Therefore, a pre-campaign 3 point calibration is sufficient to insure already a very high precision of the measurement (typically better than 0.04 ppm and 0.3 ppb for CO_2 and CH_4, respectively). As an additional quality control, a target gas (1898.99 ppb CH_4, 398.00 ppm CO_2) was measured during the cruise. Furthermore, the collected flask samples will be used as an additional control on the instrumental drift.

Flask samples were taken with the MPI-BGC flask sampler on the ship's upper deck. After a flushing period of at least 20 minutes a 1 litre flasks pair was filled with ambient air to a pressure of ~ 1.7 barg. The sample air was continuously dried by passing it through a magnesium perchlorate ($Mg(ClO_4)_2$) cartridge. A total of 100 flasks (50 pairs) were taken in the period from 4.-22. June 2010, and are in the process of being analysed for CO_2, O_2/N_2, CH_4, CO, N_2O, SF_6, H_2, Ar/N_2, ^{13}C and ^{18}O in CO_2.

7.11.2 Preliminary results

We present here continuous CO_2 and CH_4 data as 1 min averages. The H_2O content of the measured air (not shown) was for most of the time between 0.3 and 0.5 %v. These relatively low water vapour concentrations decrease further the uncertainty of the CO_2/CH_4 measurement. Figures 1 and 2 summarize the continuous data. Close to the coast, where the potential for human and/or terrestrial influence on the air masses is the largest, and particularly during 24 h stations, interesting variations in CO_2/CH_4 were observed (Fig. 3). Based also on some other preliminary results from other teams, we suggest that these events are examined in more detail.

7.11.3 Outlook

When available, the flask analysis results will provide additional constraints on the continuous data (e.g. estimate the anthropogenic influence on the measured air masses). Furthermore they will complement and help validate our and other data sets collected during the cruise (e.g. the continuous measurements of atmospheric $\delta^{13}CO_2$, etc.). Based on their composition and relation to other data sets from the cruise, some flask samples may be selected for δD and $\delta^{13}C$ isotope analysis of CH_4.

7.11.4 Acknowledgements

Enno Bahlmann and Ralf Lendt (Univ. of Hamburg) are thanked for the logistic support and operation of the instrumentation and flask sampling during the cruise. Jan Winderlich (MPI-BGC) contributed the data treatment code, performed the initial data treatment, produced Figure 1, and calibrated the $CO_2/CH_4/H_2O$ instrument. S. Baum and M. Hielscher (MPI-BGC) are thanked for technical support.

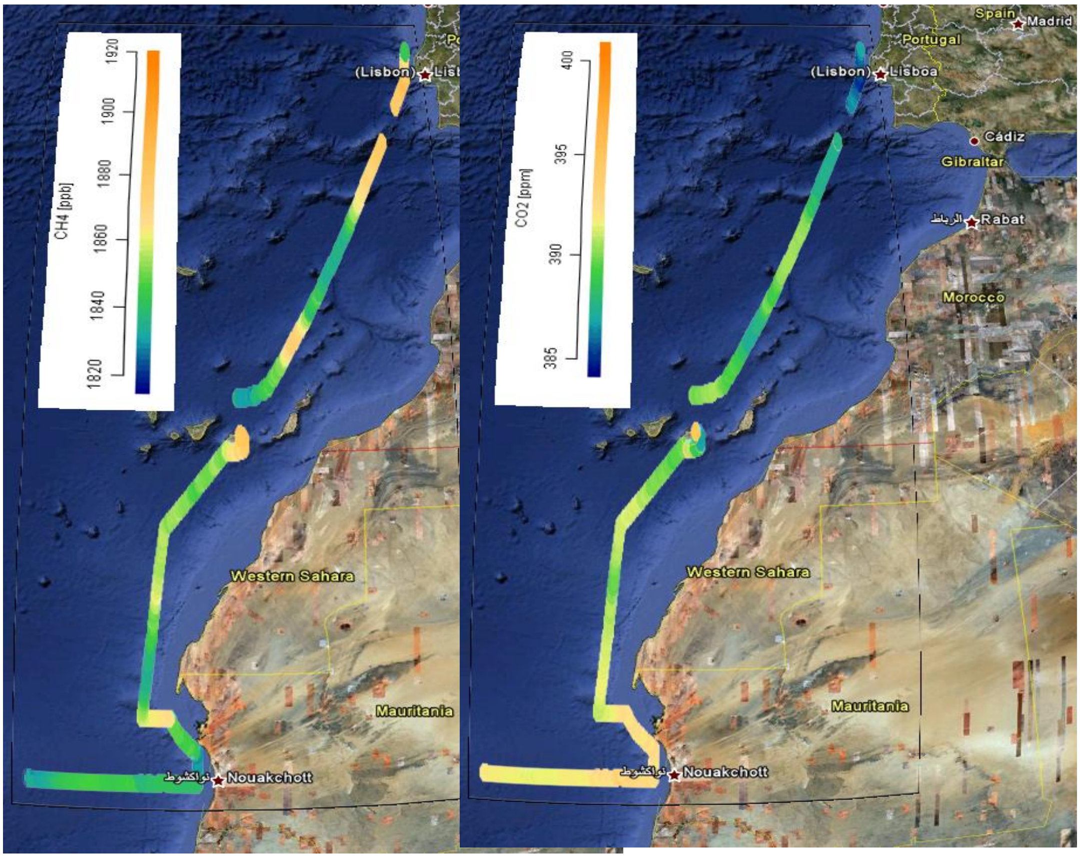

Figure 2 Dry atmospheric mixing ratios of methane (CH_4; left) and carbon dioxide (CO_2; right), traced on the path of the Poseidon cruise P399, legs 2 and 3 (31 May – 24 June 2010). (Source of the map: Google Earth 2011).

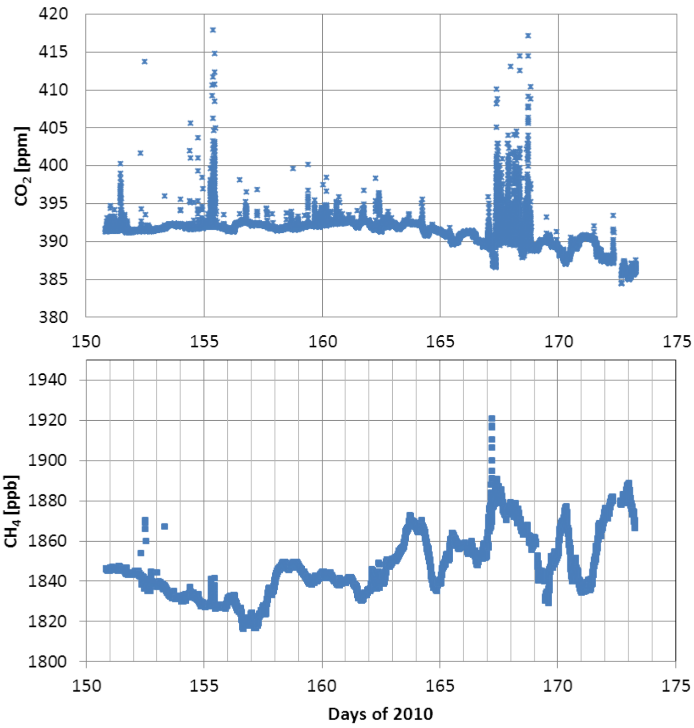

Figure 3: Dry atmospheric mixing ratios of carbon dioxide (CO2; above) and methane (CH4; below) recorded during the Poseidon cruise P399, legs 2 and 3 (31 May – 24 June 2010). Increased levels of CO2 coincide with times when the ship was close to urban areas (e.g. in a port).

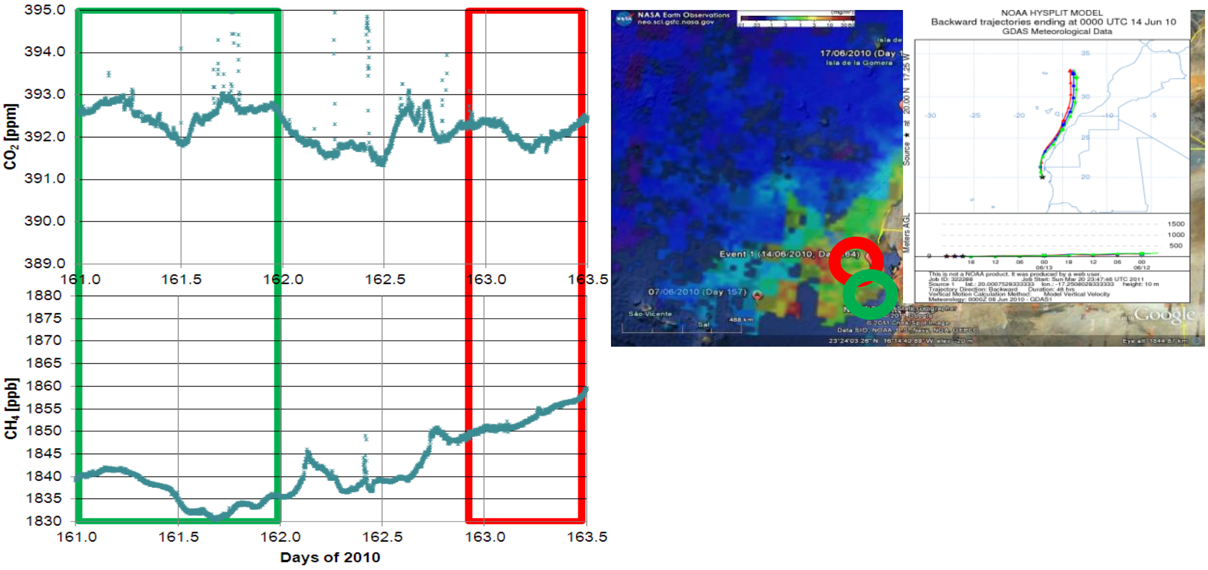

Figure 4: The green and red rectangles on the left mark two 24 hours stations off-coast Mauritania (Banc d'Arguin; the second station (red rectangle) is shown only partly). Days 161, 162, and 163 correspond to 11, 12, and 13 June 2010, respectively. Note the considerable increase of CH_4 concentrations starting at day 161.5, which is not reflected in the CO_2 concentrations. The HYSPLIT back trajectories (right) suggest that the measured air masses travelled a considerable distance over sea, but at this stage additional local/continental sources cannot be excluded. The coloured overlay on the Google Earth map (centre) is from NASA/NEO (Chlorophyll Concentration; 1 month - Aqua/MODIS; Jun 1, 2010 00:00-Jun 30, 2010 23:59). Although the atmospheric CO_2/CH_4 sometimes show a remarkable correlation with sea chlorophyll concentrations, we cannot provide, with the current data set, an estimation of the degree to which they are linked.

7.12 MAX-DOAS measurements of BrO and IO

Katja Großmann, University of Heidelberg; katja.grossmann@iup.uni-heidelberg.de

7.12.1 Scientific Background

Reactive halogen species (RHS) exert various influences on the photochemistry of the marine boundary layer. They are formed in the marine atmosphere for example from precursors released from sea salt aerosols, through the degradation of organo-halogens emitted by certain algae, or from inorganic aqueous reactions. The halogen radicals (BrO and IO) can destroy ozone catalytically, oxidize dimethyl sulfide (DMS) or cause the formation of new aerosol particles[1]. However, there are still many open questions concerning the abundance and significance of RHS in the marine boundary layer over the open ocean.

7.12.2 Measurements

Measurements of BrO and IO were carried out during the Poseidon campaign using the Multi-Axis Differential Optical Absorption Spectroscopy (MAX-DOAS)[2] technique, which analyses scattered sunlight spectra at different elevation angles. This method yields differential Slant Column Densities (dSCD) as a primary output quantity which can be converted into mixing ratios using the radiative transfer model McArtim[3].
The MAX-DOAS instrument aboard consisted of a telescope unit, which was mounted on top of the rail on the starboard side on the upper deck of the Poseidon, a spectrometer-detector-unit as well as a quartz fibre bundle that conducted the light collected by the telescope to the spectrometer. The telescope included an inclinometer to compensate for the rolling of the ship.

7.12.3 First Results

Tropospheric BrO could be detected on several days in the afternoon close to the West African Coast (Figure 1). During another Poseidon cruise in 2007 (P348) similar BrO results were found[4]. BrO profiles were retrieved assuming an aerosol box profile with a height of 1 km and an average aerosol optical depth (AOD) of 0.14 km^{-1} for the Atlantic region[5]. Figure 2 shows the contour plot of the diurnal variation of the BrO mixing ratio for one day close to the Mauretanian Coast with high BrO concentration of approximately 10 ppt in the afternoon.

IO was present above the detection limit for almost the whole duration of the cruise (Figure 3). IO profiles were also retrieved assuming an aerosol box profile with a height of 1 km and an average aerosol optical depth of 0.14 km^{-1} for the Atlantic region[5]. Figure 4 shows the contour plot of the diurnal variation of the IO mixing ratio for one day with less clouds. IO is located in the lower tropospheric layers up to approximately 1 km. A maximum surface mixing ratio of 2 ppt can be observed. However, variations in the aerosol load are a source for systematic uncertainties in the retrieved BrO and IO profiles.

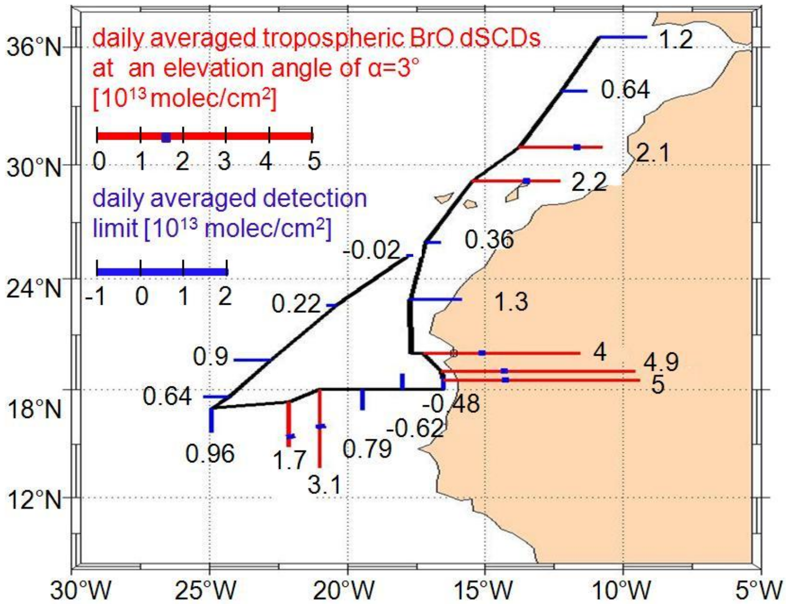

Figure 1: Daily averaged tropospheric BrO dSCDs (red) and the respective detection limit (blue) at an elevation angle of 3° plotted along the cruise track.

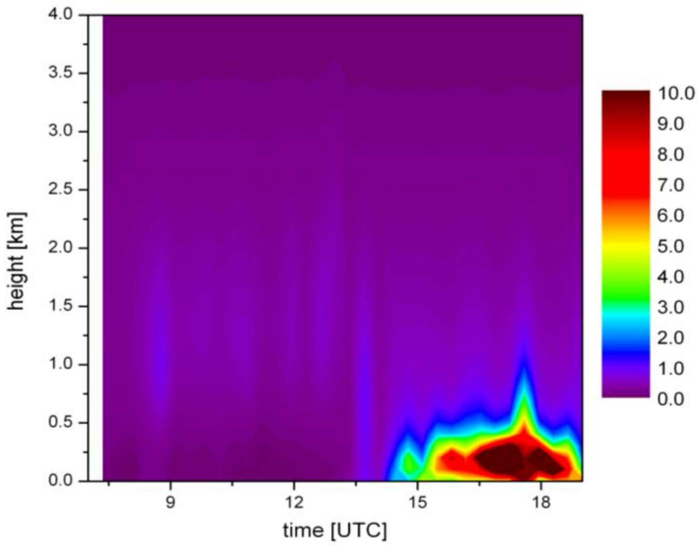

Figure 2: Retrieved BrO profile from June 13th, 2010. The different colours indicate the mixing ratio of BrO in ppt.

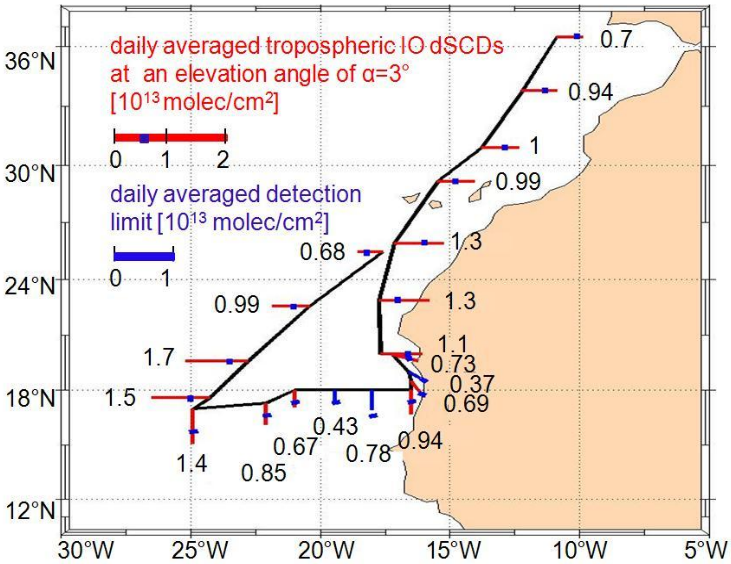

Figure 3: Daily averaged tropospheric IO dSCDs (red) and the respective detection limit (blue) at an elevation angle of 3° plotted along the cruise track.

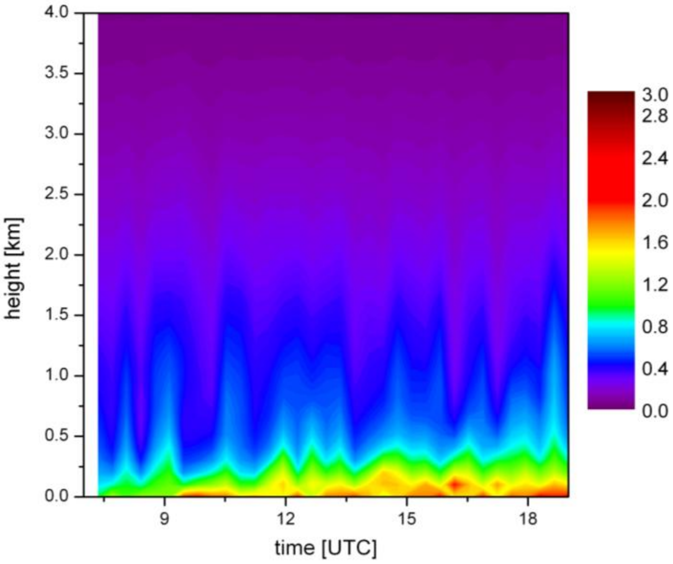

Figure 4: Retrieved IO profile from June 3rd, 2010. The different colours indicate the mixing ratio of IO in ppt.

References

[1] Platt, U. and Hönninger, G. The role of halogen species in the troposphere, Chemosphere, Vol. 52, 325–338,2003

[2] Hönninger, G., von Friedeburg, C.,and Platt, U.: Multi axis differential optical absorption spectroscopy (MAX-DOAS), Atmos. Chem. Phys., 4, 231–254, URL: http:// www.atmos-chem-phys.org/acp/4/231/, 2004

[3] Deutschmann, T. Atmospheric radiative transfer modelling using Monte Carlo methods, Diploma thesis, University of Heidelberg, 2008

[4] Martin, M., Pöhler, D., Seitz, K., Sinreich, R., and Platt, U.: BrO Measurements over the Eastern North Atlantic, Atmospheric Chemistry and Physics, 9, 9545-9554,URL: http://www.atmos-chem-phys.net/9/9545/2009/, 2009

[5] Smirnov, A., Holben, B., Kaufman, Y., Dubovik, O., Eck, T., Slutsker, I., Pietras, C., and Halthore, R.: Optical properties of atmospheric aerosol in maritime environments, American Meteorological Society, 2001

7.13 Halocarbons in the air and in the ocean

Helmke Hepach, Birgit Quack, Franziska Wittke, Karen Stange, Gert Petrick, Kirstin Krüger, Steffen Fuhlbrügge, IFM-GEOMAR, Kiel; hhepach@ifm-geomar.de

Elliot Atlas, RSMAS, Miami, Fl, USA.

Short lived halogenated substances (halocarbons) that occur naturally in the oceans contribute largely to the overall budget of reactive halogen species in the atmosphere and thus influence the ozone depletion in both the troposphere and the stratosphere. Coastal areas, as well as upwelling regions in the tropics, have been identified to be of high significance to the budget of brominated very short lived substances (VSLS) with bromoform ($CHBr_3$) generally representing the largest organic contributor to atmospheric reactive bromine.

During the cruise, halocarbons were measured in both the ocean and the atmosphere. Oceanic measurements were performed in situ on a nearly hourly basis using combined gas chromatography and mass spectrometry (GC-MS) equipped with a purge and trap system. 80 ml of sea water was purged with a stream of helium gas (30 ml /min) while it was heated concurrently to 70°C. Trace gases were captured on a trap hanging above liquid nitrogen. After 60 min purge time, the sample was injected into the GC-MS. Roughly 250 water samples, including sea surface samples and samples from vertical profiles, have been analyzed. In total, 12 halogenated compounds were targeted. This included brominated, chlorinated and iodinated substances: methyl iodide (CH_3I), dichloromethane (CH_2Cl_2), chloroform ($CHCl_3$), tetrachloromethane (CCl_4), 1,1,1-trichloroethane (CCl_3CH_3), dibromomethane (CH_2Br_2), chloroiodomethane (CH_2ClI), 1,1,2-trichloroethane ($CHCl_2CH_2Cl$), dibromochloromethane ($CHBr_2Cl$), bromoiodomethane (CH_2BrI), bromoform ($CHBr_3$), and diiodomethane (CH_2I_2).

For analysis of atmospheric samples, air was pumped into stainless steel canisters using a metal bellows pump being installed on the compass deck. Air was sampled every hour at the 24h-stations. 190 atmospheric samples were sent to Miami where they were analysed for over 50 trace gases including a range of halocarbons (CH_3I, $CHBr_3$ etc.), alkanes, and DMS. Parallel to the sampling on board of the RV Poseidon, air was collected at the Cape Verde Atmospheric Observatory (CVAOO) during the first and the second 24h-station as well.

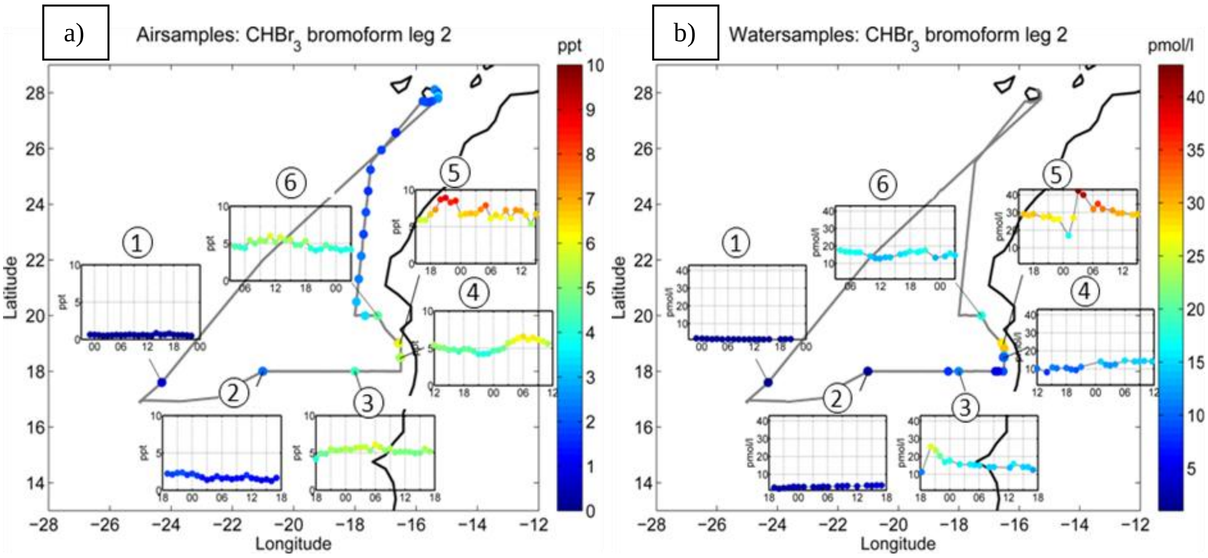

Figure 1: Atmospheric mixing ratios (a) and concentrations in the sea surface water (b) of $CHBr_3$ during P399/2. The numbers indicate the 24h-stations.

First analyses of the results for $CHBr_3$ from leg 2 for air measurements (a) and for sea surface water samples (b) reveal a decline from coastal concentrations towards the stations (1, 2 and 3) farther from the coast. Dissolved surface concentrations and saturation anomalies were in the range from 1 to 43 pmol L-1 and <0 to 225% for $CHBr_3$, indicating that the Mauritanian upwelling is generally a net source of $CHBr_3$ for the atmosphere during P399/2. At the stations farther away from the coast, the ocean and the atmosphere seemed to be in equilibrium.

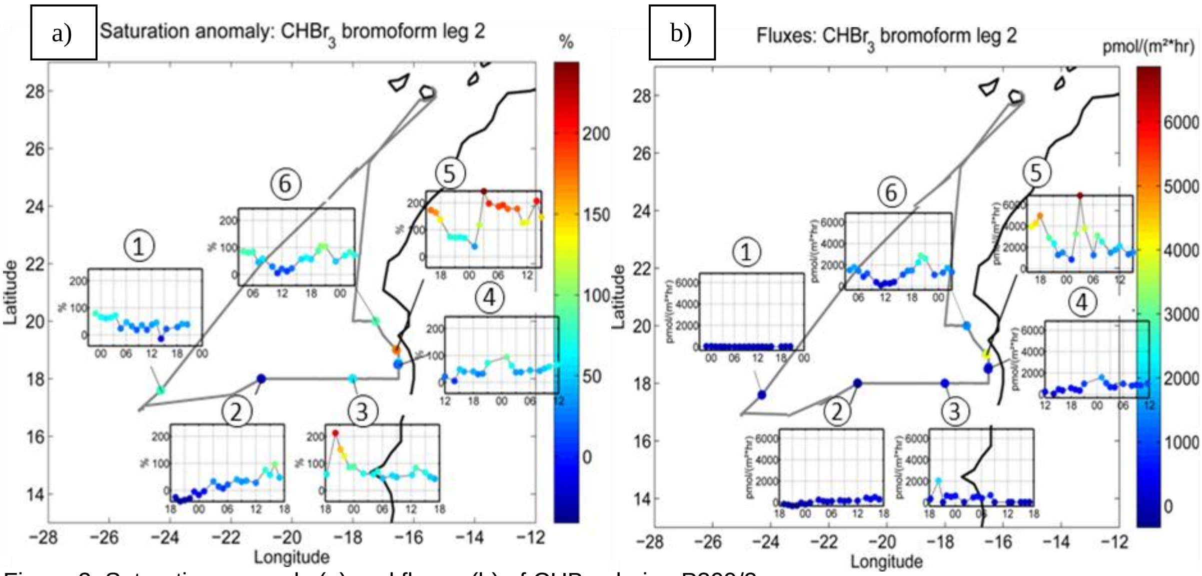

Figure 2: Saturation anomaly (a) and fluxes (b) of $CHBr_3$ during P399/2.

Dissolved $CHBr_3$ and also dibromomethane (CH_2Br_2) concentrations as well as atmospheric mixing ratios of both compounds showed a clear increasing trend towards the coast which is in line with previous observations of near shore sources. The maxima of dissolved and atmospheric $CHBr_3$ and CH_2Br_2 (station 5) were not found at the station with the most intensive upwelling (station 6). Diurnal variabilities were observed for the atmospheric and dissolved concentrations, however, there seemed to be no obvious correlation between both parameters. Computations of the saturation anomalies (Figure 2a) and sea-to-air fluxes of $CHBr_3$ (Figure 2a) indicate that even the highest saturation anomalies and fluxes at station 5 were not sufficient to explain neither the observed elevated atmospheric mixing ratios nor their rapid increases during the day and require additional sources, most likely from shallow coastal waters of the Banc d'Arguin area. This hypothesis will be further investigated.

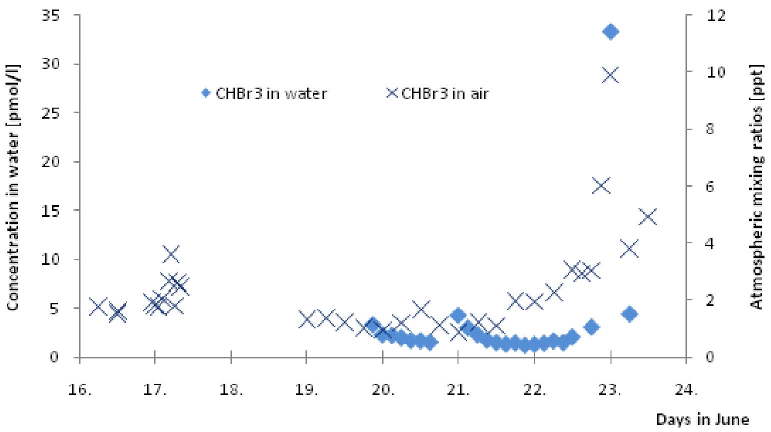

Figure 3: Concentrations of $CHBr_3$ in the atmosphere and in the water during P399/3

Atmospheric and oceanic concentrations of $CHBr_3$ during P399/3 were rather low during the whole leg except for June 23rd (Figure 3). This position was located close to Lisbon, in waters with lower salinity, originating from the inflowing river Tejo. It can therefore be assumed that the high concentrations there are associated to anthropogenic activity.

Analysis of other details of the oceanic halocarbon surface concentrations and their depth profiles is still in progress. The atmospheric distribution and origin of the compounds will also be evaluated, in cooperation and usage of the meteorological analysis of the cruise, especially the calculation of backward tracjectories and mixing layer heights from the radio soundings (Steffen Fuhlbrügge, diploma thesis).

7.14 Stable carbon isotope composition of selected naturally produced halocarbons in the atmosphere

Enno Bahlmann and Ralf Lendt, University of Hamburg;
enno.bahlmann@zmaw.de

7.14.1 Work description

The major objective of our working group was to determine the stable carbon isotope composition of selected naturally produced halocarbons in the atmosphere. The obtained isotopic data was used to investigate the sources and sinks of these halocarbons with a special emphasis regarding the contributions from near coastal emissions.

During the Poseidon cruise P399 leg 2 and 3, 31 high volume air samples (200 L– 400 L) were taken for subsequent isotope determination in the home laboratory. In addition, a total number of 22 5L surface water samples for the determination of the isotopic composition of dissolved halocarbons were taken (in cooperation with IOW). This basic sampling program was complemented by additional atmospheric measurements, which were done in cooperation with various partners to better characterize the composition, origin and chemistry of the sampled air masses. In detail, gaseous elemental mercury was measured on board with e Tekran 2380 atomic fluorescence spectrometer provided by the HGZ Research centre, Geesthacht. Ozone was continuously measured in cooperation with the Max-Planck Institute for Atmospheric Chemistry in Mainz. Together with Max Planck Institute for Biogeochemistry in Jena atmospheric CO_2 and methane have been continuously measured and 2 – 3 flask samples for the examination of the composition of major biogeochemical gases have been taken.

So far 20 of the high volume air samples have been analysed for the isotopic composition of naturally produced halocarbons by 2-dimensional GC-MS/IRMS. The method is described in detail in Bahlmann et al. (2011). The water samples have not yet been analysed.

7.14.2 First Results

The analysis of the air samples in the homelaboratory provided the first carbon isotope ratios from marine background air for a wide range of halocarbons including bromomethane (CH_3Br) and bromoform. So far the evaluation of the results has focussed on dichlorodifluoromethane (CCl_2F_2), chloromethane (CH_3Cl) and CH_3Br. The variability of the δ^{13}C-values for these compounds is depicted in Figure 1.

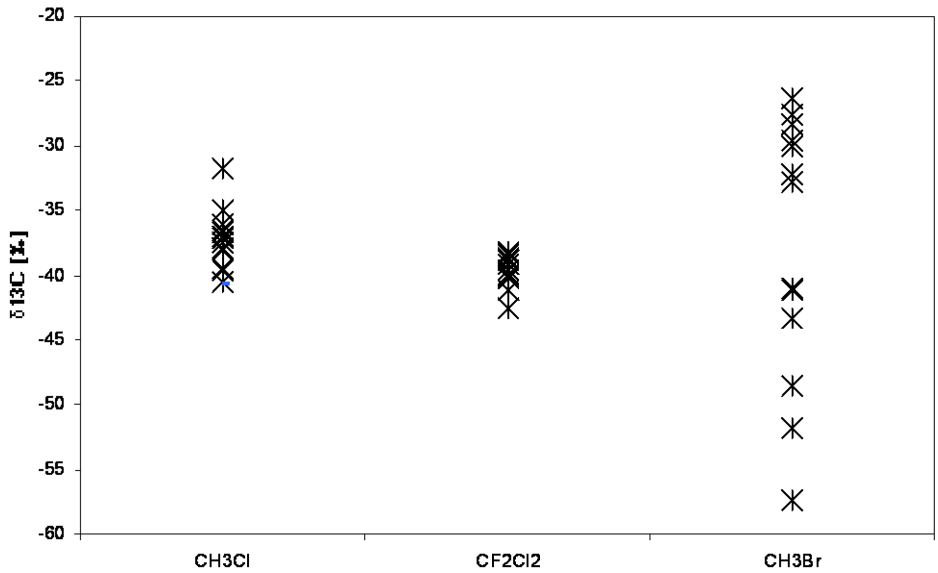

Fig. 1 Stable carbon isotope ratios of CH_3Cl, CF_2Cl_2 and CH_3Br

CCl_2F_2 and CH_3Cl show remarkable constant $\delta^{13}C$-values of –39.1± 1.7‰ and –37.0± 2.1‰, respectively. For CCl_2F_2 this is consistent with its long atmospheric residence time and uniform source distribution. For CH_3Cl our data do not suggest a significant turnover of this compound in the marine boundary layer within the tropical North-East Atlantic.

In contrast, the $\delta^{13}C$ values of CH_3Br show a much higher variability with $\delta^{13}C$ values ranging from -22‰ to -57‰. A first analysis of the CH_3Br data indicate a bimodal distribution of the stable carbon isotope ratios with isotopically enriched CH_3Br (-28‰ ± 2.7‰) in air masses that have passed over the North Atlantic and isotopically depleted CH_3Br (- 47‰ ± 6‰) in air masses that passed along the West African Coast (Fig. 1).

CH_3Br is known to be rapidly degraded in marine surface waters by biotic and abiotic processes with overall degradation rates of up to 20% per day (King & Saltzman, 1997 and references therein). The degradation due to hydrolysis and transhalogenation is assigned with a large ε of 69 ± 8‰ (King & Saltzman, 1997). Thus, the enriched $\delta^{13}C$ values for CH_3Br, which have been observed in the air masses that passed over the North Atlantic point towards a massive degradation in the surface waters of this region. These data are very promising and further detailed analysis will show how this isotope effect can be used to constrain the oceanic cycling of CH_3Br.

References

E.Bahlmann, I.Weinberg, R.Seifert, C.Tubbesing, and W.Michaelis (2011) A high volume sampling system for isotope determination of volatile halocarbons and hydrocarbons; Atmos. Meas. Tech. Discuss., 4, 2161-2188.

King, D. B., and E. S. Saltzman (1997) Removal of methyl bromide in coastal seawater: Chemical and biological rates, J. Geophys. Res., 102, 18,715– 18,721, 1997.

7.15 Dissolved volatile halogenated organic compounds (VHOCs) – the stable carbon isotope ratio

Anna Orlikowska and Detlef Schulz-Bull, Leibniz Institute for Baltic Sea Research Warnemünde (IOW), anna.orlikowska@io-warnemuende.de

Marine produced volatile halogenated organic compounds (VHOCs) are a strong source of highly reactive halogen oxide radicals catalysing the destruction of ozone. Halocarbons come from a number of chemical and biological processes and are present as trace constituents in the oceans and the atmosphere. There is an intense exchange of organohalogens between seawater and the atmosphere and the ocean can be either a source or a sink of these trace gases.

This group of compounds was intensively investigated over the years but the knowledge about the quantities and a composition of VHOCs in the ocean and their changes with the geographical location is rare and not enough to fully understand the present oceanic uptake/emission processes. The supplementary stable carbon isotope composition data ($\delta^{13}C$) can be used to further explore biogeochemical cycles and global source-sink relationships. The differences in isotopic composition of a single compound are closely related to a carbon source and an isotopic fractionation associated with the formation process. Therefore the stable carbon isotope analysis can be used to differentiate various origins of VHOCs and can serve as a valuable technique to distinguish biodegradation from physical, nondegradative processes.

The Poseidon cruise P399 gave possibility to join qualitative and quantitative measurements of VHOCs in the North Atlantic with additional information gained from their $\delta^{13}C$ values. Therefore, not only identification of the halocarbons in the target area and the calculations of the sea-air fluxes for biogenic VHOCs are possible but also additional knowledge of the transformations or sources of the compounds can be provided. During the cruise, discrete water samples were taken for the $\delta^{13}C$ analysis of VHOCs ($CHBr_3$, $CHCl_3$ and others) in the ocean surface layer. Due to a rather poor sensitivity of isotope ratio mass spectrometer a large volumes of the samples (5-10 L) were required. The samples were spiked with mercury chloride in order to stop a biological activity and the associated processes (bioproduction/biodegradation of VHOCs). The water was stored at 4 degree in the dark until further processing after the cruise. The method for VHOCs analysis used in IOW laboratory combines a preconcentration technique (purge and trap system) with a heart-cut multidimensional gas chromatography (heart-cut MDGC) and a mass spectrometry (MS) together with an isotope ratio mass spectrometry (IRMS). The qualitative information about the halocarbons present in the samples is obtained with the single column chromatography and ECD detector. The fourteen compounds of interests (including $CHBr_3$, $CHCl_3$) are transferred for further separation on the second column and determined with MS and IRMS. (Fig. 1) This instrumental set-up enables to obtain both mass spectrometric data as well as the reliable information about a carbon isotopic composition of the low level halocarbons in water. The $\delta^{13}C$ and a concentration data of chloroform and bromoform from several samples collected during the Poseidon P399 cruise are presented in Figure 2.

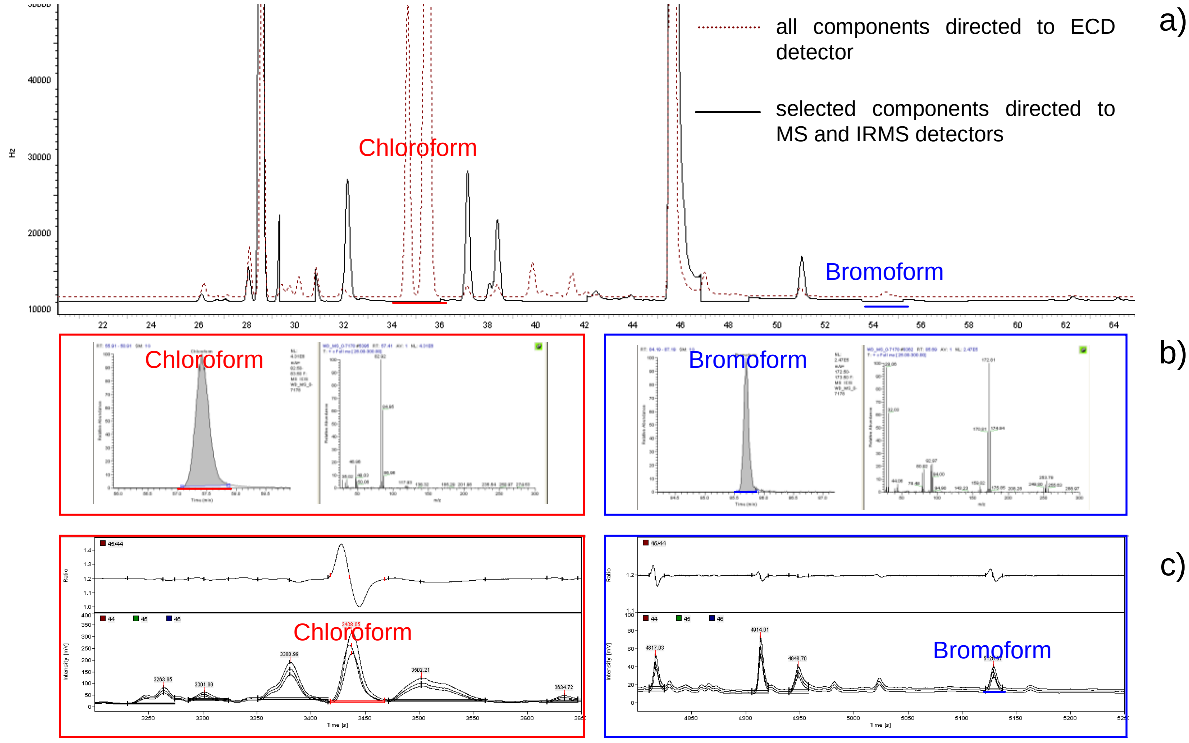

Fig. 1. The separation of halocarbons with a one column chromatography and ECD detector (a) and the heart-cut MDGC with MS (b) and IRMS (c) detectors; an example of chloroform and bromoform in surface water sample collected during the cruise.

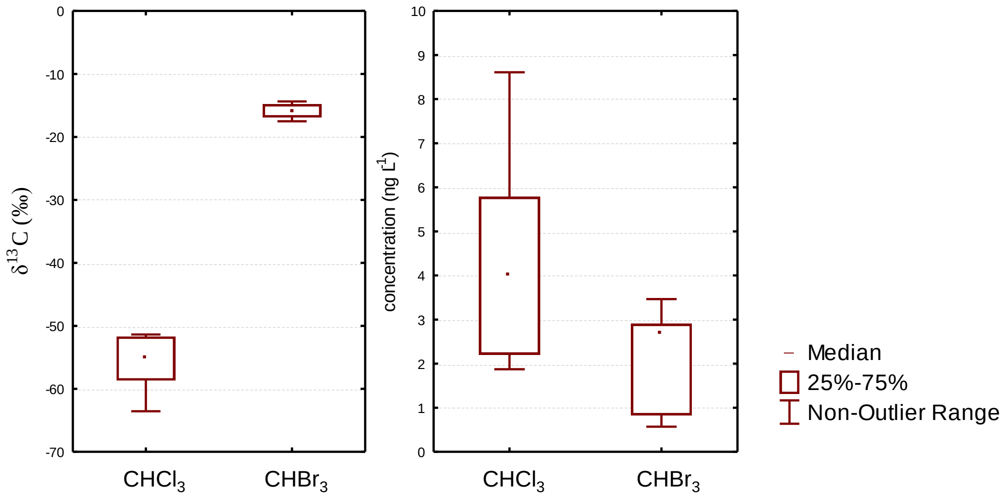

Fig. 2. The stable carbon isotope ratio (‰) and the concentration (ng L^{-1}) of chloroform and bromoform in the analysed surface water from the North Atlantic.

8. Appendices

8.1 Weekly reports, in German

8.2 Partcipants

8.3 List of e-mail addresses

DRIVE: **D**iurnal and **R**eg**i**onal **V**ariability of Halogen **E**missions - Eine Kampagne des SOPRAN Projektes -

FS Poseidon Reise P399/2, 31. Mai – 17. Juni 2010

1. Wochenbericht 31. Mai – 10. Juni 2010

Hermann W. Bange & das P399/2-Team:

Mirja Dunker, Helmke Hepach, Uwe Koy, Carolin Löscher, Gert Petrick, Jens Schafstall, Karen Stange, Franziska Wittke (IFM-GEOMAR, Leibniz-Institut für Meereswissenschaften Kiel)

Katja Grossmann (Institut für Umweltphysik (IUP), Univ. Heidelberg)

Enno Bahlmann, Ralf Lendt (Institut für Biogeochemie und Meereschemie (IfBM), Univ. Hamburg)

Seit gut einer Woche sind wir im tropischen Nordostatlantik mit der Poseidon auf dem 2. Fahrtabschnitt ihrer 399. Reise unterwegs. Unsere Forschungsreise ist Teil der Aktivitäten des BMBF-Verbundprojektes SOPRAN (Surface Ocean PRocesses in the ANthropocene: www.sopran.pangaeade), welches zum Ziel hat, die gegenseitigen Wechselwirkungen zwischen Ozean und Atmosphäre zu untersuchen. Die kontrastreiche Region zwischen den Kapverden und der mauretanischen Küste bietet hierfür ideale Voraussetzungen: Zum einen ist diese Region aufgrund ihrer Nähe zur Sahara gekennzeichnet durch einen hohen Staubeintrag in den Ozean. Dieser beeinflusst durch den Eintrag von Nährstoffen (wie z.B. Eisen) die biologischen Prozesse im küstenfernen und nährstoffarmen tropischen Nordostatlantik. Zum anderen sind die küstennahen Auftriebsgebiete vor Mauretanien gekennzeichnet durch extrem hohe Nährstoffkonzentrationen, die die Grundlage bilden für eines der biologisch produktivsten ozeanischen Gebiete weltweit. Das küstennahe Auftriebsgebiet vor Mauretanien ist ebenfalls eine bedeutende Quelle für eine Vielzahl von biologisch gebildeten klimarelevanten Spurengasen, wie z.B. halogenierten Kohlenwasserstoffen (Bromoform u.a.), Kohlendioxid (CO_2), Methan (CH_4) und Lachgas (N_2O).

Verschiedene SOPRAN-Teilprojekte des IFM-GEOMAR, des Instituts für Umweltphysik der Universität Heidelberg und des Instituts für Biogeochemie und Meereschemie der Universität Hamburg arbeiten auf dieser Reise zusammen, um die Verteilung von Spurengasen (Halogenierte Kohlenwasserstoffe, BrO, N_2O, CO_2) im Ozean und in der Atmosphäre zu untersuchen. Untypisch für gewöhnliche Schiffskampagnen, liegt der besondere Schwerpunkt der DRIVE-Kampagne auf der Charakterisierung der Zusammensetzung der Atmosphäre, um ein umfassendes Bild der Quellen und Senken der halogenierten Kohlenwasserstoffen, die nicht nur ozeanischen Ursprungs sind, zu bekommen. Deshalb werden auf dem Peildeck von Poseidon regelmäßig Luftproben zur Bestimmung der halogenierten Kohlenwasserstoffe genommen. Ergänzt werden diese Messungen durch Probennahmen zur Bestimmung der atmosphärischen Isotopensignatur der halogenierten Kohlenwasserstoffe. Ein MAX-DOAS-Instrument der Universität Heidelberg ist ebenfalls auf dem Peildeck installiert und misst die Konzentrationen von Brom- und Iodoxid (BrO, IO) in der Atmosphäre. Ferner wird kontinuierlich die Isotopensignatur von atmosphärischen CO_2 gemessen sowie die Atmosphärenkonzentrationen von

Methan, Ozon sowie Quecksilber bestimmt. Filterproben, um den Staub- bzw. Aerosoleintrag zu bestimmen, werden täglich genommen. Die luftchemischen Messungen werden durch regelmäßige Radiosondenaufstiege zur Charakterisierung der vertikalen Struktur der Atmosphäre ergänzt.

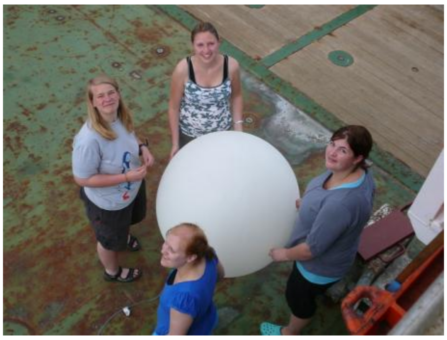

Abb. Links: Vorbereiten eines Radiosondenaufstiegs auf dem Achterdeck, Rechts: Luftprobennahme für halogenierte Kohlenwasserstoffe auf dem Peildeck

Auf der Wasserseite werden die Verteilungen der halogenierten Kohlenwasserstoffe, N_2O und CO_2 bestimmt. Ergänzend dazu wird mit Hilfe einer Mikrostruktursonde die turbulente Vermischung der oberen Wassersäule untersucht und zur Charakterisierung der Verteilung des Phytoplanktons Wasserproben gefiltert. Die Filterproben werden später auf den Gehalt an Chlorophyll und anderen Markerpigmenten untersucht.

Charakteristisch für die Probennahmestrategie der DRIVE-Kampagne sind 24h-Dauerstationen, bei denen das Schiff 24 Stunden auf einer Position verharrt. Dies ist wichtig, um die tägliche Variabilität der halogenierten Kohlenwasserstoffe zu erfassen. Insgesamt sechs 24h-Stationen sind für die DRIVE-Kampagne eingeplant. Um regionale Unterschiede zu erfassen, werden die 24h-Stationen sowohl im nährstoffreichen Küstengebiet vor Mauretanien als auch im nährstoffarmen Gebiet vor den Kapverden durchgeführt.

Das Aufbauen der Instrumente vor dem Auslaufen in Las Palmas ging vor allem Dank der tatkräftigen Unterstützung durch die Mannschaft der Poseidon und des Schiffsagenten sehr zügig voran. Beim Auslaufen am Morgen des 31. Mai waren alle Geräte aufgebaut, wenn es auch hier und da noch einige der „üblichen“ technischen Anlaufschwierigkeiten gab, die jedoch alle behoben werden konnten. Nach einem mehrtägigen Schnitt von Las Palmas in Richtung Südwesten fingen am 3. Juni die Messungen mit der ersten 24h-Station an der TENATSO-Zeitserienstation an. Dann ging es weiter nach Mindelo (Kapverden), wo bei einem kurzen Hafenaufenthalt ein Personalwechsel stattfand. Danach sind wir entlang des 18. Breitengrades in Richtung Mauretanien gedampft. Inzwischen sind zwei weitere 24h-Stationen absolviert und wir sind gerade bei der 4. 24h-Station vor der Küste Mauretaniens.

Besonders „aufregende“ Ergebnisse können wir noch nicht berichten, da wir noch am Anfang der Auswertung unserer Messungen stehen. Auftrieb, gekennzeichnet durch das Auftreten von kaltem und nährstoffreichem Wasser aus mittleren Tiefen, haben wir noch nicht beobachten können. Das Wetter während der Reise war bis jetzt hervorragend. Seit dem Auslaufen in Las Palmas begleitet uns viel Sonnenschein. Es wehen moderate Winde aus Nord und Nordost mit Windstärken bis zu 7 Bft. Mittlerweile haben wir uns auch an die manchmal hohe Dünung und das Rollen des Schiffes gewöhnt. Begleitet wurden wir von ‚fliegenden Fischen’ und kurzzeitig auch von zwei Meersschildkröten und Delfinen. Die Stimmung ist sehr gut und wir sehen dem Rest der Reise gespannt entgegen.

DRIVE: **D**iurnal and **R**eg**i**onal **V**ariability of Halogen **E**missions - Eine Kampagne des SOPRAN Projektes -

FS Poseidon Reise P399/2, 31. Mai – 17. Juni 2010
FS Poseidon Reise P399/3, 18. – 24. Juni 2010

2. Wochenbericht 10. Juni – 23. Juni 2010

Hermann W. Bange & das P399/2, /3-Team:

- Mirja Dunker, Helmke Hepach, Uwe Koy, Carolin Löscher, Jens Schafstall, Karen Stange, Franziska Wittke (IFM-GEOMAR, Leibniz-Institut für Meereswissenschaften, Kiel)
- Katja Grossmann (Institut für Umweltphysik (IUP), Univ. Heidelberg)
- Ralf Lendt (Institut für Biogeochemie und Meereschemie (IfBM), Univ. Hamburg)
- Andres Cianca (Instituto Canaria de Ciencias Marinas (ICCM), Telde, Gran Canaria, Espana)
- Ahmed Makaoui (Institut National de Recherche Halieutique (INRH), Casablanca, Maroc)

In der zweiten und dritten Woche der Reise P399/2 haben wir drei 24h-Stunden Stationen entlang der mauretanischen Küste absolviert. Je weiter wir dabei auf unserer Fahrtroute entlang der Küste nach Norden gekommen sind, desto kälter wurde das Oberflächenwasser. Mit ~18°C wurden an unserer nördlichsten 24h-Station bei 20N 17°15'W die kälteste Oberflächenwassertemperatur aufgezeichnet. Diese kälteren Wassertemperaturen sind ein eindeutiges Zeichen des küstennahen Auftriebs, den wir untersuchen wollen. Begleitet wurde die Abnahme der Wassertemperatur mit einer deutlichen Zunahme der Nährstoffkonzentrationen (z.B. Nitrat), die aus Wassertiefen bis zu 200m stammen und durch den Auftrieb an die Oberflächen transportiert werden. Durch die hohen Nährstoffkonzentrationen wird die Nahrungskette gespeist, die die mauretanischen Küstengebiete zu sehr ertragreichen Fischfanggebieten machen. Zahlreiche große Fischereifahrzeuge, die kommerziellen Fischfang betreiben, haben wir beobachten können. Ebenfalls angelockt von dem Fischreichtum, wurden wir in Küstennähe von Vögeln begleitet.

Die hochproduktiven Gewässer vor Mauretanien sind auch eine Quelle für klimarelevante atmosphärische Spurengase: Zur Bestimmung der Konzentrationen von Kohlendioxid (CO_2) und Lachgas (N_2O) haben wir deshalb für diese Reise zwei vollautomatische, kontinuierlich arbeitende Messsysteme an Bord installiert. In regelmäßigen Abständen können so die Konzentrationen von CO_2 und N_2O in der Atmosphäre und in der Oberfläche des Ozeans bestimmt werden. Dadurch wird eine hohe zeitliche und räumliche Auflösung erzielt und ermöglicht es so, die Verteilung von CO_2 und N_2O im Untersuchungsgebiet detailliert zu ermitteln. Besonders interessiert sind wir daran, die Konzentrationsunterscheide zwischen Auftriebsgebieten und dem offenen Ozean zu untersuchen. Wie vermutet, fanden wir beim Übergang in das kältere Wasser vor Mauretanien einen sehr deutlichen Anstieg sowohl für das gelöste CO_2 als auch für das gelöste N_2O. Als wir das Auftriebsgebiet in Richtung Las Palmas wieder verlassen hatten, nahmen auch die Konzentrationen von gelösten CO_2 und N_2O wieder ab. Dies unterstreicht abermals die Bedeutung des küstennahen Auftriebsgebiets vor Mauretanien als Quelle für atmosphärische Spurengase. Die Messungen der gelösten halogenierten

Kohlenwasserstoffe (KW) sind noch nicht ausgewertet, es ist aber zu vermuten, dass auch sie im Auftriebsgebiet erhöhte Konzentrationen zeigten.

Im Gegensatz zu vorherigen Reisen in den vergangenen Jahren ist der Saharastaubeintrag relativ gering gewesen. Dies zeigte sich deutlich daran, dass die für Saharastaub charakteristische rot-braune Färbung der Aerosolfilter diesmal nur an einem Tag in Küstenähe zu erkennen war. Der geringe Staubeintrag ist wohl auf die Jahreszeit zurückzuführen, in der gewöhnlicherweise die Luftmassen eher im Norden als im Osten ihren Ursprung haben.

Nach drei Tagen Dampfstrecke haben wir am 17. Juni wieder Las Palmas erreicht. Dort erwarteten uns weitere Programmhöhepunkte: Nachmittags besuchte der deutsche Konsul aus Las Palmas für einen informativen Kurzbesuch die Poseidon, dann ging es anschließend, auf freundliche Einladung des kanarischen Kollegen Andres Cianca, zu einem zweistündigen Besuch beim Instituto Canario de Ciencas Marinas in Telde (ICCM), südlich von Las Palmas. Absoluter Höhepunkt des Besuchs beim ICCM war die Besichtigung der Becken zur Aufzucht von Meeresschildkröten.

Am 18. Juni ging es dann weiter auf unseren Transit in Richtung Norden nach Vigo, unserem Zielhafen. Der Transit wurde nur durch einen kurzen Aufenthalt an der Zeitserienstation ESTOC, nördlich von Las Palmas, unterbrochen. Nach Beendigung der Station dampfen wir nun gradewegs nach Vigo, was für die „Alte Dame“ Poseidon teilweise Schwerstarbeit bedeutet: Mit zeitweilig nur 6-7 kn (ca. 11-13 km/h) dampft sie gegen Wind und den kräftigen, südwärtsgerichteten Kanarenstrom an. Wie langsam dies ist, wird einem deutlich, wenn hochbeladene Containerschiffe scheinbar mühelos innerhalb einer halben Stunde vorbeiziehen. Nach fast 4 Wochen, sehr erfolgreicher Fahrt mit Poseidon, werden wir am 24. Juni Vigo erreichen, d.h. heute ist der letzte Messtag und morgen fängt das große Kistenpacken an …





Impressionen von P399, links oben: Blick ins Nasslabor (N_2O Gaschromatograph links, Filtrationsgestelle für Chlorophyll, rechts); rechts oben: Blick ins Trockenlabor (links GC-MS für halogenierte KW, CTD Kontrollstation rechts); rechts unten: CTD/Rosette im Abendlicht; Mitte: Schildkröte, Besuch des ICCM (Telde, Gran Canaria); links unten: Feierabendstimmung auf dem Achterdeck während der Internetradioübertragung Deutschland-Australien.

31. Mai – 5. Juni 2010, Las Palmas – Mindelo

Enno Bahlmann
(IfBM Hamburg)
Halogenierte Verbind.,
Quecksilber, CH_4, O_3

Franziska Wittke
(IFM-GEOMAR)
Radiossonden,
Luftprobennahme,
Halogenierte Verb.

Mirja Dunker
(IFM-GEOMAR)
Nährstoffe, O_2

Uwe Koy
(IFM-GEOMAR)
CTD, Mikrostruktur

Jens Schafstall
(IFM-GEOMAR)
CTD, Mikrostruktur

Katja Grossmann
(IUP Heidelberg)
Reakive Halogenverb.

Helmke Hepach
(IFM-GEOMAR)
Halogenierte Verb.

Carolin Löscher
(IFM-GEOMAR)
N_2O, Chla-/DNA-Filtration

Hermann Bange
(IFM-GEOMAR)
N_2O, CO_2, Aerosole

Gert Petrick
(IFM-GEOMAR)
Halogenierte Verb.

5. – 17. Juni 2010, Mindelo - Las Palmas

Ralf Lendt
(IfBM Hamburg)
Halogenierte Verbind.,
Quecksilber, CH_4, O_3

Karen Stange
(IFM-GEOMAR)
Halogenierte Verb.

P399/3: 18. – 25. Juni 2010, Las Palmas – Vigo

Andres Cianca
(ICCM Telde)
CTD

Ahmed Makaoui
(INRH Casablanca)
Phys. Ozeanograph
Bobachter aus Marokko

K. Grossmann
MAX-DOAS: BrO, IO, ...

E. Atlas
flask samples: atm. halocarbons, hydrocarbons, CFCs, DMS, COS, alkyl nitrates, ...

E. Bahlmann
isotope composition of atm halocarbons; atm. Hg

A. Baker
aerosol composition: metals, cations, anions, nutrients , ...

M. Heimann, Jost Lavric
cont. atm. CH_4; flask samples: atm. SF_6, O_2/N_2, Ar/N_2, $^{13}C^{18}O_2$, N_2O, CO, CH_4, H_2, ...

J. Williams
atm. O_3

H. Bange
nutrients, diss. O_2, ship data: cont. meteorological data, thermosalinograph

A. Kock
underway atm/diss N_2O, N_2O dp

T. Steinhoff
underway atm/diss pCO_2,
underway diss O_2

B. Quack, H. Hepach, F. Wittke
diss. halocarbons, radio sondes

K. Krüger, S. Fuhlbrügge
meteorology; air mass trajectories

M. Dengler, J. Schafstall
CTD; microstructure measurement

C. Löscher
cont. atm/diss N_2O, N_2O dp;
DNA/RNA sampling

G. Friedrichs
cont. atm. $^{13}CO_2$

I. Peeken, A. Bracher
chl a/pigments, flow cytometry; pigments by remote sensing

A. Cianca
CTD and Chl a/pigments at ESTOC

A. Orlikowska
^{13}C in diss. VOC

INSTITUT FÜR UMWELTPHYSIK

K. Grossmann
katja.grossmann@iup.uni-heidelberg.de

UNIVERSITY OF MIAMI

E. Atlas
eatlas@rsmas.miami.edu

E. Bahlmann
enno.bahlmann@zmaw.de

University of East Anglia

A. Baker
alex.baker@uea.ac.uk

Max-Planck-Institut für Biogeochemie

Jost Lavric
jlavric@bgc-jena.mpg.de

MPI für Chemie Mainz

J. Williams
jonathan.williams@mpic.de

IFM-GEOMAR

H. Bange
hbange@ifm-geomar.de

A. Kock
akock@ifm-geomar.de

T. Steinhoff
tsteinhoff@ifm-geomar.de

B. Quack, H. Hepach, F. Wittke
bquack@ifm-geomar.de
hhepach@ifm-geomar.de
fwittke@ifm-geomar.de

K. Krüger, S. Fuhlbrügge
kkrueger@ifm-geomar.de
sfuhlbruegge@ifm-geomar.de

M. Dengler
mdengler@ifm-geomar.de

Christian-Albrechts-Universität zu Kiel

C. Löscher
cloescher@ifam.uni-kiel.de

G. Friedrichs
gfriedr@phc.uni-kiel.de

I. Peeken, A. Bracher
ilka.peeken@awi.de
astrid.bracher@awi.de

A. Cianca
andres@iccm.rcanaria.es

A. Orlikowska
anna.orlikowska@io-warnemuende.de


INSTITUT FÜR UMWELTPHYSIK Univ. Heidelberg
MPI für Chemie Mainz
University of East Anglia
Max-Planck-Institut für Biogeochemie
UNIVERSITY OF MIAMI
Universität Hamburg
DRIVE
Poseidon Cruise P399 Legs 2 and 3
IFM-GEOMAR
Leibniz-Institut für Meereswissenschaften an der Universität Kiel
AWI
INSTITUTO CANARIO DE CIENCIAS MARINAS
ICCM
C A U
Christian-Albrechts-Universität zu Kiel
Leibniz-Institut für Ostseeforschung Warnemünde
iow

IFM-GEOMAR
Leibniz-Institut für Meereswissenschaften
an der Universität Kiel

IFM-GEOMAR Reports

No.	Title
1	RV Sonne Fahrtbericht / Cruise Report SO 176 & 179 MERAMEX I & II (Merapi Amphibious Experiment) 18.05.-01.06.04 & 16.09.-07.10.04. Ed. by Heidrun Kopp & Ernst R. Flueh, 2004, 206 pp. In English
2	RV Sonne Fahrtbericht / Cruise Report SO 181 TIPTEQ (from The Incoming Plate to mega Thrust EarthQuakes) 06.12.2004.-26.02.2005. Ed. by Ernst R. Flueh & Ingo Grevemeyer, 2005, 533 pp. In English
3	RV Poseidon Fahrtbericht / Cruise Report POS 316 Carbonate Mounds and Aphotic Corals in the NE-Atlantic 03.08.–17.08.2004. Ed. by Olaf Pfannkuche & Christine Utecht, 2005, 64 pp. In English
4	RV Sonne Fahrtbericht / Cruise Report SO 177 - (Sino-German Cooperative Project, South China Sea: Distribution, Formation and Effect of Methane & Gas Hydrate on the Environment) 02.06.-20.07.2004. Ed. by Erwin Suess, Yongyang Huang, Nengyou Wu, Xiqiu Han & Xin Su, 2005, 154 pp. In English and Chinese
5	RV Sonne Fahrtbericht / Cruise Report SO 186 – GITEWS (German Indonesian Tsunami Early Warning System 28.10.-13.1.2005 & 15.11.-28.11.2005 & 07.01.-20.01.2006. Ed. by Ernst R. Flueh, Tilo Schoene & Wilhelm Weinrebe, 2006, 169 pp. In English
6	RV Sonne Fahrtbericht / Cruise Report SO 186 -3 – SeaCause II, 26.02.-16.03.2006. Ed. by Heidrun Kopp & Ernst R. Flueh, 2006, 174 pp. In English
7	RV Meteor, Fahrtbericht / Cruise Report M67/1 CHILE-MARGIN-SURVEY 20.02.-13.03.2006. Ed. by Wilhelm Weinrebe und Silke Schenk, 2006, 112 pp. In English
8	RV Sonne Fahrtbericht / Cruise Report SO 190 - SINDBAD (Seismic and Geoacoustic Investigations Along The Sunda-Banda Arc Transition) 10.11.2006 - 24.12.2006. Ed. by Heidrun Kopp & Ernst R. Flueh, 2006, 193 pp. In English
9	RV Sonne Fahrtbericht / Cruise Report SO 191 - New Vents "Puaretanga Hou" 11.01. - 23.03.2007. Ed. by Jörg Bialas, Jens Greinert, Peter Linke, Olaf Pfannkuche, 2007, 190 pp. In English
10	FS ALKOR Fahrtbericht / Cruise Report AL 275 - Geobiological investigations and sampling of aphotic coral reef ecosystems in the NE-Skagerrak, 24.03. - 30.03.2006, Eds.: Andres Rüggeberg & Armin Form, 39 pp. In English

IFM-GEOMAR
Leibniz-Institut für Meereswissenschaften
an der Universität Kiel

No.	Title
11	FS Sonne / Fahrtbericht / Cruise Report SO 192-1: MANGO: Marine Geoscientific Investigations on the Input and Output of the Kermadec Subduction Zone, 24.03. - 22.04.2007, Ernst Flüh & Heidrun Kopp, 127 pp. In English
12	FS Maria S. Merian / Fahrtbericht / Cruise Report MSM 04-2: Seismic Wide-Angle Profiles, Fort-de-France – Fort-de-France, 03.01. - 19.01.2007, Ed.: Ernst Flüh, 45 pp. In English
13	FS Sonne / Fahrtbericht / Cruise Report SO 193: MANIHIKI Temporal, Spatial, and Tectonic Evolution of Oceanic Plateaus, Suva/Fiji – Apia/Samoa 19.05. - 30.06.2007, Eds.: Reinhard Werner and Folkmar Hauff, 201 pp. In English
14	FS Sonne / Fahrtbericht / Cruise Report SO195: TOTAL TOnga Thrust earthquake Asperity at Louisville Ridge, Suva/Fiji – Suva/Fiji 07.01. - 16.02.2008, Eds.: Ingo Grevemeyer & Ernst R. Flüh, 106 pp. In English
15	RV Poseidon Fahrtbericht / Cruise Report P362-2: West Nile Delta Mud Volcanoes, Piräus – Heraklion 09.02. - 25.02.2008, Ed.: Thomas Feseker, 63 pp. In English
16	RV Poseidon Fahrtbericht / Cruise Report P347: Mauritanian Upwelling and Mixing Process Study (MUMP), Las-Palmas - Las Palmas, 18.01. - 05.02.2007, Ed.: Marcus Dengler et al., 34 pp. In English
17	FS Maria S. Merian Fahrtbericht / Cruise Report MSM 04-1: Meridional Overturning Variability Experiment (MOVE 2006), Fort de France – Fort de France, 02.12. – 21.12.2006, Ed.: Thomas J. Müller, 41 pp. In English
18	FS Poseidon Fahrtbericht /Cruise Report P348: SOPRAN: Mauritanian Upwelling Study 2007, Las Palmas - Las Palmas, 08.02. - 26.02.2007, Ed.: Hermann W. Bange, 42 pp. In English
19	R/V L'ATALANTE Fahrtbericht / Cruise Report IFM-GEOMAR-4: Circulation and Oxygen Distribution in the Tropical Atlantic, Mindelo/Cape Verde - Mindelo/Cape Verde, 23.02. - 15. 03.2008, Ed.: Peter Brandt, 65 pp. In English
20	RRS JAMES COOK Fahrtbericht / Cruise Report JC23-A & B: CHILE-MARGIN-SURVEY, OFEG Barter Cruise with SFB 574, 03.03.-25.03. 2008 Valparaiso – Valparaiso, 26.03.-18.04.2008 Valparaiso - Valparaiso, Eds.: Ernst Flüh & Jörg Bialas, 242 pp. In English
21	FS Poseidon Fahrtbericht / Cruise Report P340 – TYMAS "Tyrrhenische Massivsulfide", Messina – Messina, 06.07.-17.07.2006, Eds.: Sven Petersen and Thomas Monecke, 77 pp. In English

IFM-GEOMAR
Leibniz-Institut für Meereswissenschaften
an der Universität Kiel

No.	Title
22	RV Atalante Fahrtbericht / Cruise Report HYDROMAR V (replacement of cruise MSM06/2), Toulon, France - Recife, Brazil, 04.12.2007 - 02.01.2008, Ed.: Sven Petersen, 103 pp. In English
23	RV Atalante Fahrtbericht / Cruise Report MARSUED IV (replacement of MSM06/3), Recife, Brazil - Dakar, Senegal, 07.01. - 31.01.2008, Ed.: Colin Devey, 126 pp. In English
24	RV Poseidon Fahrtbericht / Cruise Report P376 ABYSS Test, Las Palmas - Las Palmas, 10.11. - 03.12.2008, Eds.: Colin Devey and Sven Petersen, 36 pp, In English
25	RV SONNE Fahrtbericht / Cruise Report SO 199 CHRISP Christmas Island Seamount Province and the Investigator Ridge: Age and Causes of Intraplate Volcanism and Geodynamic Evolution of the south-eastern Indian Ocean, Merak/Indonesia – Singapore, 02.08.2008 - 22.09.2008, Eds.: Reinhard Werner, Folkmar Hauff and Kaj Hoernle, 210 pp. In English
26	RV POSEIDON Fahrtbericht / Cruise Report P350: Internal wave and mixing processes studied by contemporaneous hydrographic, current, and seismic measurements, Funchal – Lissabon, 26.04.-10.05.2007 Ed.: Gerd Krahmann, 32 pp. In English
27	RV PELAGIA Fahrtbericht / Cruise Report Cruise 64PE298: West Nile Delta Project Cruise - WND-3, Heraklion - Port Said, 07.11.-25.11.2008, Eds.: Jörg Bialas & Warner Brueckmann, 64 pp. In English
28	FS POSEIDON Fahrtbericht / Cruise Report P379/1: Vulkanismus im Karibik-Kanaren-Korridor (ViKKi), Las Palmas – Mindelo, 25.01.-12.02.2009, Ed.: Svend Duggen, 74 pp. In English
29	FS POSEIDON Fahrtbericht / Cruise Report P379/2: Mid-Atlantic-Researcher Ridge Volcanism (MARRVi), Mindelo- Fort-de-France, 15.02.-08.03.2009, Ed.: Svend Duggen, 80 pp. In English
30	FS METEOR Fahrtbericht / Cruise Report M73/2: Shallow drilling of hydrothermal sites in the Tyrrhenian Sea (PALINDRILL), Genoa – Heraklion, 14.08.2007 – 30.08.2007, Eds.: Sven Petersen & Thomas Monecke, 235 pp. In English
31	FS POSEIDON Fahrtbericht / Cruise Report P388: West Nile Delta Project - WND-4, Valetta – Valetta, 13.07. - 04.08.2009, Eds.: Jörg Bialas & Warner Brückmann, 65 pp. In English
32	FS SONNE Fahrtbericht / Cruise Report SO201-1b: KALMAR (Kurile-Kamchatka and ALeutian MARginal Sea-Island Arc Systems): Geodynamic and Climate Interaction in Space and Time, Yokohama, Japan - Tomakomai, Japan, 10.06. - 06.07.2009, Eds.: Reinhard Werner & Folkmar Hauff, 105 pp. In English
33	FS SONNE Fahrtbericht / Cruise Report SO203: WOODLARK Magma genesis, tectonics and hydrothermalism in the Woodlark Basin, Townsville, Australia - Auckland, New Zealand 27.10. - 06.12.2009, Ed.: Colin Devey, 177 pp. In English

IFM-GEOMAR
Leibniz-Institut für Meereswissenschaften
an der Universität Kiel

No.	Title
34	FS MARIA S. MERIAN Fahrtbericht / Cruise Report MSM 03-2: HYDROMAR IV: The 3rd dimension of the Logatchev hydrothermal field, Fort-de-France - Fort-de-France, 08.11. - 30.11.2006, Ed.: Sven Petersen, 98 pp. In English
35	FS SONNE Fahrtbericht / Cruise Report SO201-2 **KALMAR: K**urile-Kamchatka and **AL**eutian **MAR**ginal Sea-Island Arc Systems: Geodynamic and Climate Interaction in Space and Time Busan/Korea – Tomakomai/Japan, 30.08. - 08.10.2009, Eds.: Wolf-Christian Dullo, Boris Baranov, and Christel van den Bogaard, 233 pp. In English
36	RV CELTIC EXPLORER Fahrtbericht / Cruise Report CE0913: Fluid and gas seepage in the North Sea, Bremerhaven – Bremerhaven, 26.07. - 14.08.2009, Eds.: Peter Linke, Mark Schmidt, CE0913 cruise participants, 90 pp. In English
37	FS SONNE Fahrtbericht / Cruise Report: TransBrom SONNE, Tomakomai, Japan - Townsville, Australia, 09.10. - 24.10.2009, Eds.: Birgit Quack & Kirstin Krüger, 84 pp. In English
38	FS POSEIDON Fahrtbericht / Cruise Report POS403, Ponta Delgada (Azores) - Ponta Delgada (Azores), 14.08. - 30.08.2010, Eds.: Torsten Kanzow, Andreas Thurnherr, Klas Lackschewitz, Marcel Rothenbeck, Uwe Koy, Christopher Zappa, Jan Sticklus, Nico Augustin, 66 pp. In English
39	FS SONNE Fahrtbericht/Cruise Report SO208 Leg 1 & 2 Propagation of Galápagos Plume Material in the Equatorial East Pacific (PLUMEFLUX), Caldera/Costa Rica – Guayaquil/Ecuador 15.07. - 29.08.2010, Eds.: Reinhard Werner, Folkmar Hauff and Kaj Hoernle, 230 pp, In English
40	Expedition Report "Glider fleet", Mindelo (São Vincente), Republic of Cape Verde, 05. – 19.03.2010, Ed.: Torsten Kanzow, 26 pp, In English
41	FS SONNE Fahrtbericht / Cruise Report SO206, Caldera, Costa Rica – Caldera, Costa Rica, 30.05. – 19.06.2010, Ed.: Christian Hensen, 95 pp, In English
42	FS SONNE Fahrtbericht / Cruise Report SO212, Talcahuano, Chile – Valparaiso, Chile, 22.12. – 26.12.2010, Ed.: Ernst Flüh, 47 pp, in English
43	RV Chakratong Tongyai Fahrtbericht / Cruise Report MASS-III, Morphodynamics and Slope Stability of the Andaman Sea Shelf Break (Thailand), Phuket - Phuket (Thailand), 11.01. - 24.01.2011, Ed.: Sebastian Krastel, 42 pp, in English.
44	FS SONNE Fahrtbericht / Cruise Report SO-210, Identification and investigation of fluid flux, mass wasting and sediments in the forearc of the central Chilean subduction zone (ChiFlux), Valparaiso – Valparaiso, 23.09. – 01.11.2010, Ed.: Peter Linke, 112 pp, in English.
45	RV Poseidon POS389 & POS393 & RV Maria S. MerianMSM15/5, TOPO-MED - Topographic, structural and seismotectonic consequences of plate re-organization in the Gulf of Cadiz and Alboran Sea – POS 389: Valletta, Malta – Malaga, Spain, 06.–17.08.2009, POS393: Malaga, Spain – Faro, Portugal, 14.–24.01.2010, MSM15/5: Valletta, Malta - Rostock, Germany, 17.–29.07.2010, I. Grevemeyer, xx pp.

IFM-GEOMAR
Leibniz-Institut für Meereswissenschaften
an der Universität Kiel

No.	Title
46	FS POSEIDON Fahrtbericht / Cruise Report, P408 - The Jeddah Transect, Jeddah - Jeddah, Saudi Arabia, 13.01.–02.03.2011, M. Schmidt, C. Devey, A. Eisenhauer and cruise participants, 80 pp.
47	FS SONNE Fahrtbericht / Cruise Report, SO-214 NEMESYS, Wellington – Wellington, 09.03. - 05.04.2011, Wellington - Auckland 06. - 22.04.2011, Ed.: J. Bialas, 174 pp.
48	FS POSEIDON Fahrtbericht / Cruise Report, P399 - 2&3, Las Palmas - Las Palmas (Canary Islands), 31.05.2010 – 17.06.2010 & Las Palmas (Canary Islands), Vigo (Spain), 18. – 24.06.2010, Ed.: H. Bange, 84 pp.

IFM-GEOMAR
Leibniz-Institut für Meereswissenschaften
an der Universität Kiel

Das Leibniz-Institut für Meereswissenschaften ist ein Institut der Wissenschaftsgemeinschaft Gottfried Wilhelm Leibniz (WGL)

The Leibniz-Institute of Marine Sciences is a member of the Leibniz Association (Wissenschaftsgemeinschaft Gottfried Wilhelm Leibniz).

Leibniz-Institut für Meereswissenschaften / Leibniz-Institute of Marine Sciences
IFM-GEOMAR
Dienstgebäude Westufer / West Shore Building
Düsternbrooker Weg 20
D-24105 Kiel
Germany

Leibniz-Institut für Meereswissenschaften / Leibniz-Institute of Marine Sciences
IFM-GEOMAR
Dienstgebäude Ostufer / East Shore Building
Wischhofstr. 1-3
D-24148 Kiel
Germany

Tel.: ++49 431 600-0
Fax: ++49 431 600-2805
www.ifm-geomar.de